UNIVERSIDADE FEDERAL DE MINAS GERAIS

Gabriel Henrique Campolina Silva

INVESTIGAÇÃO DE COMPONENTES RELACIONADOS AO SISTEMA ENDÓCRINO VITAMINA D NA PRÓSTATA DE RATOS DURANTE O ENVELHECIMENTO

Belo Horizonte

2020

GABRIEL HENRIQUE CAMPOLINA SILVA

Versão final

INVESTIGAÇÃO DE COMPONENTES RELACIONADOS AO SISTEMA ENDÓCRINO VITAMINA D NA PRÓSTATA DE RATOS DURANTE O ENVELHECIMENTO

Tese apresentada ao Programa de Pós-Graduação em Biologia Celular da Universidade Federal de Minas Gerais como requisito parcial para a obtenção do título de Doutor em Ciências.

Orientadora: Profa. Dra. Cleida Aparecida de Oliveira

Belo Horizonte
2020

043 Silva, Gabriel Henrique Campolina.
Investigação de componentes relacionados ao sistema endócrino vitamina D na próstata de ratos durante o envelhecimento [manuscrito] / Gabriel Henrique Campolina Silva. – 2020.

143 f. : il. ; 29,5 cm.

Orientadora: Profa. Dra. Cleida Aparecida de Oliveira.
Tese (doutorado) – Universidade Federal de Minas Gerais, Instituto de Ciências Biológicas. Programa de Pós-Graduação em Biologia Celular.

1. Próstata. 2. Envelhecimento. 3. Vitamina D. 4. Receptores de Calcitriol. 5. Receptores X Retinoide. 6. 25-Hidroxivitamina D3 1-alfa-Hidroxilase. 7. Vitamina D3 24-Hidroxilase. I. Oliveira, Cleida Aparecida de. II. Universidade Federal de Minas Gerais. Instituto de Ciências Biológicas. III. Título.

CDU: 576

Ficha catalográfica elaborada pela bibliotecária Rosilene Moreira Coelho de Sá – CRB 6 – 2726

Universidade Federal de Minas Gerais - Instituto de Ciências Biológicas
Programa de Pós-Graduação em Biologia Celular

ATA DA DEFESA DE TESE DE DOUTORADO DE

GABRIEL HENRIQUE CAMPOLINA SILVA

227/2020
entrada
1°/2016
2016705927

Às **quatorze horas** do dia **21 de agosto de 2020**, reuniu-se, no Instituto de Ciências Biológicas da UFMG, a Comissão Examinadora da Tese, indicada pelo Colegiado do Programa, para julgar, em exame final, o trabalho final intitulado: **"INVESTIGAÇÃO DE COMPONENTES RELACIONADOS AO SISTEMA ENDÓCRINO VITAMINA D NA PRÓSTATA DE RATOS DURANTE O ENVELHECIMENTO"**, requisito final para obtenção do grau de Doutor em Biologia Celular. Abrindo a sessão, a Presidente da Comissão, **Dra. Cleida Aparecida de Oliveira**, após dar a conhecer aos presentes o teor das Normas Regulamentares do Trabalho Final, passou a palavra ao candidato, para apresentação de seu trabalho. Seguiu-se a arguição pelos examinadores, com a respectiva defesa do candidato. Logo após, a Comissão se reuniu, sem a presença do candidato e do público, para julgamento e expedição de resultado final. Foram atribuídas as seguintes indicações:

Prof./Pesq.	Instituição	Indicação
Dra. Cleida Aparecida de Oliveira	UFMG	Aprovado
Dra. Catarina Segreti Porto	UNIFESP	Aprovado
Dr. Sérgio Luiz Felisbino	UNESP - Botucatu/SP	Aprovado
Dr. Guilherme Mattos Jardim Costa	UFMG	Aprovado
Dr. José Carlos Nogueira	UFMG	Aprovado

Pelas indicações, o candidato foi considerado: Aprovado
O resultado final foi comunicado publicamente ao candidato pela Presidente da Comissão. Nada mais havendo a tratar, a Presidente encerrou a reunião e lavrou a presente ATA, que será assinada por todos os membros participantes da Comissão Examinadora. **Belo Horizonte, 21 de agosto de 2020.**

Drª. Cleida Aparecida de Oliveira (Orientadora) _____

Drª. Catarina Segreti Porto _____

Dr. Sérgio Luiz Felisbino _____

Dr. Guilherme Mattos Jardim Costa _____

Dr. José Carlos Nogueira _____

Obs: Este documento não terá validade sem a assinatura e carimbo do Coordenador

Prof. Erika Cristina Jorge
Coordenadora do Programa de Pós Graduação
em Biologia Celular ICB/UFMG

A presente tese de doutorado foi realizada no Laboratório de Biologia da Reprodução (LABRE) sediado no Departamento de Morfologia do Instituto de Ciências Biológicas da Universidade Federal de Minas Gerais - UFMG, sob a orientação da Dra. Cleida Aparecida de Oliveira, e contou com o auxílio financeiro da Coordenação de Aperfeiçoamento de Pessoa de Nível Superior (CAPES), Conselho Nacional de Desenvolvimento Científico e Tecnológico (CNPq), Fundação de Amparo à Pesquisa do Estado de Minas Gerais (FAPEMIG), e da Pró-Reitora de Pós-Graduação da UFMG.

DEDICATÓRIA

Somos nós que fazemos a vida [...]
Como der, ou puder, ou quiser!

Gonzaguinha.

Dedico essa tese às pessoas mais importantes pra mim:

- Aos meus pais e familiares, em especial às minhas tias Arlete, Diva e Normélia, que acompanharam de perto minha trajetória pessoal e profissional, e sobretudo, me ensinaram que o amor justifica todo o sacrifício.

- À minha doce e amada esposa, Daiane, por toda cumplicidade e por me fazer enxergar a vida além dos olhos.

- À minha querida orientadora, Dra. Cleida Aparecida de Oliveira, pelos ensinamentos, amizade e por não medir esforços para que eu concluísse esse trabalho.

AGRADECIMENTOS

Uma tese de doutorado ou qualquer trabalho acadêmico dessa natureza pode transmitir ao leitor a ideia de ser um projeto individual, ao trazer explicitado, logo em suas primeiras páginas, somente um único nome de autoria. Porém, esse é um trabalho que requer o envolvimento de muitas pessoas – ou melhor – de uma equipe toda! Em primeiro lugar, sou grato aos meus familiares e amigos, por me proporcionar o apoio e espaço necessário para concluir mais esse projeto. Também sou imensamente grato aos meus companheiros do Laboratório de Biologia da Reprodução da UFMG, pela agradável convivência e por sempre estarem dispostos a compartilhar conhecimentos, sorrisos, e aquela ajuda de sempre nos experimentos. À Cleida, minha orientadora, deixo meus eternos agradecimentos. Obrigado pela oportunidade de crescimento profissional e pessoal, e por me fazer exigir sempre mais de mim mesmo. Aos meus companheiros do Grupo Triatomíneos/FIOCRUZ-MG, do Laboratorio de Oncología y Andrología da Universidad de Chile, e do CHU de Quebec Research Center - Canada, obrigado pela imensa troca de experiência e por toda amizade. Também não poderia faltar meu muito obrigado aos meus companheiros do PPG-Biocel e aos professores e funcionários do Departamento de Morfologia do ICB/UFMG, por terem contribuído com a minha formação e pelo companheirismo durante a jornada. Por fim, agradeço aos membros da banca examinadora, pelo precioso tempo despendido em avaliar e contribuir com a melhoria deste trabalho, e a você, caro leitor, que independente de quem seja, se interessou sobre esse trabalho que, para mim, é a minha maior conquista como discente.

A todos, meu mais sincero OBRIGADO!

RESUMO

Evidências experimentais e epidemiológicas têm atribuído ao metabólito ativo da vitamina D, o 1α,25$(OH)_2$D ou calcitriol, um papel protetor contra o desenvolvimento e progressão do câncer de próstata, uma desordem proliferativa que afeta 1 a cada 6 homens acima dos 65 anos de idade. Entretanto, pouco se sabe sobre a distribuição e possível variação idade-dependente dos componentes associados à via de sinalização da vitamina D no tecido prostático. Portanto, o presente trabalho teve como objetivo caracterizar o padrão de expressão do receptor de vitamina D (VDR) e seu parceiro RXR, bem como das enzimas-chave envolvidas com a síntese (CYP27B1) e degradação (CYP24A1) do calcitriol na próstata, desde a fase adulta até a senescência. Por meio da utilização de um modelo animal que recapitula com fidelidade o processo de carcinogênese prostática com o avançar da idade em associação ao emprego combinatório de técnicas histológicas, de biologia molecular e análise de imagens, nós mostramos que a próstata é um órgão sensível ao calcitriol e capaz de metabolizá-lo localmente, uma vez que ambas enzimas e receptores avaliados estão altamente expressos no epitélio da glândula. Entretanto, à medida que os animais envelheceram, uma drástica redução no número de células positivas e na imunoreatividade para VDR, RXR e CYP27B1 foi detectada na próstata, ocorrendo restrita tanto a ácinos e ductos atróficos, hiperplásicos e metaplásicos, quanto naqueles acometidos por lesões pré-malignas e adenocarcinomas. Em contraste, a expressão de CYP24A1 aumentou com o avançar da idade e manteve-se acentuada inclusive nas áreas de alterações histopatológicas. Esse intricado desbalanço entre os níveis de CYP27B1 e CYP24A1 foram associados a uma biodisponibilidade reduzida de calcitriol na próstata senil, o que somado à redução da expressão de VDR e RXR, limita ainda mais a conhecida ação anti-proliferativa mediada pela sinalização da vitamina D nas células da próstata. Essa evidência foi corroborada pelo aumento da atividade proliferativa celular exatamente nas regiões em que a maquinaria de síntese e reposta ao calcitriol teve sua expressão inibida. Juntos, nossos resultados destacam um conjunto de modificação ao longo do envelhecimento com alto potencial de prejudicar os efeitos protetores mediados pela sinalização de vitamina D na próstata e assim favorecer o surgimento de alterações histopatológicas que pertubam a homeostase tecidual e podem inclusive progredir para tumores.

Palavras-chave: Próstata. Envelhecimento. Vitamina D. Rato Wistar.

ABSTRACT

A growing body of experimental and epidemiological evidence has addressed to the active metabolite of vitamin D, the 1α,25$(OH)_2$D or calcitriol, a protective role against the development and progression of prostate cancer, a proliferative disorder that affects 1 in every 6 men over 65 years old. However, little is known about the distribution and putative age-dependent variation of vitamin D signaling related components in the prostatic tissue. Therefore, the present study aimed to characterize the expression pattern of the vitamin D receptor (VDR) and its heterodimeric partner RXR, as well as the key enzymes involved with the synthesis (CYP27B1) and degradation (CYP24A1) of calcitriol in the prostate, from adulthood to senility. By using an animal model that faithfully recapitulates the carcinogenesis process taking place in the prostate with advancing age and the combinatory implement of histological techniques, molecular biology and image analyses, we showed that the prostate is sensitive to calcitriol and capable to metabolize it locally, since both target enzymes and receptors were expressed at high levels in the glandular epithelium. However, as the animals aged, a drastic reduction in the number of positive cells and immunoreactivity for VDR, RXR, and CYP27B1 was detected in the prostatic tissue, occurring restricted to ducts and acini exhibiting atrophies, hyperplasia and metaplasias, as well as to those affected by premalignant lesions and adenocarcinomas. On the other hand, the CYP24A1 expression significantly increased with advancing age and remained sharply even in those histopathological altered areas. This intricate imbalance between the levels of CYP27B1 and CYP24A1 was associated with a reduced bioavailability of calcitriol in the senile prostate, which in addition to decreased expression of VDR and RXR expression, further limits the classic anti-proliferative action mediated by vitamin D signaling in prostate cells. This evidence was corroborated by the increased proliferative activity at sites where the factors implicated with calcitriol synthesis and responsiveness had its expression inhibited. Taken together, our results highlight a set of modifications over the course of aging with a high potential to impair the protective effects of vitamin D signaling on the prostate, thereby favoring the arising of histopathological alterations that disturb tissue homeostasis and may even progress to cancer.

Keywords: Prostate. Aging. Vitamin D. Wistar rat.

LISTA DE ILUSTRAÇÕES

Página

Figura 1: Estrutura anatômica da próstata humana e de roedores 15

Figura 2: Histologia da próstata humana e de rato destacando sua composição celular epitelial 17

Figura 3: Estrutura química das vitaminas D_2 (ergocalciferol), D_3 (colecalciferol) e seus percursores 22

Figura 4: Fontes, metabolismo e mecanismo de ação da vitamina D, evidenciando as principais enzimas e órgãos envolvidos 27

Figura 5: Valores de referência da vitamina D de acordo com parâmetros internacionais e nacionais..... 30

Figura 6: Atividade do calcitriol nas células da próstata 33

Figura 7: Heterogeneidade da atividade transcricional dos genes VDR, RXRa, CYP27B1 e CYP24A1 em 494 tumores de próstata humana 125

LISTA DE ABREVIATURAS E SIGLAS

(Apresentadas em ordem alfabética)

1α,25(OH)$_2$D:	1α,25-diidroxivitamina D
25(OH)D:	25-hidroxivitamina D
7-DHC:	7-dihidrocolesterol
AMP:	Adenosina 3',5'-monofosfato
AP:	Próstata anterior
AR:	Receptor de andrógeno
ChrA:	Cromogranina A
CK5:	Citoqueratinas 5
CK8:	Citoqueratinas 8
CK14:	Citoqueratinas 14
CK18:	Citoqueratinas 18
CYP:	Citocromo P450
DAG:	Diacilglicerol
DNA:	Ácido desoxirribonucleico
DLP:	Próstata dorso-lateral
DP:	Próstata dorsal
HPB:	Hiperplasia prostática benigna
INCA:	Instituto Nacional do Câncer
IP3:	Inositol trifosfato

LP:	Próstata lateral
Nkx3.1	Proteína Homeobox Nkx-3.1
p63:	Proteína tumoral 63
PIN:	Neoplasia intraepitelial prostática
PSA:	Antígeno prostático específico
PTH:	Paratormônio
RNAm:	Ácido ribonucleico mensageiro
RXR:	Receptor retinoide X
RXRα:	Receptor retinoide X, isoformas α
SBEM:	Sociedade Brasileira de Endocrinologia Médica
SBPC:	Sociedade Brasileira de Patologia Clínica
Syn:	Sinaptofisina
UVB:	Raios solares ultravioleta B
VDR:	Receptor de vitamina D
VDRE:	Elementos responsivos à vitamina D
VP:	Próstata ventral

SUMÁRIO

I. **INTRODUÇÃO** 13

1. A próstata 13

1.1 *Características anatômicas e histológicas da próstata* 14

2. Vitamina D 21

2.1 *Fontes, metabolismo e mecanismo de ação da vitamina D* 22

2.2 *O sistema endócrino vitamina D e sua importância* 27

3. Relação entre vitamina D, próstata e envelhecimento 31

II. **OBJETIVOS** 38

1. Objetivo geral 38

2. Objetivos específicos 38

III. **ARTIGOS RESULTANTES** 40

1. Reduced vitamin D receptor (VDR) expression and plasma vitamin D levels are associated with aging-related prostate lesions 41

2. Altered expression of the vitamin D metabolizing enzymes CYP24A1 and CYP27B1 under the context of prostate aging and pathologies 57

3. Targeting Wistar rats as a model for studying benign, premalignant and malignant lesions of the prostate 99

IV. **DISCUSSÃO INTEGRA DOS RESULTADOS** 119

V. **CONCLUSÃO** 127

REFERÊNCIAS BIBLIOGRÁFICAS 128

I. INTRODUÇÃO

I. INTRODUÇÃO

1. A próstata

A próstata é uma das principais e maiores glândulas anexas ao sistema genital masculino de mamíferos. Situada na cavidade pélvica, logo inferior à bexiga urinária e circundando a uretra, a próstata é composta por numerosas unidades glandulares com atividade principalmente exócrina (Flint et al. 2015). Sua função central é produzir o líquido prostático, uma secreção leitosa e levemente alcalina (pH 7,3) que constitui aproximadamente 30% do plasma seminal (Fair & Cordonnier, 1978; Verze et al. 2016). A composição diversificada do líquido prostático, a qual abrange água, lípides, minerais como zinco, cálcio, magnésio e sódio, além de ácido cítrico e uma variedade de enzimas e outras moléculas, é importante para conferir, juntamente com a secreção das demais glândulas sexuais anexas, as condições necessárias à sobrevivência dos espermatozoides durante sua veiculação tanto pelas vias espermáticas do sistema genital masculino quanto pelo trato genital feminino (Aumüller, 1989; Kumar & Majumder, 1995). Além da função exócrina, as células parenquimais e/ou estromais da próstata expressam uma maquinaria enzimática capaz de metabolizar hormônios específicos, com destaque para a conversão de testosterona em dihidrotestostorena ou estradiol (Schiffer et al. 2018; Morais-Santos et al. 2018), os quais exercem seus efeitos localmente ou podem atingir a circulação sanguínea, adicionando assim, uma função endócrina à glândula.

Além de sua importância fisiológica, a próstata é também alvo de hiperplasia prostática benigna (HPB) e câncer, ambas doenças de alto impacto na saúde pública e que acometem homens, principalmente, com idade avançada (Lackzo et al. 2005; Begley

et al. 2008; Zhou et al. 2016). Em especial, o câncer de próstata ocupa a segunda posição no *ranking* de tumores que mais acometem homens no mundo inteiro (1.276.106 novos casos em 2018!), ficando atrás apenas do câncer de pulmão, sendo também um dos líderes mundiais de mortalidade associada a doenças malignas (Bray et al. 2018). No Brasil, estima-se cerca de 65.840 novos casos de câncer de próstata para 2020, número bastante similar àquele esperado para o câncer de mama em mulheres (66.280 novos casos) no mesmo período (INCA, 2020). Dessa forma, a próstata tem sido um dos órgãos genitais mais estudados na atualidade, havendo uma busca eminente por novos alvos com funções preventivas e/ou terapêuticas, assim como por modelos experimentais capazes de recapitular as mudanças histopatológicas que acometem a glândula.

1.1 Características anatômicas e histológicas da próstata

A próstata consiste em um sistema de ductos túbulo-alveolares circundados por um estroma de sustentação. Diferenças na disposição do tecido prostático existem entre os mamíferos, podendo ocorrer na forma de lobos, como observado em roedores (Hayashi et al. 1991; Risbridger & Taylor, 2006), ou como formações concêntricas ao redor da uretra, como observado em primatas (McNeal, 1988).

Em humanos, a próstata é um órgão ímpar que pode ser anatomicamente dividido em três regiões glandulares (zona central, zona de transição e zona periférica) e uma região constituída apenas por tecido fibromuscular, denominada zona anterior (Figura 1A). Vale ressaltar que as regiões glandulares da próstata humana possuem significâncias patológicas distintas. Nesse sentido, a zona de transição, localizada em torno da porção proximal da uretra prostática, é a região de maior incidência de HPB,

enquanto que a zona central, a qual situa-se circundando os ductos ejaculatórios, é raramente acometida por patologias. Já a zona periférica envolve as demais zonas glandulares, sendo este o local mais suscetível ao desenvolvimento de prostatites e tumores prostáticos (McNeal, 1981; Shappell et al. 2004; Risbridger & Taylor, 2006). Além disso, diferenças volumétricas entre as regiões glandulares existem, sendo que na próstata de um indivíduo adulto e sadio, a zona de transição corresponde cerca de 10% do tecido glandular, seguido da zona central (20-25%) e da zona periférica (70%).

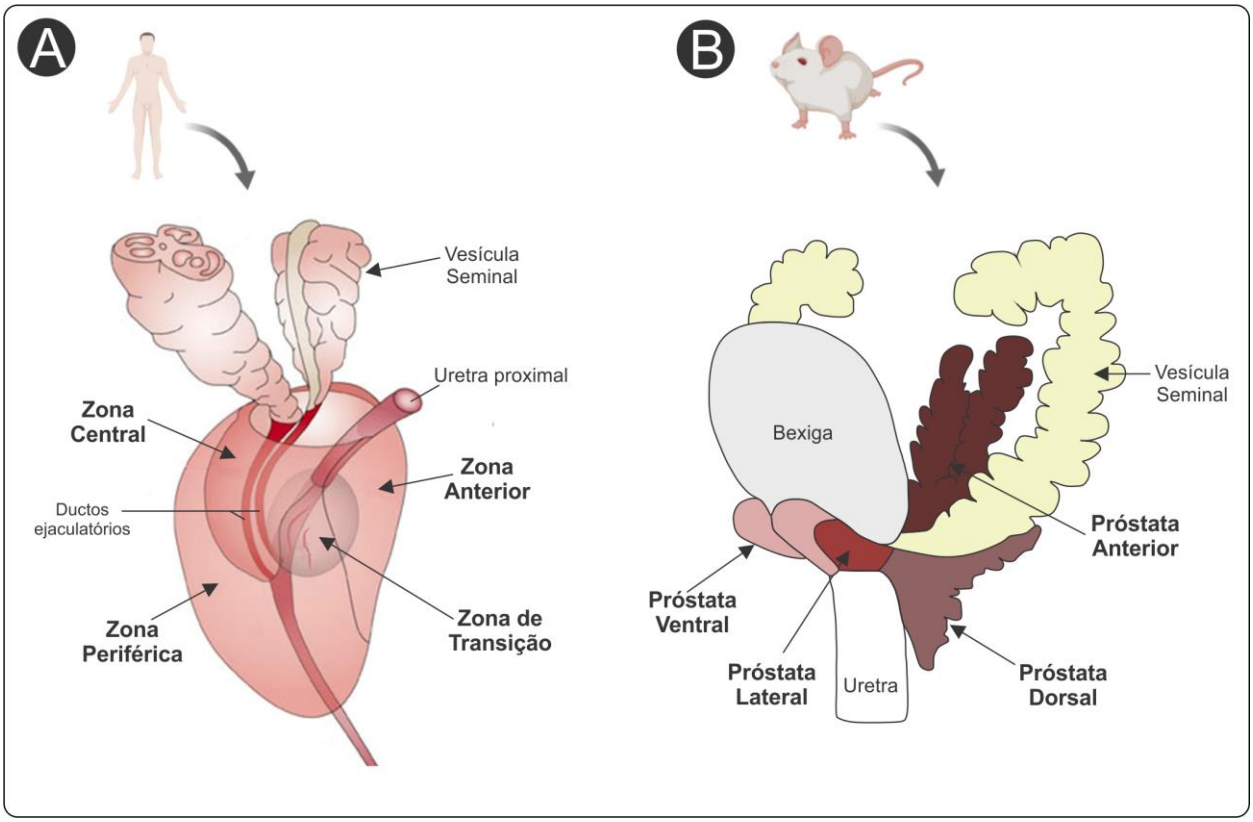

Figura 1 | Estrutura anatômica da próstata humana e de roedores. (A) Em humanos, o tecido prostático se dispõe em zonas concêntrica em torno da uretra. (B) Em roedores, a próstata é subdividida em quatro pares de lobos denominados de acordo com sua posição em relação à uretra**.** Adaptado de Sugimura et al. (1986) e Wadhera (2013).

Em roedores, a próstata pode ser anatomicamente dividida em pares de lobos classificados de acordo com sua disposição em relação à uretra, sendo eles: próstata

ventral (VP), próstata lateral (LP), próstata dorsal (DP) e próstata anterior (AP) (Figura 1B). O conjunto dos lobos da próstata é usualmente referido como complexo prostático. Essa organização lobar tem sido observada tanto em roedores silvestres quanto naqueles rotineiramente utilizados em laboratórios (Sugimura et al. 1986; Hayashi et al. 1991; Gonçalves et al. 2013; Chaves et al. 2015). Vale ressaltar que a VP é um dos principais lobos estudados, por estar localizada inferior à bexiga urinária e sendo de fácil acesso, além de abranger cerca da metade da massa de todo o complexo prostático. Além disso, este é um dos principais lobos dependentes de andrógenos (Banerjee et al. 2000; Desai et al. 2004). Já a LP, compreende cerca de 14% do complexo prostático e localiza-se ladeando a VP e se apoiando caudalmente à DP. Devido a sua intricada associação com a DP, a qual se dispõe inferoposterior à vesícula seminal e também compreende cerca de 14% da massa do complexo prostático (Hayashi et al. 1991), muitos estudos consideram ambas DP e LP como sendo um único par de lobos, denominado próstata dorso-lateral (DLP). Por fim, a AP (também conhecida como glândula de coagulação) abrange cerca de 25% do complexo prostático e localiza-se adjacente à face côncava da vesícula seminal (Hayashi et al. 1991). Embora alguns estudos têm demonstrado a existência de um acometimento lobo-específico por alterações benignas e malignas induzidas quimicamente ou geneticamente, bem como por aquelas que surgem espontaneamente ao longo do envelhecimento (Banerjee et al. 1998; Gingrich et al. 1999; Morais-Santos et al. 2018; Ozten et al. 2019), ainda é prematuro assumir que um determinado lobo prostático seja mais relevante que outro na compreensão da fisiopatologia prostática. Enquanto isso, roedores têm sido amplamente utilizados como valiosos modelos experimentais no estudo de prostatites, hiperplasia e

câncer de próstata, e se faz importante adotar uma estratégia que aborde o complexo prostático como um todo.

Apesar das diferenças anátomo-histológicas existentes, a próstata humana e de roedores possui estrutura histológica parenquimatosa similar (Ittmann, 2018). Nesse sentido, o epitélio geralmente prismático que reveste os ácinos e ductos prostáticos é basicamente composto por três tipos celulares fenotipicamente e funcionalmente distintos, sendo eles: células luminais, células basais e células neuroendócrinas (Figura 2).

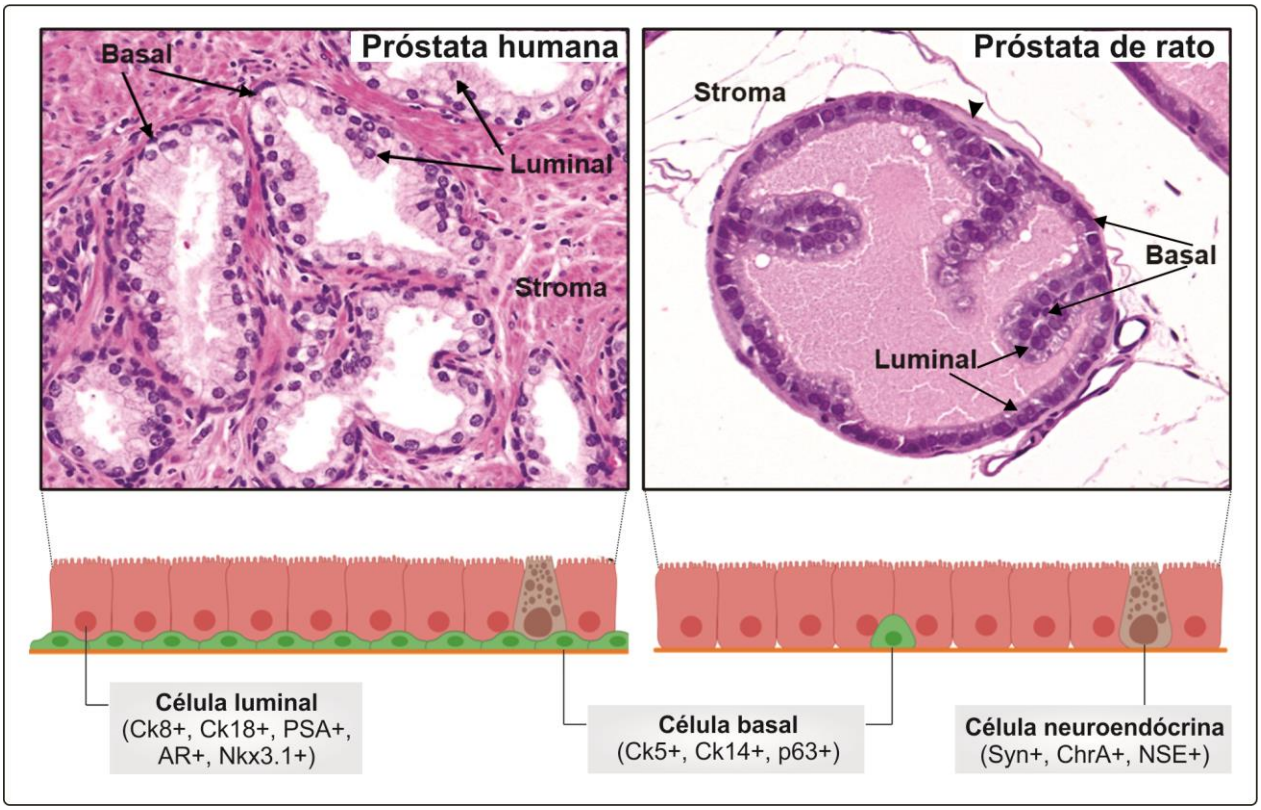

Figura 2 | Histologia da próstata humana e de rato destacando sua composição celular epitelial. Cada tipo celular presente no epitélio expressa marcadores específicos que permitem sua distinção das demais células. Cabeça de seta: indica musculatura lisa que na próstata de roedores está organizada em camadas celulares circundando os ácinos e ductos glandulares. Fonte: autoria própria.

As células luminais ou secretoras constituem o tipo celular mais numeroso do epitélio e são responsáveis por produzir o líquido prostático. São rotineiramente distinguidas das demais células epiteliais por serem altas, possuírem núcleo arredondado e por expressarem marcadores clássicos como as citoqueratinas 8 e 18 (CK8/18, Figura 2). Condizendo com sua função secretora, essas células apresentam retículo endoplasmático rugoso abundante e complexo de Golgi bem desenvolvido, além de inúmeros grânulos de secreções no citoplasma apical (Hayward et al. 1996a; El-Alfy et al. 2000; Risbridger & Taylor, 2006). A detecção de níveis séricos elevados do antígeno prostático específico (PSA), uma protease principalmente produzida pelas células luminais, constitui uma importante ferramenta aliada ao diagnóstico do câncer de próstata e acompanhamento da doença (Lilja et al. 2008).

As células basais possuem morfologia característica, sendo células relativamente pequenas e de formato irregular, com citoplasma escasso e núcleo heterocromático e geralmente semicircular (El-Alfy et al. 2000). Apesar de se localizarem apoiadas à membrana basal, sabe-se que tanto as células basais da próstata como àquelas de outros epitélios (ex: vias aéreas e epidídimo) não estão restritas à base dos epitélios. Essas células geralmente emitem longas projeções citoplasmáticas capazes de ultrapassar as junções de oclusão existentes entre as células epiteliais e assim, atingirem o lúmen (Shum et al. 2008; Roy et al. 2016). As células basais prostáticas, interessantemente, constituem uma população heterogênea, que expressa diferentes combinações de marcadores (ex: p63, citoqueratinas 5 e 14), e acredita-se que dentre elas estão as células-tronco, multipotentes e auto-renováveis, as quais podem diferenciar em células luminais, neuroendócrinas e basais (Wang et al. 2013; Lee et al. 2014). A

capacidade tronco das células basais, a qual é corroborada pela sua assinatura gênica (Zhang et al. 2016), é alvo de intensas investigações que colocam essa população celular, apesar de algumas controvérsias (Wang et al. 2014), como sendo a principal provedora das células que sofrem transformação oncogênica e iniciam a formação do tumor prostático (Taylor et al. 2012; Stoyanova et al. 2013; Park et al. 2016). Tal transformação ocorre ao passo que a maioria das lesões malignas não apresenta positividade para os marcadores clássicos de células basais, ausência esta que tem sido utilizada como um dos critérios diagnósticos em biopsias prostáticas. De maneira oposta, as células basais também exercem papeis cruciais na homeostase do órgão, sendo componentes indispensáveis no desenvolvimento, além de auxiliar na correta diferenciação, funcionamento e manutenção da sobrevivência de suas vizinhas, as células luminais e neuroendócrinas (Signoretti et al. 2000; Kurita et al. 2004). Desse modo, é evidente que as células basais podem ter diferentes contribuições estruturais e funcionais para próstatas normais ou cancerosas. Vale ressaltar que diferenças quanto à proporção de células basais/células luminais são observadas entre espécies, sendo: 1/1 em humanos, 1/4 em camundongo, 1/7 em cachorro e macaco, e 1/10 em rato (El-Alfy et al. 2000).

As células neuroendócrinas compõem o terceiro tipo epitelial da próstata (Figura 3). Além de corresponderem a população menos observada no epitélio prostático, essas células são dificilmente identificadas através de colorações histológicas de rotina (Ittmann, 2018). Sabe-se que a frequência de células neuroendócrinas é maior durante o desenvolvimento prostático e acredita-se que elas possam exercer ações regulatórias sobre o crescimento e atividade secretora da glândula. Além disso, as células

neuroendócrinas estão envolvidas com a secreção do neuropeptídeo Y, serotonina, cromograninas A e B, calcitonina e somatostatina (Abrahamsson, 1999; Rodriguez et al. 2003; Risbridger & Taylor, 2006), os quais podem ser utilizados como marcadores específicos dessa população celular. Apesar das informações existentes, pouco se sabe sobre a ontogenia e função das células neuroendócrinas do epitélio prostático.

Por fim, o epitélio da próstata é circundado por um estroma de sustentação onde se encontram células e fibras do tecido conjuntivo, nervos, vasos sanguíneos e linfáticos, além de células musculares lisas que se contraem espasmodicamente e promovem a ejeção do líquido prostático no lume da uretra, durante a ejaculação (Hayward et al. 1996b). Na próstata de roedores, essa musculatura lisa organiza-se em camadas celulares circundando os ductos e ácinos glandulares, divergindo do observado em humanos, onde a musculatura lisa é mais abundante e está amplamente distribuída por todo o estroma (Figura 2) (Aumüller, 1979; Hayward et al. 1996b; McNeal, 1988).

Vale ressaltar que o desenvolvimento, diferenciação e morfofisiologia, tanto das células epiteliais quanto das células presentes no estroma da próstata, dependem dos níveis de andrógenos, sendo a dihidrotestosterona o principal esteroide androgênico atuante no local (Grossmann et al. 2001; Tan et al. 2015). Entretanto, a regulação da próstata é complexa e envolve a participação de outros esteroides e seus receptores, tais como estrógenos e vitamina D, os quais também têm sido referenciados como importantes hormônios para a manutenção da morfofisiologia glandular (Prins & Korach, 2008; Swami et al. 2011). Nesse cenário, as funções dos estrógenos no tecido prostático já são melhor estabelecidas (Risbridger et al. 2007; Cooke et al. 2017), enquanto que o

papel da sinalização da vitamina D no local ainda não é totalmente conhecido, sendo este o hormônio alvo do presente estudo.

2. Vitamina D

Vitamina D é um termo originalmente designado para referir-se ao ergocalciferol (vitamina D_2, origem vegetal) e colecalciferol (vitamina D_3, origem animal), os quais são hormônios secosteroides erroneamente referidos como vitaminas e oriundos da conversão fotolítica do ergosterol e 7-deidrocolesterol (7-DHC), respectivamente (Figura 3). Estima-se que os primeiros seres vivos a produzirem vitamina D residiam no fitoplâncton e zooplâncton marinho a cerca de 1 bilhão de anos atrás (Holick, 2009). Hoje em dia se sabe que as mais diversas formas de vida da Terra produzem vitamina D mediante exposição direta à luz solar. Apesar da função da vitamina D ser incerta nas plantas e formas de vida inferiores, sabe-se que a produção da vitamina D e seu posterior catabolismo em compostos metabolicamente ativos foi um processo criticamente importante para garantir aos vertebrados terrestres uma quantidade de cálcio suficiente para a manutenção de atividades celulares e a correta mineralização de seus esqueletos (Holick, 1989). Atualmente, além de ser reconhecida pelo seu papel central na homeostase de cálcio e mineralização óssea (DeLuca, 2004), diversas funções têm sido atribuídas à vitamina D e incluem ações anti-inflamatórias e anti-neoplásicas (Feldman et al. 2014; Wang et al. 2017), as quais serão exploradas mais adiante.

Vale ressaltar que o termo vitamina D também tem sido utilizado para se referir ao grupo de moléculas derivadas da vitamina D e abrange tanto o metabólito ativo 1α,25-diidroxivitamina D [$1\alpha,25(OH)_2D$] ou calcitriol quanto seu percursor 25-hidroxivitamina D

[25(OH)D] ou calcidiol (Bikle, 2014). Para um melhor entendimento, no presente trabalho a vitamina D e seus metabólitos foram considerados separadamente. Adicionalmente, uma maior atenção foi dada à vitamina D_3 por se tratar da principal forma presente nos animais.

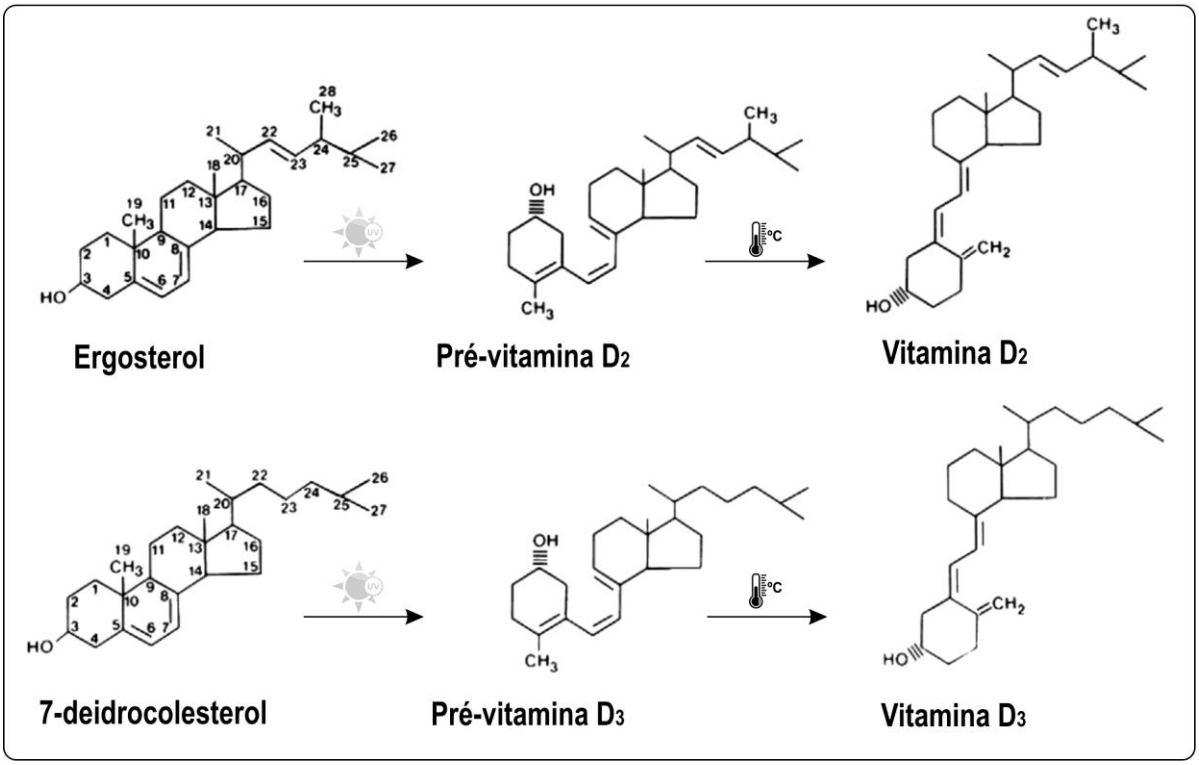

Figura 3 | Estrutura química das vitaminas D_2 (ergocalciferol), D_3 (colecalciferol) e seus percursores. Note que a vitamina D_2 difere da D_3 por apresentar uma ligação dupla entre os carbonos 22 e 23, além de um grupo metil no carbono 24. Fonte: autoria própria.

2.1 Fontes, metabolismo e mecanismo de ação da vitamina D

Grande parte dos alimentos naturais são isentos ou possuem pouca quantidade de vitamina D. Uma exceção são os cogumelos comestíveis (ex: Paris, shitake ou shimeji) que provêm variadas quantidades de vitamina D_2, assim como a carne e óleo de fígado de alguns peixes como bacalhau, sardinha e salmão, ricos em vitamina D_3 (Holick et al. 2004). Na tentativa de contornar a baixa disponibilidade desse composto na dieta comum,

vários alimentos industrializados foram enriquecidos com vitamina D e incluem pães, sucos, leite e seus derivados. Entretanto, a quantidade de vitamina D geralmente adicionada aos alimentos (100 UI/porção), apesar de ajudar a prevenir o raquitismo em crianças, está muito aquém dos valores de ingestão diária preconizado para crianças (400 – 1.000 UI) e adultos (1.000 – 2.000 UI) (Holick, 2009). Portanto, cerca de 80 – 90% da vitamina D necessária para manter a adequada função do organismo é resultante da síntese endógena após exposição direta à luz solar e ocorre principalmente na forma de vitamina D_3 (Holick, 2004).

Como mencionado previamente, a vitamina D_3 deriva da conversão fotolítica do 7-DHC, um processo não enzimático e termo-sensível que ocorre na pele sob influência dos raios ultravioleta B provenientes do sol (UVB, Holick, 2004). A exposição direta aos raios UVB (máxima eficiência em 290 a 320 nm) desencadeia a quebra do anel B do ciclo pentanoperidrofenantreno do 7-DHC, presente principalmente nas células da epiderme, formando assim a molécula secosteroide denominada pré-vitamina D_3. Essa nova substância logo sofre isomerização devido ao aumento da temperatura local e resulta em uma molécula cuja configuração espacial é mais estável, a vitamina D_3 (Figura 3). Portanto, o tempo de exposição à luz solar assim como a área do corpo exposta são fatores diretamente relacionados ao aporte de vitamina D produzido.

É importante ressaltar que tanto a vitamina D_3 quanto a D_2 são biologicamente inativas. Portanto, para que a sinalização de vitamina D ocorra nas células-alvo, a vitamina D produzida na pele ou aquela adquirida através da dieta é subsequentemente metabolizada por enzimas da superfamília do citocromo P450, as quais adicionam grupos hidroxilas à estrutura da molécula. Tal processo de metabolismo para ativação da

vitamina D ocorre em duas etapas principais conforme descrito a seguir, e culmina na síntese de seu metabólito ativo conhecido como 1α,25(OH)$_2$D ou calcitriol.

Na primeira etapa do metabolismo da vitamina D, a qual ocorre principalmente no fígado, um grupo hidroxila é adicionado ao carbono 25 da molécula, dando origem ao 25(OH)D ou calcidiol. Este primeiro metabólito é considerado a principal forma circulante da vitamina D e tem sido utilizado com sucesso na avaliação do *status* de vitamina D no organismo, por apresentar tempo de vida (~2 semanas) superior ao seu precursor inativo (Vitamina D$_2$ e D$_3$, ~1 dia) e ao calcitriol (~4 horas) (Holick, 2004). Várias enzimas com atividade 25-hidroxilase já foram identificadas em mamíferos, e compreendem as enzimas CYP27A1, CYP3A4, CYP2C11, CYP2D25, CYP2J2, CYP2J3 e CYP2R1 (Hayashi et al. 1986; Hosseinpour & Wikvall, 2000; Sawada et al. 2000; Cheng et al. 2003; Yamasaki et al. 2004; Gupta et al. 2004). Entretanto, estudos utilizando ensaios de gene repórter, modelos *knockouts*, análises mutacionais de regiões codificantes e atividade enzimática, demonstraram que a CYP2R1 é a principal 25-hidroxilase envolvida na produção do 25(OH)D (Cheng et al. 2003; 2004; Shinkyo et al. 2004; Zhu et al. 2013). Não coincidentemente, altos níveis de CYP2R1 são encontrados no parênquima hepático (Barchetta et al. 2012).

Em seguida, o 25(OH)D é hidroxilado na posição C-1α pela enzima CYP27B1, originando assim, o calcitriol. Diferentemente do observado para seu percursor 25(OH)D, apenas uma enzima está envolvida na etapa final de síntese do calcitriol. É nos túbulos proximais dos rins, os quais apresentam elevada expressão da 1α-hidroxilase CYP27B1, que ocorre a principal produção de calcitriol. Vale ressaltar que a conversão renal de 25(OH)D em calcitriol é estimulada pela ação do paratormônio (PTH) e inibida pela

elevação dos níveis do fator de crescimento fibroblástico 23 (FGF-23) e do próprio calcitriol (Gao et al. 2002; Bikle, 2014). No entanto, RNAm e/ou proteína CYP27B1 tem sido detectados em uma variedade de tecidos, tais como placenta, pele, pulmão, cérebro, intestino, tireoide, pâncreas, glândulas mamárias, testículo e até mesmo próstata, evidenciando a possibilidade de produção extra-renal de calcitriol (Jones et al. 1999; Hsu et al. 2001; Zehnder et al. 2001; Segersten et al. 2002; 2005; Bikle, 2009). Fora dos rins, é provável que a expressão e atividade 1α-hidroxilase da CYP27B1 sejam influenciadas por citocinas e fatores locais específicos (Flanagan et al. 2003; Bikle, 2009; 2014; Kagi et al. 2018). Ainda, o calcitriol, e em menor proporção a 25(OH)D, podem ser reduzidos a compostos menos ativos pela CYP24A1, uma enzima importante para o controle dos níveis locais e magnitude de ação dos metabólitos da vitamina D, e cuja expressão e atividade é estimulada pelo próprio calcitriol (Zierold et al. 2003; Bikle, 2014).

Nas células-alvo, o calcitriol exerce seus efeitos hormonais através da ligação ao receptor de vitamina D (VDR), um fator de transcrição pertencente à superfamília dos receptores nucleares (Mangelsdorf et al. 1995). A ligação do calcitriol ao VDR desencadeia uma modificação na conformação do receptor, permitindo a sua heterodimerização com uma das três isoformas (α, β, γ) do receptor retinoide X (RXR). Posteriormente, este complexo ligante-VDR/RXR acopla-se em regiões específicas do DNA conhecidas como elementos responsivos à vitamina D (VDRE) e modulam a transcrição de vários genes (Haussler et al. 1997). Alvos clássicos dessa modulação incluem genes que codificam proteínas envolvidas no transporte transepitelial de cálcio, tais como TRPV5, TRPV6, PMCA, NCX1 e Calbindina-D28K (Fleet et al. 2002; Okano et al. 2004; Hoenderop et al. 2005). Tamanha importância é atribuída à sinalização da

vitamina D para manutenção da calcemia que cerca de 80% a 90% de todo o cálcio absorvido da dieta depende da ação do calcitriol no epitélio intestinal (Holick, 2006). No entanto, a regulação transcricional mediada pelo heterodímero VDR-RXR é mais ampla e abrange genes envolvidos em diversas funções fisiológicas, o que vai de encontro com a detecção de milhares de VDRE distribuídos ao longo do genoma humano (Pike et al. 2016). Ainda, o calcitriol pode agir de uma maneira mais rápida por meio da via não-genômica, a qual envolve a participação de receptores VDR localizados em cavéolas na membrana plasmática e ativação de mediadores intermediários como IP_3, DAG, AMP cíclico, fosfolipase C, entre outros (Huhtakangas et al. 2004; Nemere et al. 2004). Portanto, além de ser uma peça-chave na homeostase de cálcio, a sinalização da vitamina D também está envolvida em diversos processos fisiológicos e incluem a síntese e secreção de hormônios (ex: PTH e a insulina), modulação do sistema imune e do desenvolvimento cerebral, controle da pressão arterial e função cardíaca, além de regular os processos de diferenciação e proliferação celular em uma gama de tipos celulares (Bourlon et al. 1997; Li et al. 2002; van Etten & Mathieu, 2005; Liu et al. 2006; Marini et al. 2010; Feldman et al. 2014; Wang et al. 2017). As fontes de vitamina D, assim como seu metabolismo e mecanismo de ação, podem ser visualizados na figura 4.

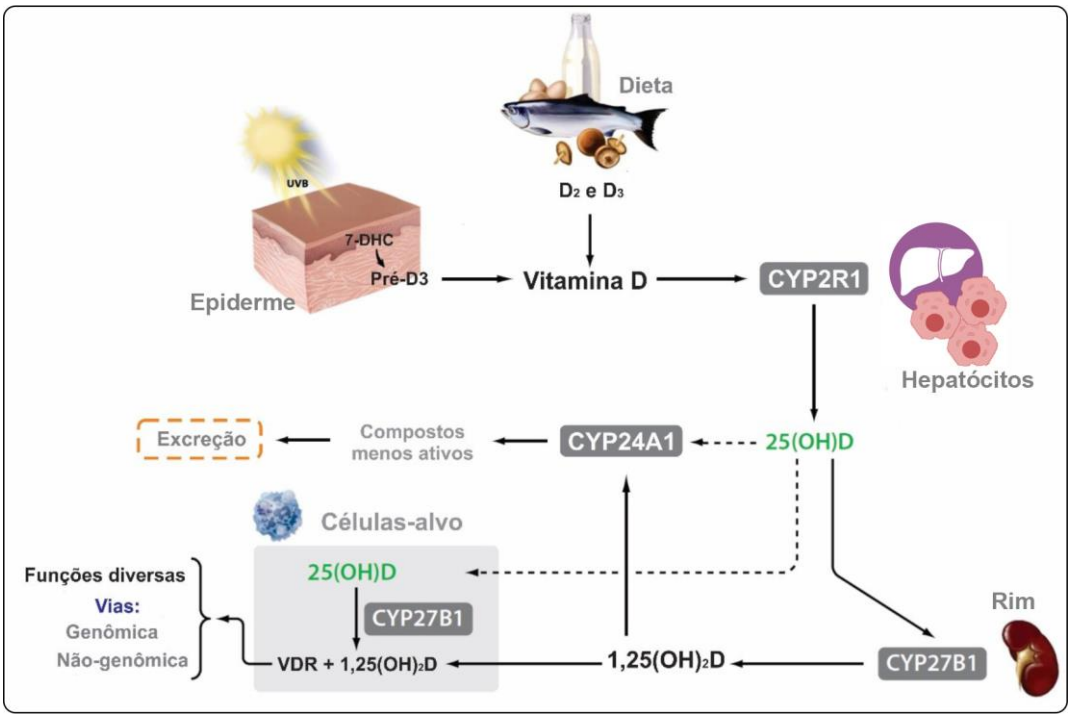

Figura 4 | Fontes, metabolismo e mecanismo de ação da vitamina D, evidenciando as principais enzimas e órgãos envolvidos. Adaptado de Krishnan & Feldman, 2011.

2.2 O sistema endócrino vitamina D e sua importância

A vitamina D e seus metabólitos, assim como as enzimas participantes de seu metabolismo e o receptor VDR, compõem um fascinante eixo hormonal, conhecido como sistema endócrino vitamina D. Com base nas multifunções mediadas pelo calcitriol, tem sido atribuído à esse sistema um papel central na regulação da homeostase corporal, cujo funcionamento apropriado é indispensável ao longo de toda a vida para a prevenção de várias doenças, incluindo aquelas que afetam o sistema endócrino, digestivo, cardiovascular, nervoso, genital e ósseo (Hypponen et al. 2001; Raman et al. 2011; Danik & Manson, 2012; Blomberg Jensen, 2014; Wang et al. 2017; Mokry et al. 2016). Para exemplificar tamanha importância, a simples exposição de pacientes à luz solar (10 - 15 minutos por dia), juntamente ou não com o consumo de alimentos ricos em ou

enriquecidos com vitamina D, foi uma medida essencial para erradicar o raquitismo em vários países, uma doença óssea altamente prevalente em crianças do mundo todo nos séculos XVII a XIX (Holick, 2009). Outro exemplo vem de um importante estudo conduzido na Finlândia, onde a suplementação diária com 2.000 UI de vitamina D, durante o primeiro ano de vida, foi capaz de reduzir em até 80% o risco de desenvolvimento de diabetes tipo I na fase adulta (Hyppönen et al. 2001). Mais atualmente, grande debate envolvendo vitamina D e prevenção de câncer surgiu na comunidade científica (Feldman et al. 2014), sendo que há evidências demonstrando que tanto homens quanto mulheres com baixos níveis de 25(OH)D e, consequentemente, baixa produção de calcitriol e ativação do sistema endócrino vitamina D, são em média 20% mais propensos a desenvolverem câncer de qualquer natureza (Budhathoki et al. 2018).

No entanto, essa proteção múltipla atribuída ao sistema endócrino vitamina D está ameaçada pela deficiência de vitamina D, uma pandemia reemergente que atualmente afeta mais de 1 bilhão de pessoas, independentemente da idade, raça, situação econômica e região geográfica (Holick, 2017). Apesar de fatores adicionais como dieta, grau de pigmentação da pele, faixa etária e o ângulo de incidência dos raios solares na Terra influenciarem os níveis de vitamina D (Holick et al. 1980; MacLaughlin & Holick, 1985; Webb et al. 1989), o principal fator atrelado a essa deficiência é a baixa exposição à luz solar. Não concidentemente, a deficiência de vitamina D ressurge em um cenário em que o uso de protetores solar e a falta de apreciação direta da luz solar constituem a principal medida preventiva contra o câncer de pele. Não há questionamentos quanto a relação entre exposição excessiva e crônica à radiação solar e o risco elevado de

desenvolvimento de danos na pele, incluindo carcinomas cutâneos (Housman et al. 2003). Entretanto, não há também evidências indicando que a exposição limitada ao sol (10 a 15 minutos), para satisfazer a necessidade de vitamina D diária, possa substancialmente aumentar o risco de câncer de pele. Enquanto isso, a comunidade científica alerta que cerca de 40% a 60% da população mundial carece de vitamina D, e por isso, está sob risco elevado de contrair enfermidades diversas (Holick, 2017; 2018).

Uma dessas enfermidades e que está atualmente impactando a saúde global é a COVID-19, uma pandemia causada pelo novo coronavirus Sars-CoV-2. Ainda que substancial, há evidências epidemiológicas sugerindo que indivíduos deficientes de vitamina D possuem maior chance de contrair a COVID-19 e até mesmo de progredirem para o pior quadro clínico da doença (Grant et al. 2020; Alipio, 2020). Relação similar também tem sido observada para outras infecções virais como dengue, hepatites, herpes e influenza (Grant et al. 2020). Tal relação é sustentada pela conhecida atuação do sistema endócrino vitamina D na modulação do sistema imune, a qual envolve basicamente dois mecanismos: (i) melhora das barreiras físicas célula-célula, estimulando a expressão de proteínas das junções de oclusão, adesão e comunicantes; e (ii) potencialização da imunidade inata e adquirida, por meio da indução de peptídeos antimicrobianos (ex: catelicidina, defensinas e IL-37) e regulação dos níveis de citocinas pró- e anti-inflamatórias (Rondanelli et al. 2018). Portanto, no atual cenário, a suplementação diária com vitamina D emerge como uma alternativa para fortalecer os sistemas fisiológicos e assim evitar o desenvolvimento de doenças, inclusive aquelas de caráter infeccioso (Grant et al. 2020; Ebadi & Montano-Loza, 2020).

É importante ressaltar que a definição do *status* de vitamina D (Figura 5), a qual leva em consideração os níveis circulantes de 25(OH)D, pode variar de acordo com a entidade especializada no assunto (Figura 5). De modo geral, pessoas apresentando níveis de 25(OH)D abaixo de 20 ng/mL de sangue são classificadas como deficientes no mundo todo. Entretanto, em 2018, a Sociedade Brasileira de Patologia Clínica (SBPC) juntamente com a Sociedade Brasileira de Endocrinologia Médica (SBEM) se distanciaram dos parâmetros mundiais por definirem a deficiência de vitamina D no Brasil como níveis de 25(OH)D $\leq$ 10ng/ml, valor este considerado como deficiência severa pelas demais agências mundiais especializadas no assunto. Essa situação definida pelas SBPC e SBEM, transferem a grande parcela da população brasileira que atualmente se encontra deficiente pelo padrão mundial para o *status* de insuficiente, fato este que afetam as estratégias utilizadas para elevar os níveis de vitamina D.

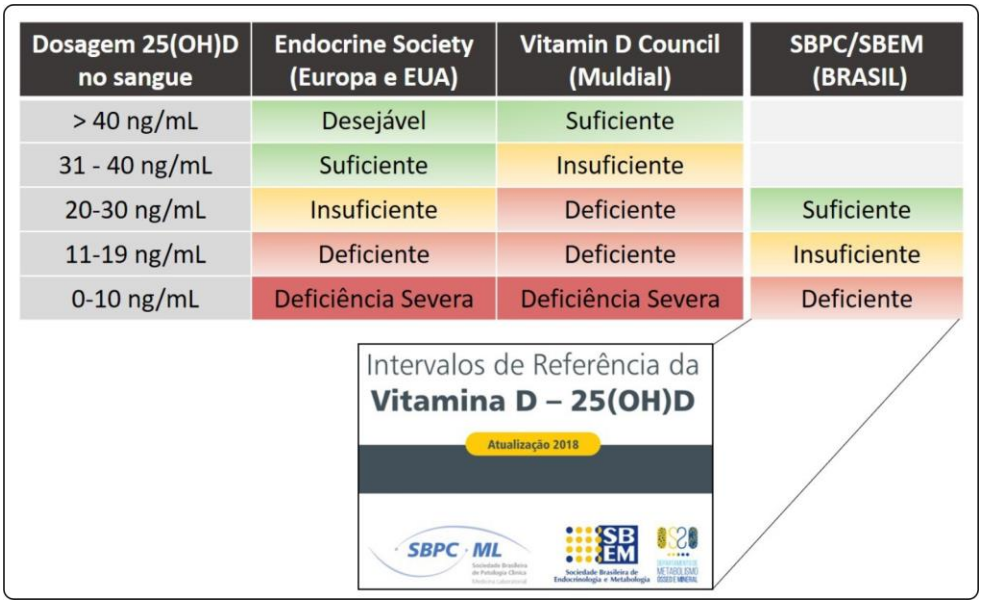

Dosagem 25(OH)D no sangue	Endocrine Society (Europa e EUA)	Vitamin D Council (Muldial)	SBPC/SBEM (BRASIL)
> 40 ng/mL	Desejável	Suficiente	
31 - 40 ng/mL	Suficiente	Insuficiente	
20-30 ng/mL	Insuficiente	Deficiente	Suficiente
11-19 ng/mL	Deficiente	Deficiente	Insuficiente
0-10 ng/mL	Deficiência Severa	Deficiência Severa	Deficiente

Figura 5: Valores de referência da vitamina D de acordo com parâmetros internacionais e nacionais. Note que as definições de suficiência, insuficiência e deficiência de vitamina D variam dependendo da organização especializada no assunto. Fonte: autoria própria.

3. Relação entre vitamina D, próstata e envelhecimento

Desde a década de 80, estudos já apontavam que a deficiência de vitamina D em ratos machos ou fêmeas levava a uma redução significativa das taxas de fertilidade (Halloran & DeLuca, 1980; Kwiecinski et al. 1989). Atualmente, a atuação da vitamina D na atividade reprodutiva já é mais clara e, mais especificamente nos machos, o calcitriol tem sido indicado como um importante hormônio participante da manutenção da função testicular e das glândulas sexuais anexas, além de estar envolvido na regulação da biossíntese de estrógenos (Johnson et al. 1996; Kinuta et al. 2000; Blomberg Jensen, 2014). Tal participação só é permitida pela presença do receptor VDR, o qual medeia os efeitos hormonais do metabólito ativo da vitamina D e está presente nos órgãos que compõem o sistema genital masculino, inclusive na próstata (Johnson et al. 1996; Kivineva et al. 1998; Blomberg Jensen et al. 2010). Além da presença do VDR, interessantemente, a expressão de enzimas participantes do metabolismo da vitamina D já foi demonstrada na próstata humana e de roedores, em especial as enzimas CYP27B1 e CYP24A1 (Blomberg Jensen et al. 2010; Giangreco et al. 2015). Essas evidências sugerem que a próstata seja capaz de produzir e inativar o calcitriol localmente, reforçando a participação desse sistema hormonal na regulação da glândula.

Diversos estudos epidemiológicos têm apontado a vitamina D como um importante fator preventivo na ocorrência e progressão das doenças prostáticas, especialmente se tratando do câncer de próstata, baseando-se no fato de que a incidência desse tumor é maior com o avançar da idade, em indivíduos que residem em regiões de altas latitudes e também em homens negros, todos estes considerados grupos propícios a apresentarem deficiência de vitamina D (John et al. 2005; Trump et al. 2010; van der

Rhee et al. 2012; Xie et al. 2017). De fato, evidências experimentais demonstraram que os efeitos anti-tumorais atribuídos à sinalização da vitamina D no tecido prostático estão associados a modulação da transcrição de vários genes (alguns representados na figura 6) e resultam em parada do crescimento celular, promoção de diferenciação celular e apoptose, bem como supressão da angiogênese, inflamação e metástase (Hsu et al. 2001; Chen & Holick, 2003; Krishnan & Feldman 2011; Swami et al. 2011). Entretanto, vale ressaltar que alguns estudos também encontraram pouca ou nenhuma associação entre os níveis de vitamina D e a incidência ou progressão do tumor prostático (Park et al. 2010; Holt et al. 2013; Wong et al. 2014). Além disso, efeitos anti-tumorais limitados contra o câncer de próstata foram obtidos por ensaios clínicos de fase I e II utilizando a vitamina D_3 ou o calcitriol como agente terapêutico (Beer et al. 2004; Flaig et al. 2006; Marshall et al. 2012). Esses dados conflitantes podem estar associados a uma expressão diferencial dos componentes do sistema endócrino vitamina D, uma vez que evidencias *in vitro* mostraram que a ação anti-tumoral observada em células de câncer de próstata após a administração de vitamina D dependem positivamente da expressão de CYP27B1 e VDR, e inversamente dos níveis e atividade da CYP24A1 (Skowronski et al. 1993; Hsu et al. 2001; Tannour-Louet et al. 2014).

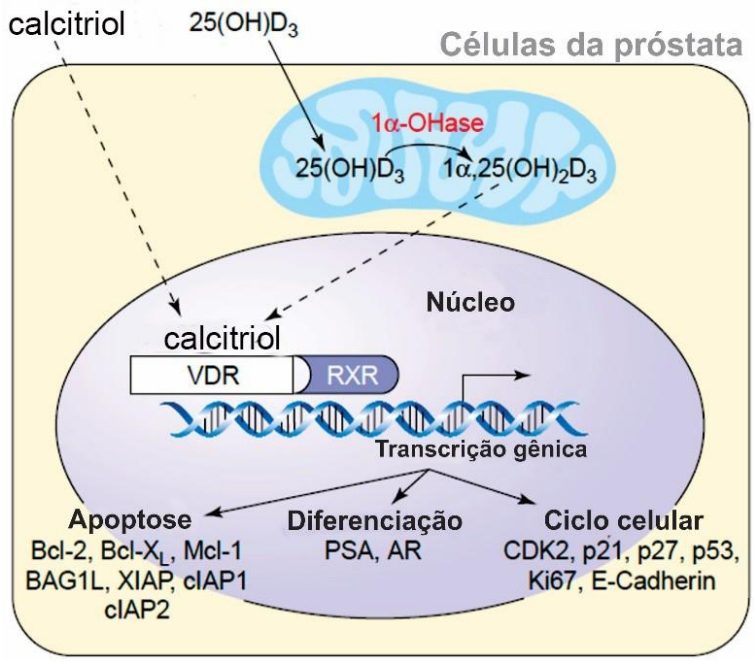

Figura 6 | Atividade do calcitriol nas células da próstata. A sinalização da vitamina D, mediada pelo complexo calcitriol-VDR/RXR, desempenha papéis protetores no tecido prostático através da regulação transcricional de vários genes envolvidos com processos importantes. Adaptado de Chen & Holick, 2003.

Embora seja bem conhecido que a idade é o principal fator de risco para HPB e câncer de próstata (Leitzmann & Rohrmann, 2012; Lim, 2017), e que os níveis de vitamina D reduzem significativamente durante o envelhecimento (MacLaughlin & Holick, 1985), pouco se sabe sobre a variação idade-dependente de componentes do sistema endócrino vitamina D na próstata. Até o momento, apenas o estudo conduzido por Krill e colaboradores (2001) avaliou a expressão de um dos componentes na próstata humana durante o envelhecimento, sendo este o receptor de vitamina D. Através da avaliação por imunohistoquímica de tecidos prostáticos de doadores de órgãos em idades variadas (10 a 70 anos), os autores observaram que a expressão de VDR aumentou da primeira década de vida até atingir seu pico na quinta década, reduzindo a partir de então (Krill et al. 2001). Entretanto a redução do receptor em idades mais avançadas não foi estatisticamente significativa, muito provavelmente pelo baixo tamanho amostral (em

média 4 por grupo), e os autores selecionaram apenas tecidos livres de adenocarcinoma ou lesões suspeitas.

Nesse cenário, um trabalho recente do nosso grupo de pesquisa (Campolina-Silva, 2016) teve como objetivo investigar o padrão de expressão do VDR na próstata ao longo do envelhecimento, através de um modelo animal que desenvolve lesões histopatológicas espontâneas que se assemelham àquelas que acometem a próstata humana senil. Para isso, ratos Wistar machos em diferentes idades foram considerados (3, 6, 12, 18, 24 meses), de forma a abranger animais adultos jovens a idosos. Este estudo mostrou que o VDR está amplamente distribuído na próstata e que seus níveis teciduais aumentam significativamente a partir dos 12 meses de idade, paralelo a marcante redução de cerca de 2,8 vezes nas concentrações circulantes de 25(OH)D. Ainda, observou-se uma maior intensidade de imunomarcação para VDR nas células epiteliais com morfologia e localização de células basais, e uma redução significativa do número de células imunorreativas em áreas proliferativas, especialmente naquelas correspondentes à lesão pré-maligna conhecida como neoplasia intraepitelial prostática (PIN), o principal local de origem do tumor prostático (Woenckhaus & Fenic, 2008).

Os resultados de Campolina-Silva (2016) apresentados acima confirmam a existência de variação idade-dependente em um importante componente do sistema endócrino vitamina D e trazem evidências de que, para se interpretar a magnitude da sinalização da vitamina D, não se deve focar somente na concentração de 25(OH)D no sangue, como tem sido empregado de maneira conflitante nos estudos que visam investigar a relação protetora entre vitamina D e as doenças prostáticas, mas também em outros fatores tais como a concentração de VDR nas células-alvo, a qual pode ser

inversamente proporcional aos níveis circulantes da vitamina D. Nesse sentido, a avaliação das concentrações intraprostáticas de calcitriol e da expressão das principais enzimas participantes de seu metabolismo durante o envelhecimento, assim como do RXR, pode ser fundamental para melhor compreender o impacto e variação observada na expressão de VDR, visto que o calcitriol pode regular a expressão de seu próprio receptor (Giangreco et al. 2015), e que o RXR é um componente essencial para que o VDR ativado exerça seus efeitos nas células-alvo.

Sabe-se que a próstata é um órgão sensível a hormônio, e nesse sentido, as células luminais (ou secretoras) do epitélio recebem o papel de protagonistas em mediar a resposta hormonal na glândula. Entretanto, a mais intensa positividade para VDR observada nas células do epitélio prostático com características de células basais (Campolina-Silva, 2016), chama atenção para a participação desse tipo celular em mediar os efeitos não só da vitamina D, mas também de outros hormônios atuantes na próstata. Nesse sentido, embora seja muito discutido que as células basais prostáticas não expressam receptores de andrógenos, sabe-se que elas são altamente responsíveis a hormônios, expressando receptores de estrógenos (ERα e ERβ, GPER), receptores de retinoides (RXR e RAR), e muito provavelmente, de vitamina D (VDR) (Hu et al. 2011; 2012; Rago et al. 2016; Campolina-Silva, 2016).

As células basais da próstata constituem uma população heterogênea que abriga as células-tronco, multipotentes e auto-renováveis, as quais podem diferenciar em células luminais, neuroendócrinas ou basais (Wang et al, 2013; Lee et al, 2014). Acredita-se que diferentes subtipos de células basais podem exercer diferentes contribuições estruturais e funcionais para próstatas normais ou cancerosas, destacando uma

necessidade eminente de caracterização desse tipo celular. Interessantemente, a expressão da principal isoforma do receptor retinoide X atuante na próstata, o RXRα, é mais proeminente nas células basais do epitélio, e o número de células basais positivas para tal receptor reduz significativamente tanto em lesões pré-malignas PIN quanto no tumor prostático (Mao et al. 2004). Esses dados reforçam a participação das células basais em mediar os efeitos protetores do calcitriol na próstata e, somado a redução da expressão de VDR nas áreas de PIN (Campolina-Silva, 2016), é possível que a perda da sinalização do complexo VDR/ RXRα, inclusive nas células basais, possa ser um fator importante para a carcinogênese prostática.

Portanto, a presente proposta visa investigar o padrão de expressão dos principais componentes que integram o sistema endócrino vitamina D no tecido prostático, como um importante passo para melhor compreender a relação da vitamina D na fisiopatologia da próstata em envelhecimento. Para isso, ratos Wistar machos em diferentes idades foram adotados como modelo experimental, visto que esses animais possuem a vantagem de desenvolver naturalmente alterações histopatológicas na próstata, em especial lesões epiteliais benignas e pré-malignas (Morais-Santos et al. 2015). Adicionalmente, um modelo de indução crônica da carcinogênese prostática também foi estabelecido para confirmar possíveis diferenças entre a expressão das proteínas-alvo desse estudo em áreas normais e malignas da próstata.

II. OBJETIVOS

II. OBJETIVOS

1. Objetivo geral

Investigar o efeito do envelhecimento na expressão de componentes do sistema endócrino vitamina D no complexo prostático de ratos Wistar, por meio da avaliação dos níveis circulantes e teciduais de calcitriol e da expressão das enzimas CYP27B1 e CYP24A1, bem como do receptor RXR, correlacionando os resultados obtidos com o padrão de expressão observado para o receptor de vitamina D (VDR) no local.

2. Objetivos específicos

a) Mapear a distribuição celular e subcelular das enzimas CYP27B1 e CYP24A1, bem como do receptor retinoide X (RXR) nos lobos prostáticos.

b) Investigar se o padrão de expressão das proteínas-alvo desse estudo altera com o envelhecimento, especialmente em áreas de alterações epiteliais comuns na próstata senil, ou em lesões prostáticas induzidas pela exposição prolongada a hormônios esteroides.

c) Determinar os níveis plasmáticos e intraprostáticos de calcitriol;

d) Correlacionar a expressão da CYP27B1, CYP24A1 e RXR com os níveis mensurados de calcitriol e o padrão de expressão previamente observado para VDR no complexo prostático durante o envelhecimento;

e) Confirmar a identidade das células do epitélio prostático similares a células basais que apresentaram expressão diferencial para o VDR.

III. ARTIGOS RESULTANTES

III. ARTIGOS RESULTANTES

Os resultados assim como a metodologia empregada foram compilados em três artigos científicos que resultaram diretamente do projeto desenvolvido, a saber:

1. **Reduced vitamin D receptor (VDR) expression and plasma vitamin D levels are associated with aging-related prostate lesions**
    - Artigo publicado em 2018, no volume 78 do periódico internacional “The Prostate”, sob o registro DOI:10.1002/pros.23498.

2. **Altered expression of the vitamin D metabolizing enzymes CYP24A1 and CYP27B1 under the context of prostate aging and pathologies**
    - Manuscrito enviado em 14 de maio de 2020 para avaliação pelo corpo editorial do periódico internacional “The Journal of Steroid Biochemistry and Molecular Biology”.
    -

3. **Targeting Wistar rat as a model for studying benign, premalignant and malignant lesions of the prostate**
    - Artigo publicado em 2020, no volume 242 do periódico internacional “Life Sciences”, sob o registro DOI: 10.1016/j.lfs.2019.117149

ARTIGO 1: Reduced vitamin D receptor (VDR) expression and plasma vitamin D levels are associated with aging-related prostate lesions. Prostate, 78: 1-15.

Received: 25 October 2017 | Accepted: 5 February 2018
DOI: 10.1002/pros.23498

ORIGINAL ARTICLE

WILEY The Prostate

Reduced vitamin D receptor (VDR) expression and plasma vitamin D levels are associated with aging-related prostate lesions

Gabriel H. Campolina-Silva | Bruna T. Maria | Germán A.B. Mahecha | Cleida A. Oliveira

Department of Morphology, Universidade Federal de Minas Gerais, Belo Horizonte, Minas Gerais, Brazil

Correspondence
Cleida A. Oliveira, Av. Antônio Carlos, 6627, 31270-901, Belo Horizonte, Minas Gerais, Brasil.
Email: cleida@icb.ufmg.br

Funding information
Conselho Nacional de Desenvolvimento Científico e Tecnológico, Grant number: 473619/2013-0; Fundação de Amparo à Pesquisa do Estado de Minas Gerais, Grant number: Grant PPM-00334-14

Background: Protective roles have been proposed for vitamin D in prostate cancer, which has the advanced age as the major risk factor. However, little is known about the expression of the vitamin D receptor (VDR) in the aging prostate and its association with the development of epithelial lesions that affect tissue homeostasis and may precede prostate tumors.

Methods: VDR expression in the prostatic complex of young adults to senile Wistar rats, a natural model to study age-related prostatic disorders, was evaluated by immunohistochemical, Western blotting, and image-assisted analyzes. Results were correlated with the plasma levels of vitamin D and testosterone, the occurrence of punctual histopathological changes in the aging prostate, and the expression of retinoid X receptors (RXR).

Results: VDR was widely distributed in the prostatic complex at all ages analyzed, with the highest immunoexpression found in basal epithelial cells. As the animals aged, VDR levels increased, except in punctual areas with intraepithelial proliferation, metaplasia, or proliferative inflammatory atrophy, which had reduced expression of this receptor concomitantly with increased cell proliferation. Interestingly, RXR expression in the aging prostate was similar to that found for its partner VDR, indicating that components of the VDR/RXR complex required for vitamin D signaling are affected in aging-related prostatic lesions. Moreover, plasma vitamin D levels declined at the same ages when prostatic alterations appeared. Although circulating levels of testosterone also decreased with aging, the changes observed in the components of the vitamin D system were not correlated with androgens.

Conclusions: Our data indicate that the aging prostate suffers from an imbalance on the intricate mechanism of tissue regulation by the vitamin D responsive system. We argue that the status of VDR expression might be determinant for the development of histopathological alterations in the aging prostate, which include premalignant lesions.

KEYWORDS
aging, prostate, prostate lesions, vitamin D receptor, vitamin D signaling

1 | INTRODUCTION

Although vitamin D is recognized by its classic role in bone health, a growing body of evidence has linked its deficiency, a re-emerging global health problem, with increased risk for several diseases[1,2] including prostate cancer.[3–5] Prostate cancer is one of the most commonly diagnosed neoplasms and the fifth leading cause of cancer death worldwide.[6]

Experimental studies involving primary cultures,[7,8] cell lines,[8,9] xenograft systems,[10] and transgenic models of prostate cancer[11,12] showed that vitamin D in its biologically active form, the 1,25-dihydroxyvitamin D, plays a growth-inhibitory effect on the prostate. Despite these encouraging results, epidemiological data have kept an ongoing debate concerning vitamin D and prostate cancer. Indeed, while studies have associated the low circulating levels of vitamin D with increased prostate cancer risk or progression,[4,5,13,14] other investigations did not support this association.[15–20] One possible explanation for these conflicting data may be differences in prostatic levels of the vitamin D receptor (VDR), which varies in normal and tumor tissues.[21–23] Upon binding to 1,25-dihydroxyvitamin D, VDR forms a heteromeric complex with retinoid X receptors (RXR) to mediate most of the vitamin D signaling effects on target cells.

It is well known that advancing age is the major risk factor for the development of prostate lesions that affect tissue homeostasis and may even progress to cancer.[24–27] However, the occurrence of age-dependent variation in VDR expression as well as its association with prostatic disorders is still poorly understood. Therefore, in the present study, we mapped the expression pattern of VDR in the prostates of young adults to senile Wistar rats, since this animal model has the advantage of naturally developing aging-related prostate lesions that mimic most of those affecting the human prostate. We correlated VDR expression in the prostatic tissue with the expression of its partner RXR and the circulating levels of Vitamin D. Furthermore, as the prostate is an androgen-dependent organ and some studies indicate a relationship between vitamin D and the androgen responsive system,[28–31] we also compared the results with testosterone levels and investigated whether the expression pattern of VDR in the prostatic tissue is influenced by androgens.

2 | MATERIALS AND METHODS

2.1 | Ethics statement

All the experimental procedures described herein were approved by the Ethical Committee for Animal Experimentation of the Universidade Federal de Minas Gerais-UFMG, Brazil (CEUA, process 286/2008).

2.2 | Animals and sample collection

The investigation was performed in the prostates of adult male Wistar rats at different ages (3, 6, 12, 18, and 24 months). The rats were purchased with approximately 1 month of age from the Central Animal House (UFMG) and then housed in the animal facility at the Institute of Biological Sciences (UFMG) under a constant light cycle (12 h of light and 12 h of darkness) and temperature (22°C). The animals received ad libitum access to water and standard pelleted chow containing 2.000 IU vitamin D_3/kg (Nuvital Nutrientes S.A, Colombo, Brazil). No changes in food consumption were observed between groups along the experiment.

After reaching the ages of interest, the animals were weighed, anesthetized, and perfused transcardially with Ringer's solution followed by 10% neutral buffered formalin (NBF). The NBF-fixed prostatic complex, comprising the ventral, dorsal, lateral, and anterior prostate lobes, was dissected and embedded in paraffin for immunohistochemistry and immunofluorescence. In addition to aging, the ventral prostates of castrated and sham rats (4 months of age) were obtained as described[26] and processed for paraffin embedding.

For Western blotting assays, anesthetized animals were perfused only with Ringer's solution and the fresh tissues from each prostate lobe were dissected, frozen in liquid nitrogen, and stored at −80°C until use. The kidney and liver were also processed for Western blotting and immunohistochemistry to be used as high and low control of VDR levels, respectively.

2.3 | Antibodies

All antibodies used herein were checked for amino acid sequence homology, purchased commercially, and tested by serial dilutions to determine the optimal concentration before being used in the techniques described below.

2.4 | Immunohistochemistry

In order to map the expression pattern of VDR in the rat prostate during aging, NBF-fixed and paraffin-embedded fragments from all prostate lobes of rats at different ages (n = 5 per age) were sectioned at 5 µm. Additionally, immunostainings for RXR, androgen receptor (AR), and the cell proliferation marker Minichromosome Maintenance 7 (MCM7), were also performed. For this purpose, the obtained sections were deparaffinized in xylol, rehydrated through a graded series of ethanol, rinsed briefly in distilled water, and immersed in a 0.6% methanol-hydrogen peroxide solution for blocking endogenous peroxidase. After antigen retrieval with 0.01 M sodium citrate buffer (pH 6.0) and microwave heating (30 min at 70% power), the sections were exposed to the avidin/biotin blocking solution (Vector Laboratories, Burlingame, CA) for 10 min. To prevent non-specific binding of antibodies, the sections were incubated with 10% rabbit (for VDR) or goat normal serum (for RXR and MCM7) for 1 h at room temperature. Then, we incubated the sections for approximately 40 h at 4°C with rat monoclonal anti-VDR antibody (clone 9A7γ, Thermo Scientific, Fremont, CA), diluted 1:1500 in phosphate buffer saline (PBS, pH 7.4), or overnight at 4°C with mouse monoclonal anti-RXR (clone F-1, Santa Cruz Biotechnology, Dallas, TX) or anti-MCM7 (clone 47DC141, Thermo Scientific), and rabbit polyclonal anti-AR (clone PG21, Millipore, Burlington, MA), diluted 1:400 in PBS. Negative controls received only PBS in place of the primary antibody. After washing in

PBS, the sections were exposed for 1 h at room temperature to the biotinylated rabbit anti-rat (for VDR), goat anti-mouse (for RXR and MCM7), or goat anti-rabbit (for AR) secondary antibodies (Dako, Carpinteria, CA) diluted 1:100 in PBS, and then incubated with the avidin-biotin complex (Vectastain Elite ABC Kit, Vector Laboratories) for 30 min. Finally, the immunoreaction was visualized by immersion in 0.05% 3,3′ diaminobenzidine solution containing 0.01% hydrogen peroxide in 0.05 M Tris-HCl buffer (pH 7.4), followed by slight Mayer's hematoxylin counterstaining. To confirm the results, the assays were performed in triplicates.

2.5 | Immunofluorescence

Colocalization of VDR with high molecular weight cytokeratins (CH HMW), a basal cell marker, as well as with MCM7 was performed in the rat prostates following the protocol previously described,[27] with a few modifications. After blocking with 10% normal goat serum, the sections were exposed at 4°C for approximately 40 h to the rat monoclonal anti-VDR antibody (clone 9A7y, Thermo Scientific), diluted 1:50 in Tris-HCl buffer solution (TBS, pH 7.4). After washes in TBS, the sections were incubated overnight at 4°C with mouse monoclonal anti-CK HMW (clone 34βE12, Dako) or anti-MCM7 (clone 47DC141, Thermo Scientific) antibodies, diluted 1:25 and 1:300 in TBS, respectively. Negative controls received only TBS in place of the primary antibodies. Then, the sections were incubated for 2 h at room temperature with the secondary antibodies Alexa Fluor 546-conjugated goat anti-mouse and Alexa Fluor 488-conjugated goat anti-rat (Thermo Scientific) diluted 1:100 in TBS. The immunofluorescence was examined using a Zeiss ApoTome microscope (Carl Zeiss, Göttingen, Germany) equipped with filters suitable for detection of Alexa Fluor 488 and 546 signals.

2.6 | Western blotting

Western blotting assays were performed in the prostatic complex (n = 5 per age) to evaluate changes in total VDR protein levels during aging. Rat kidney and liver were used as control. For this purpose, frozen samples were macerated in dry ice and the pulverized tissues (100 mg) were homogenized in 300 µL of protein extraction buffer (8M urea, 20 mM Tris-HCl pH 7.5, 0.5 mM EDTA pH 8.0) containing 10% protease inhibitor cocktail (Sigma-Aldrich, Dorset, UK). The protein extract was collected of the supernatant fraction after sample centrifugation for 10 min at 14 000 g at 4°C, and the protein content was determined by using the NanoDrop ND-1000 spectrophotometer (Thermo Scientific). The proteins (40 µg/lane) were separated by 10% SDS-PAGE and transferred to nitrocellulose membranes. Non-specific bindings were blocked with 10% normal rabbit serum. After incubation overnight at 4°C with the rat monoclonal anti-VDR antibody (clone 9A7y, Thermo Scientific) diluted 1:1000 in PBS (pH 7.4), the membranes were washed with PBS-Tween 0.05% followed by incubation for 1 h at room temperature with the biotinylated rabbit anti-rat antibody (Dako), also diluted 1:1000 in PBS. The avidin-biotin complex solution (Vector Laboratories) was used to amplify the signal. After several washes with PBS-Tween 0.05%, the immunolabeling was visualized with a solution of 0.1% of 3,3′ diaminobenzidine in PBS containing 0.05% (w/v) chloronaphthol, 16.6% (v/v) methanol, and 0.04% (v/v) hydrogen peroxide. β-actin was used as internal control, being detected by incubation overnight at 4°C with the mouse monoclonal anti-β-actin antibody (clone AC-74) and then, with the peroxidase conjugated goat anti-mouse antibody (Sigma-Aldrich, St. Louis, MI) for 1 h at room temperature, both antibodies diluted 1:5000 in PBS. The Western blotting assays were performed in triplicates for each prostate lobe to confirm the results.

2.7 | Quantitative studies

A systematic evaluation of VDR immunostaining in the prostate epithelium was conducted using computer-assisted image analysis. This approach is a useful tool to evaluate punctual changes in protein content, which eventually may not be clearly detected by Western blotting or other techniques that evaluate total extracts.[27] For this purpose, five pictures of different areas of the glandular epithelium of each prostate lobe per animal were randomly obtained by using the Panoramic MIDI II slide scanner (3DHISTECH, Budapest, Hungary). When present, the VDR staining intensity was quantified in 20-positive epithelial cell nuclei per area of hyperplasic, atrophic, metaplastic, or intraepithelial proliferative epithelium and compared with the adjacent normal epithelium.[27] The values obtained for luminal and basal cells within the normal epithelium were also compared. The amount of immunoreactive cells per 100 epithelial cells was counted and compared according to epithelial regions of the glands (normal or altered), prostate lobes, and ages. Immunostaining for RXR was also evaluated in the ventral and lateral prostates as described above.

Total VDR protein levels in the ventral, dorsal, lateral, and anterior prostates were quantified in Western blotting membranes, as previously described.[32] The staining intensity of the VDR specific bands was normalized with those found for β-actin and thus graphically showed as relative VDR expression.

2.8 | Assessment of circulating levels of vitamin D and testosterone

It has been established that the best form to evaluate vitamin D levels is through the quantification of its intermediate metabolite 25-dihydroxyvitamin D [25(OH)D].[33] Therefore, circulating levels of 25 (OH)D were measured by Enzyme-linked immunosorbent assay (ELISA). Testosterone levels were also measured by ELISA in order to evaluate the androgenic status of male rats during aging. To this end, plasma samples (n = 5 per age) were obtained after centrifugation of total blood (2200g for 10 min) in heparin-coated tubes before 25(OH) D and testosterone were measured. The assays were performed by using the commercial ELISA kits EIA-5396 and EIA-1559 (DRG Instruments GmbH, Marburg, Germany), respectively, following the manufacturer's instructions. All samples were evaluated in triplicates in two independent assays to confirm the results.

2.9 | Statistical analysis

Quantitative data were statistically analyzed by using the GraphPad Prism 5 software (GraphPad Software, La Jolla, CA). Initially, Q-Q plot and Shapiro-Wilk test were used to check normality of the datasets. When normality was confirmed, the data were analyzed by Student's *t*-test or ANOVA plus Tukey post hoc test to compare means between two or more groups. Otherwise, nonparametric data were analyzed using the Mann-Whitney test or Kruskal-Wallis plus Dunn's post hoc test for comparisons between two or more groups, respectively. Correlations between circulating levels of 25(OH)D, testosterone, and total VDR protein levels were calculated by using Pearson's correlation coefficient. The data were expressed as the mean ± standard error of the mean (SEM), and the significance level used for all tests was $P < 0.05$.

3 | RESULTS

3.1 | Immunolocalization and distribution of VDR in the prostatic complex

Regardless the animals' age, intense positivity for VDR was detected in the nuclei of cells localized in both epithelial and stromal compartments of the ventral, dorsal, lateral, and anterior prostates (Figure 1). Prostatic cells also presented weak cytoplasmic staining. VDR expression was mainly detected in the glandular epithelium, as most epithelial cells were positive for the receptor. Some stromal, endothelial, and perialveolar smooth muscle cells showed positive nuclear staining for VDR (Figure 1).

In all prostate lobes, the staining intensity for VDR was significantly stronger in many epithelial cells with localization and morphology compatible with basal cells, compared to the intensity observed in the adjacent luminal cells (Figure 2A-D). Other basal-like cells, albeit at a much lower number, showed moderate or negative immunoreaction for VDR (inserts in Figures 2B and 2C). The colocalization of VDR and the basal cell marker CK HMW confirmed the identity of these cells more intensely stained for VDR as basal epithelial cells (Figure 2). This data was contrasted with the expression pattern of androgen receptor in the prostate epithelium, which occurred primarily in luminal cells, being low or absent in basal cells (Figure 3A). Moreover, the expression of VDR in the prostate epithelium appears to be independent of androgen, as castrated and sham rats presented similar VDR expression (Figures 3B and 3C).

The number of VDR-positive cells in the glandular epithelium varied significantly between prostate lobes, with ventral > dorsal = lateral > anterior (Figure 3D). In line with the immunohistochemical results, total VDR protein levels determined by Western blotting were higher in the ventral and dorsal prostates than the lateral and anterior prostates (Figure 3E). Western blotting assays specifically detected two main reactive bands of 55 kDa and 50 kDa, corresponding to the expected molecular weights of VDR in the prostate.[30,31]

Comparisons with other tissues known to present high (kidney) or low (liver) VDR expression revealed as high VDR protein levels in the ventral prostates as in the kidney, whereas the liver had the lowest level of VDR (Figure 3F). The kidney has been classically indicated as the major organ responsive to vitamin D, where VDR expression is 24-fold higher in the distal than proximal convoluted tubules.[34] The image assisted analysis revealed that the prostate basal cells presented as strong nuclear staining intensity for VDR as the distal renal convoluted tubule cells. The prostate luminal cells showed higher VDR intensity than both proximal renal convoluted tubule and hepatic cells (data not shown).

3.2 | Aging affects the expression pattern of VDR in rat prostatic complex

As the animals aged, the number of VDR-positive epithelial cells in the prostatic complex was similar in acini with normal morphology (Figure 4A). However, animals aged 12 months and older showed a discrete but significant increase in the nuclear staining intensity of these cells, as determined by the image analysis of the ventral and dorsal prostates (Figures 4B and 4C). Western blotting further confirmed that the total protein extracts from each prostate lobe of young adult rats (3 and 6 months) had lower VDR levels compared to those from older animals (12, 18, and 24 months) (Figure 4D-G).

Recently, we showed that aging Wistar rats naturally develop epithelial prostatic lesions similar to many of those found in human prostate such as hyperplasia, intraepithelial proliferation, metaplasia, and atrophies.[27,35] Therefore, we also evaluated VDR expression in the prostate epithelium with histopathological alterations related to aging.

Interestingly, a heterogeneous positivity for VDR was observed in areas of intraepithelial proliferation (IP), including those presenting characteristics compatible with prostate intraepithelial neoplasia, which have been previously recognized as premalignant lesions of the prostate.[36] These punctual areas were more frequent in senile rats (18 and 24 months) and we found a high proportion of unstained cells alongside with epithelial cells stained for VDR (Figures 5A and 5B). Image analysis revealed that, although the nuclear VDR intensity did not change when positive epithelial cells were considered (Figure 5C), a significant increase in the number of VDR-negative cells in IP areas was observed when compared to the adjacent normal epithelium (Figure 5D). As higher rates of cell proliferation are found in these punctual areas of the aging rat prostates,[26] we investigated whether the increased number of cells lacking VDR were proliferating cells. Colocalization of VDR and the proliferation marker MCM7 revealed that many of the proliferating cells found in IP areas, but not in the adjacent normal epithelium, were also negative for VDR.

In some acini, especially in the ventral prostate, epithelial proliferation led to cribriform architecture, where we observed a reduced number and staining intensity of VDR-positive cells in comparison to the adjacent normal epithelium (Figure 5F-J). On the other hand, the expression pattern of VDR did not change in the atrophic acini of the ventral prostate nor in the hyperplastic epithelium of all aging prostate lobes (data not shown).

In the lateral prostate, inflammatory foci were frequently seen in the prostate stroma of animals aged 18 and 24 months (Figure 6). Morphological changes were observed in acini nearby the

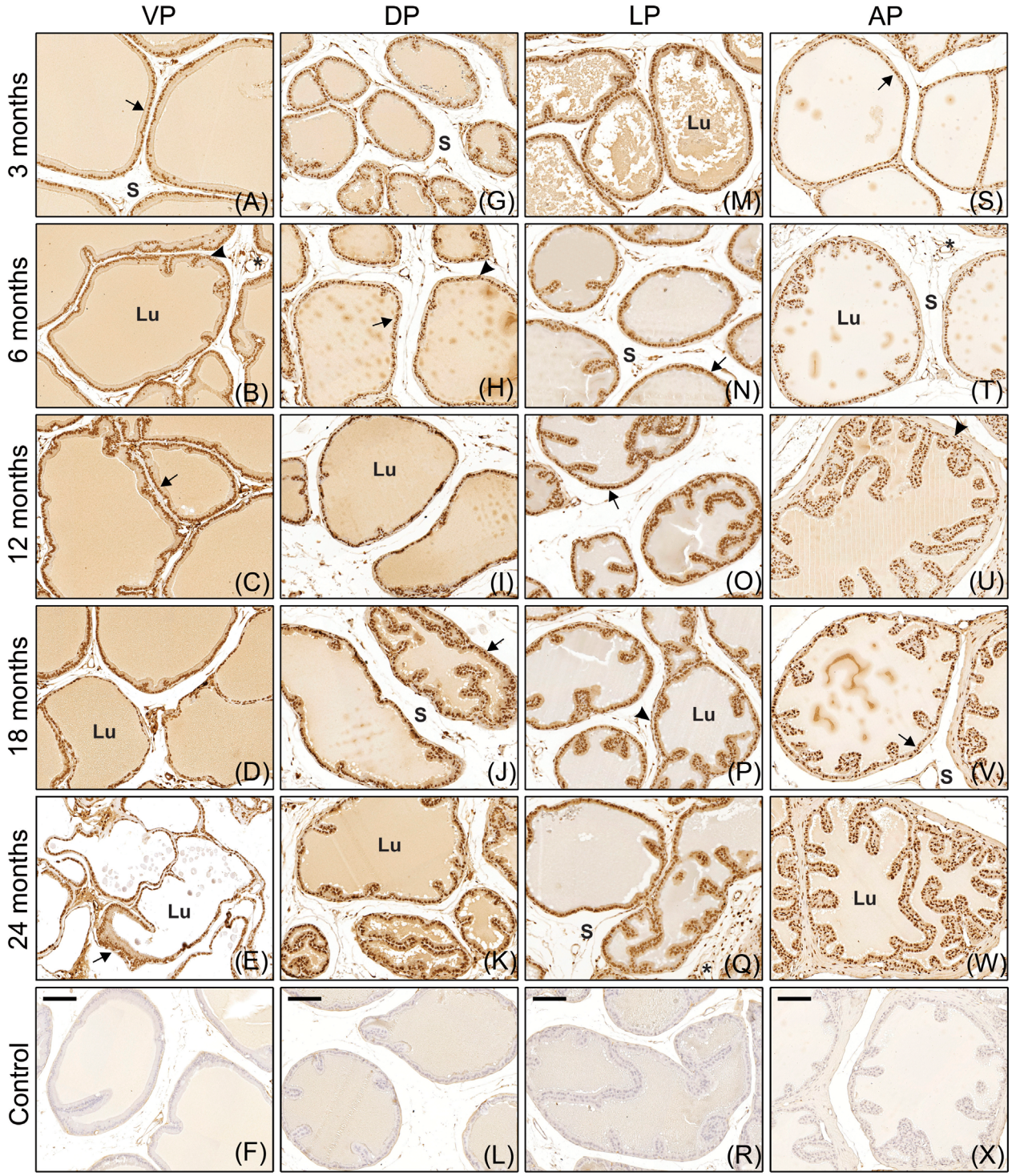

FIGURE 1 Distribution of VDR in the prostatic complex of Wistar rats at different ages. Arrows: indicate immunoreactive glandular epithelium. Arrowheads: indicate immunoreactive perialveolar smooth muscle cells. S: stroma. Lu: lumen. *: blood vessel. VP: ventral prostate. DP: dorsal prostate. LP: lateral prostate. AP: anterior prostate. Negative control of each prostate lobe in F, L, R, and X. Scale bars = 100 μm

inflammatory foci, which included metaplasia and proliferative inflammatory atrophy (PIA), as well as in the IP areas, with cells frequently presenting atypical nucleus. Compared to the normal epithelium, there was a significant reduction in VDR staining intensity in these punctual lesions of the senile lateral prostate, which also presented proliferating cells stained for MCM7 (Figure 6).

3.3 | Expression pattern of RXR in rat prostates is similar to that for VDR

It is well known that, upon binding to its ligand 1,25-dihydroxyvitamin D, VDR heterodimers with RXR to mediate most of the vitamin D effects on target cells. Therefore, we also investigated whether RXR, besides VDR, is

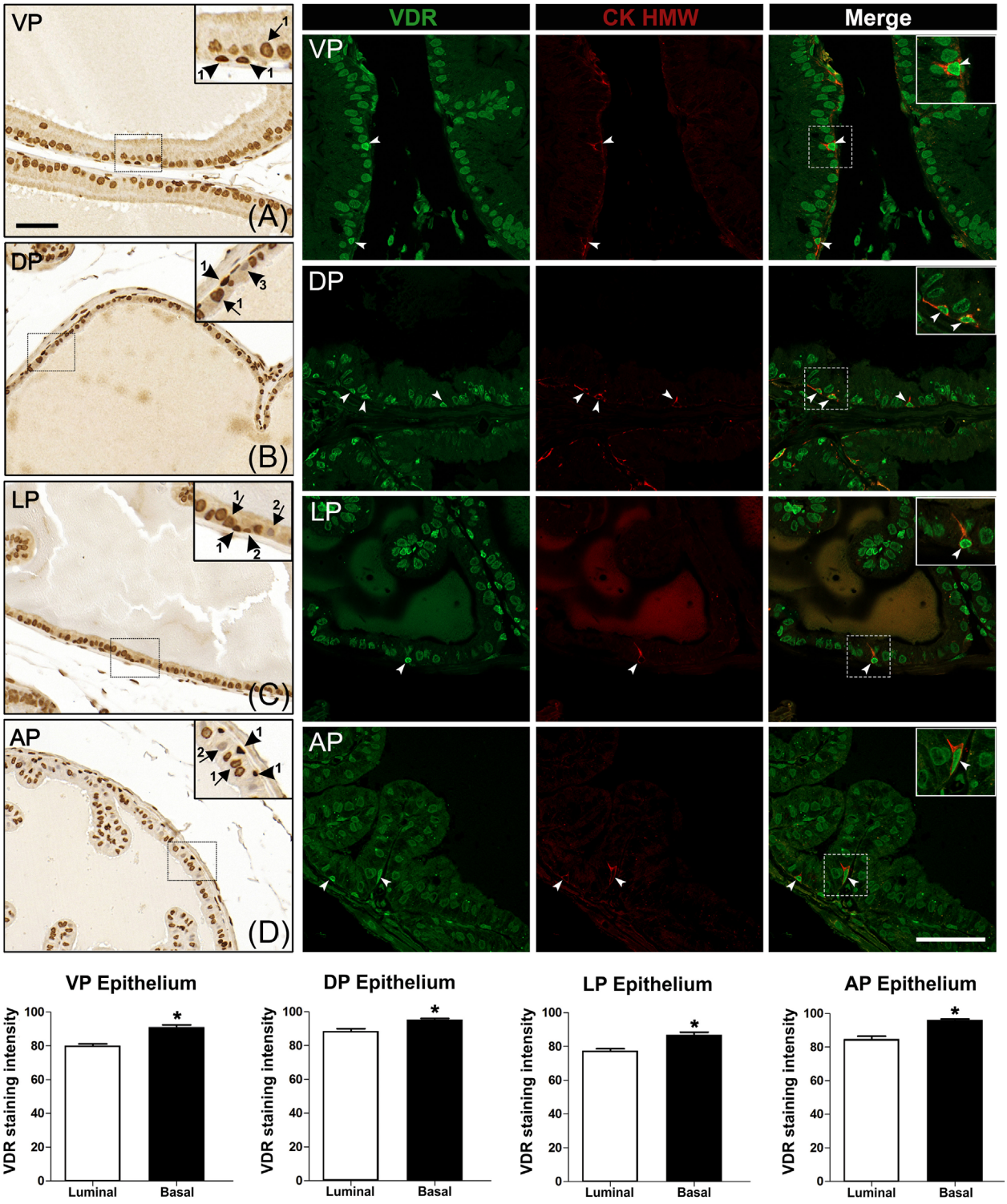

FIGURE 2 VDR expression between basal and luminal epithelial cells. (A-D) Immunoexpression of VDR in different prostate lobes. Upper inserts in A-D show many basal-like cells with stronger nuclear immunostaining (arrowheads 1) compared to the adjacent VDR-positive luminal cells (arrows 1). Eventually, a lower number of basal-like cells presented moderate nuclear staining (arrowhead 2, insert in C) or were negative for the receptor (arrowhead 3, insert in B). Some VDR-negative luminal cells were also observed (arrows 2). Colocalization of VDR and the basal cell marker CK HMW, as well as staining quantification, confirmed that basal cells presented a significantly higher nuclear VDR staining intensity than adjacent luminal cells. The figures were taken from middle-aged rats (12 months) and are representative of all ages analyzed. VP: ventral prostate. DP: dorsal prostate. LP: lateral prostate. AP: anterior prostate. Scale bars = 50 µm. * = $P < 0.05$

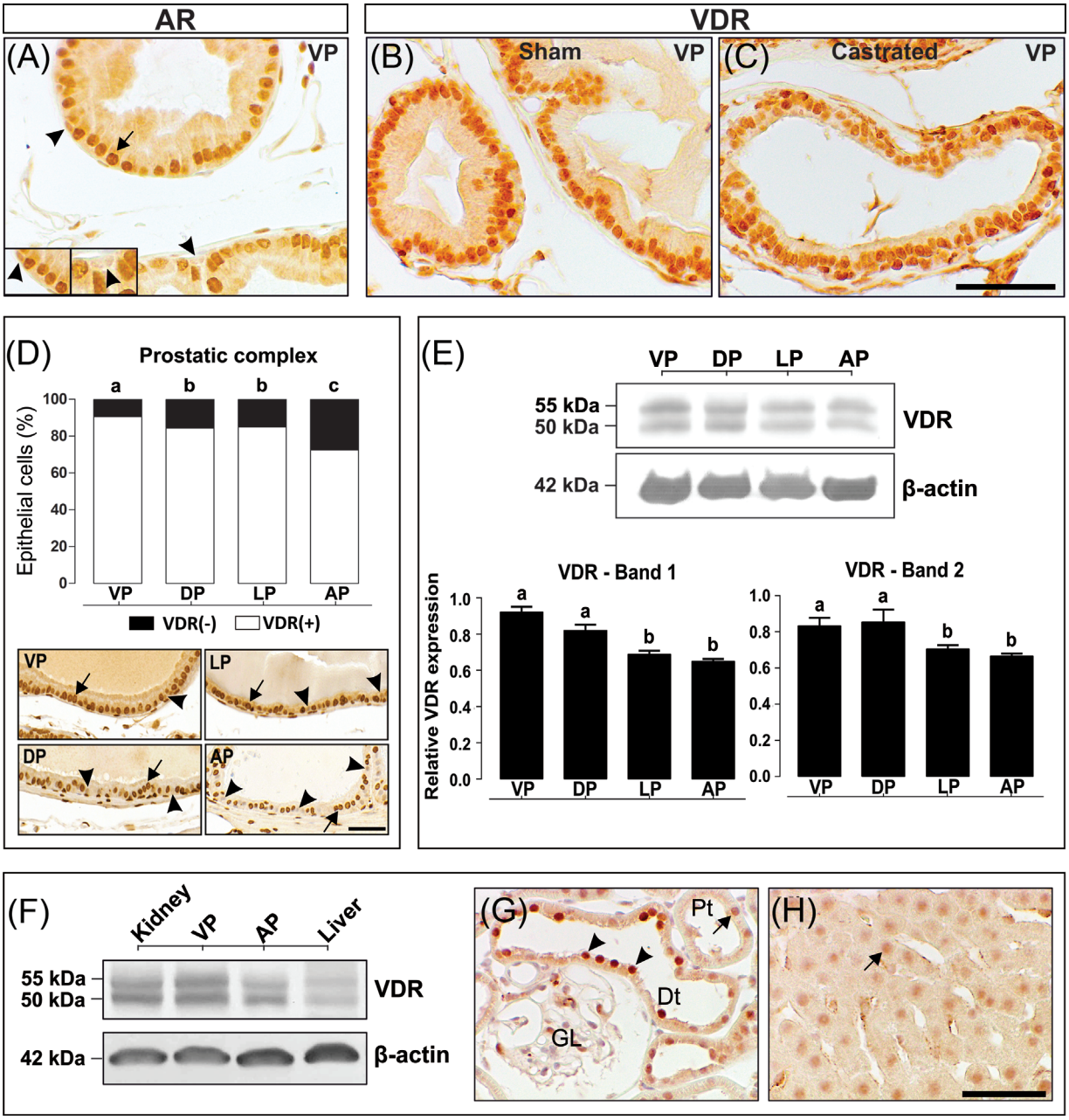

FIGURE 3 VDR expression in the rat prostatic tissues is independent of androgen and varies according to the prostate lobe. A, Androgen receptor (AR) was mainly detected in luminal cells (arrow), being low or absent in basal cells (arrowheads) of the prostate epithelium. (B and C) The expression pattern of VDR in the ventral prostate epithelium was similar between sham and castrated rats. D, Percentage of epithelial cells positive (arrows) or negative (arrowheads) for VDR in the prostatic complex of adult rats at 3-24 months of age. E, Western blotting comparing the VDR levels measured in protein extracts from the different prostate lobes, as well as (F) from the kidney and liver of rats aged 12 months. G, Immunostaining of VDR showing a higher immunoreaction in the distal (arrowheads) than proximal convoluted tubule cells (arrow). H, VDR expression in hepatic cells (arrow). VP: ventral prostate. DP: dorsal prostate. LP: lateral prostate. AP: anterior prostate. Dt: distal renal tubule. Pt: proximal renal tubule. GL: glomerulus. Scale bars = 50 μm. Mean values with different letters represent statistically significant differences ($P < 0.05$)

affected in punctual areas of the aging prostate. For this purpose, RXR was immunoreacted in the ventral and lateral prostates, the prostate lobes that presented the most significant age-related alterations.

Interestingly, the distribution pattern of RXR in the prostate was similar to that found for VDR. Positivity for RXR was detected in the nucleus of most epithelial cells, with the highest expression in many cells with localization and morphology of basal cells (Figure 7). Some stromal, endothelial, and perialveolar smooth muscle cells also stained for RXR. As the animal aged, the percentage of RXR-positive cells increased in the normal epithelium. However, compared to the adjacent normal epithelium, RXR expression significantly reduced in punctual lesions of the aging prostates, including IP, metaplasia, and PIA (Figure 7), a pattern matched by VDR as presented herein.

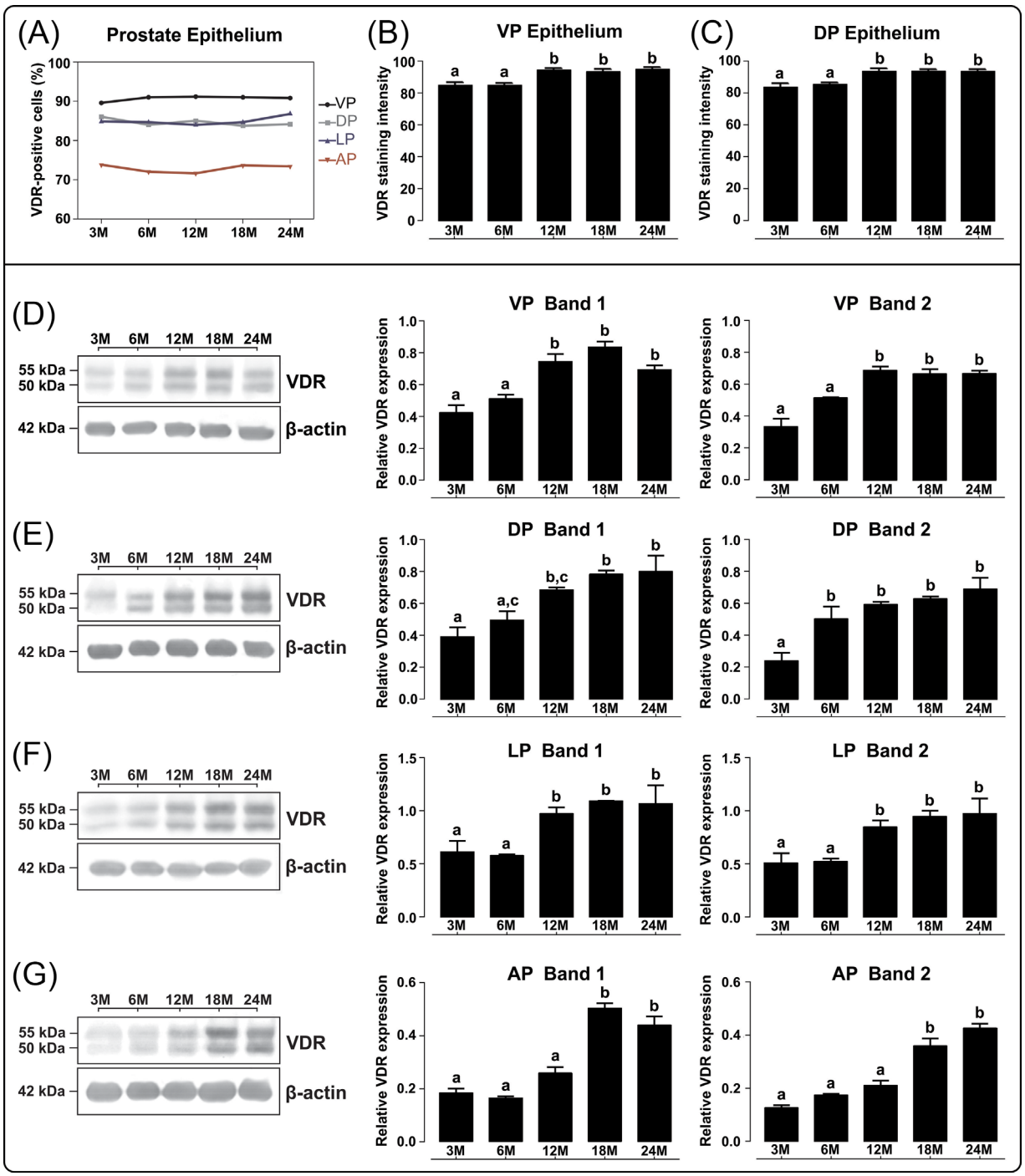

FIGURE 4 Age-related variation of VDR expression in the rat prostates. The percentage of VDR-positive cells in the normal prostatic epithelium was similar at all ages analyzed (A). However, these cells showed increased VDR staining intensity from 12 months of age onwards, as determined by image analysis of the VP (B) and DP (C). Western blotting assays also detected increased VDR levels in total protein extracts of the VP (D), DP (E), LP (F), and AP (G) with aging, as evidenced by the graphical representation of the band densitometric analysis. β-actin was used as the internal control. 3M, 6M, 12M, 18M, and 24M: age of the animals expressed in months. VP: ventral prostate. DP: dorsal prostate. LP: lateral prostate. AP: anterior prostate. Mean values with different letters represent statistically significant differences ($P < 0.05$)

3.4 | Aging decreases the circulating levels of vitamin D and testosterone

Young adult rats at 3 and 6 months of age had plasma 25(OH)D levels around 35 and 45 ng/mL, respectively. From 6 months of age onwards, there was a significant reduction (2.8-fold) in plasma 25(OH)D concentrations, reaching levels below 20 ng/mL in animals aged 12 months and older (Figure 8A). A strong inverse correlation between plasma 25(OH)D and total VDR levels in the prostatic complex was detected (Pearson $r = -0.85$, $P < 0.001$) (Figure 8B).

Senile rats also presented decreased plasma testosterone levels (Figure 8C). However, the changes observed during aging were not correlated with plasma 25(OH)D (Pearson $r = 0.09$, $P = 0.638$, Figure 8D) or total VDR protein levels (Pearson $r = -0.07$, $P = 0.768$, Figure 8E), as circulating testosterone reduced gradually from 3 months of age onwards, reaching statistical significance just at 24 months (Figure 8C).

4 | DISCUSSION

Herein, we mapped the expression pattern of VDR in the prostatic complex of young adults to senile Wistar rats. Although VDR was found widely distributed in the prostate lobes of all groups analyzed, its expression varied according to cell type, regions of the gland, and age. Interestingly, VDR expression was higher in basal cells than in luminal

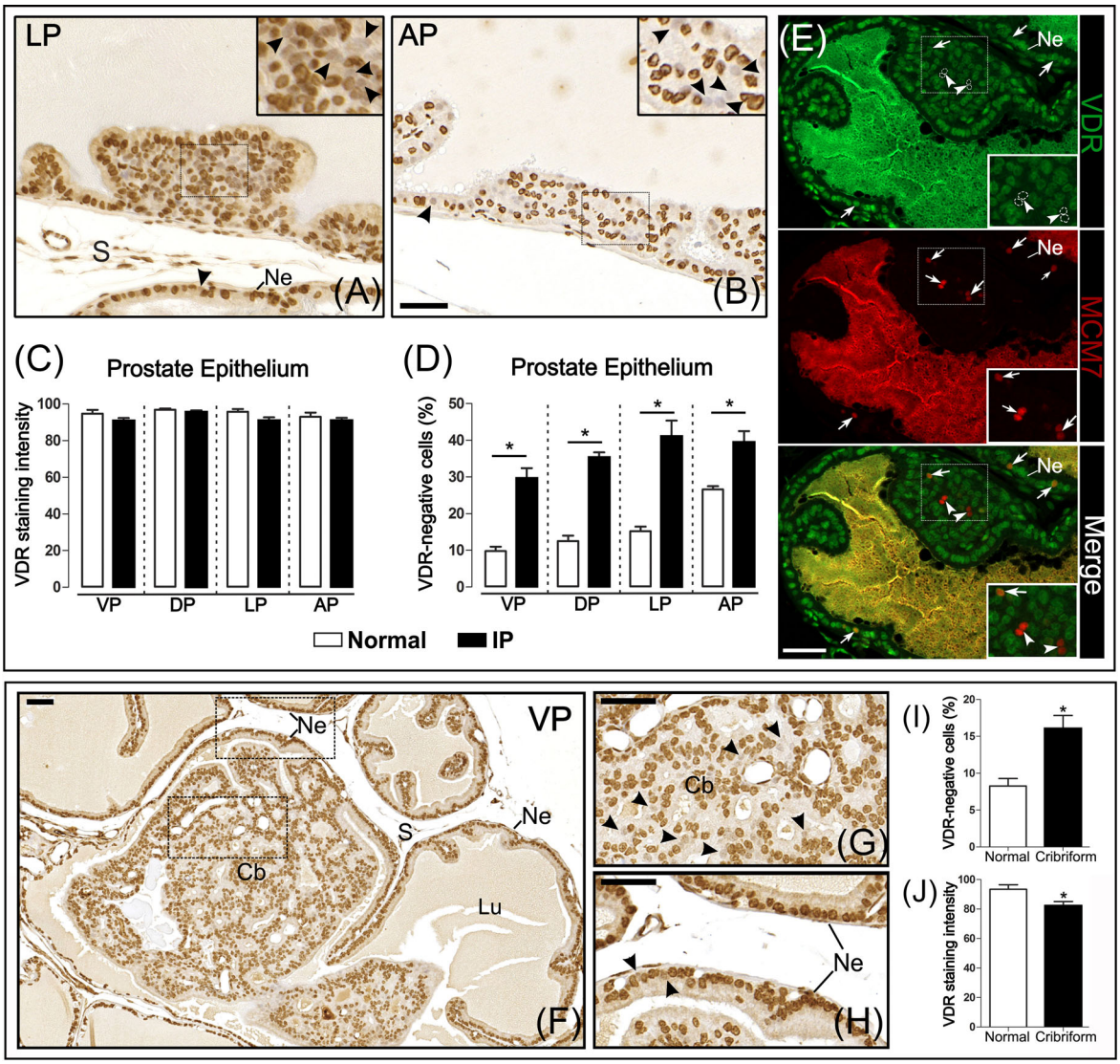

FIGURE 5 VDR expression is affected in epithelial proliferative lesions of rat aging prostates. (A and B) Heterogenous positivity for VDR in areas of intraepithelial proliferation (IP), where a high proportion of unstained cells (arrowheads) are found along with VDR-positive epithelial cells (see upper inserts). Although the nuclear staining intensity did not change (C), there was a significant increase in the number of VDR-negative cells in IP areas, compared to the adjacent normal epithelium (D). Colocalization of VDR and the proliferation marker MCM7 showed that many of the VDR-negative cells (arrowheads) restricted to IP areas were also positive for MCM7 (E). Epithelial proliferation led to a cribriform architecture with intraluminal growing in some acini (F) that also presented a higher proportion of cells lacking VDR (G), in comparison to the adjacent normal epithelium (H). Image analysis confirmed a significant reduction in positivity (I) and staining intensity (J) for VDR in this proliferative lesion. IP: intraepithelial proliferation. Arrowheads: VDR-negative epithelial cells. Arrows: MCM7-positive epithelial cells. Cb: proliferation with cribriform architecture. Ne = normal epithelium. S: stroma. Lu: lumen. VP: ventral prostate. LP: lateral prostate. AP: anterior prostate. Scale bars = 50 μm. * = $P < 0.05$

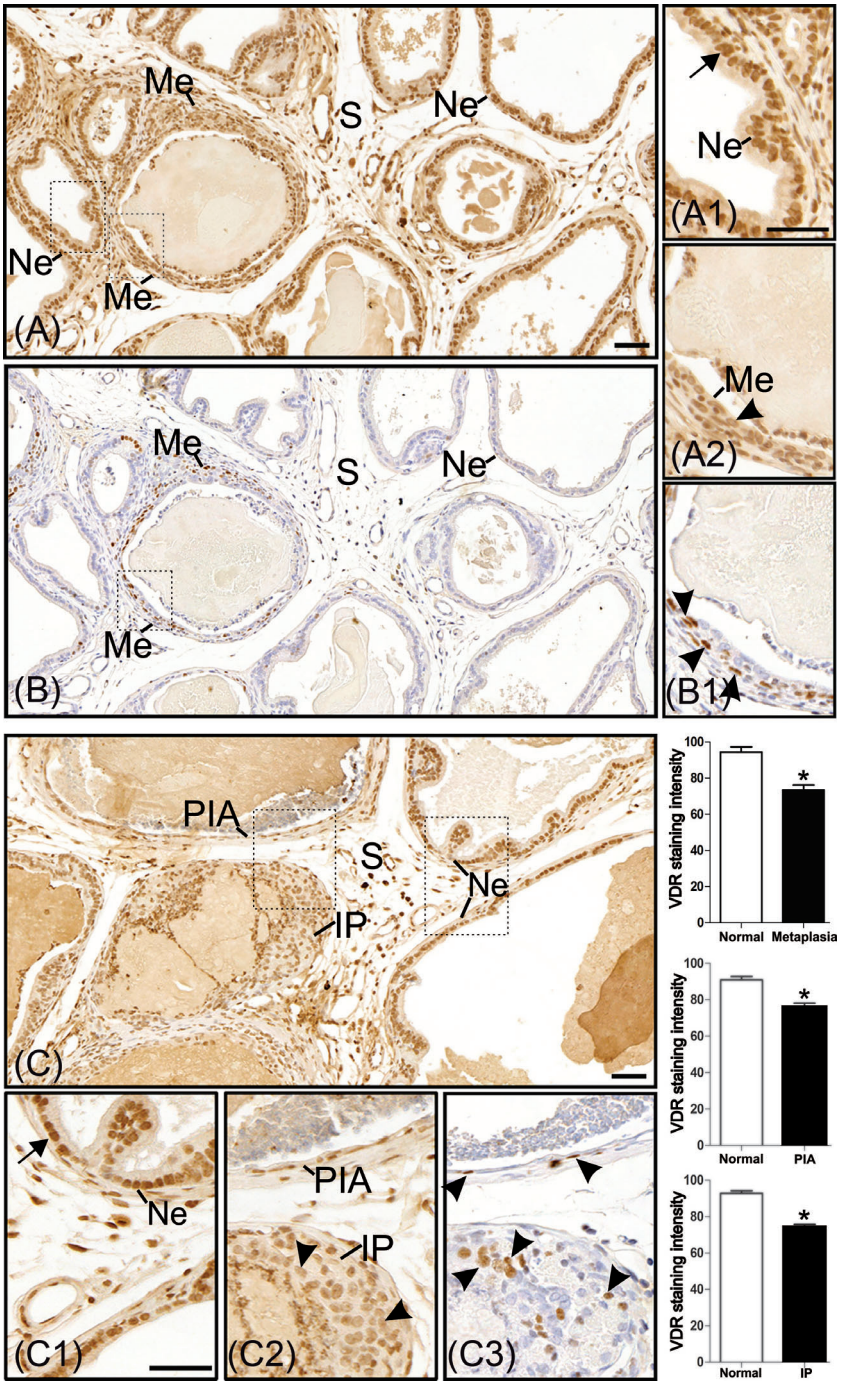

FIGURE 6 VDR expression and cell proliferation in the lateral prostate of senile Wistar rats. A, VDR staining in areas of the senile lateral prostate presenting acini with normal epithelium (Ne) or metaplasia (Me). Note the presence of inflammatory foci in the stroma. As highlighted by the magnification of panel A, the VDR-positive cells in normal epithelium (arrow in A_1) had higher VDR intensity than positive cells in metaplasia (arrowhead in A_2). B, Serial section of the same area represented in A showing high proportion of proliferating cells stained for MCM7 in metaplasia. (B_1) Magnification of panel B highlighting high cell proliferation in the same area of the metaplastic epithelium that showed reduced VDR staining intensity. Note that MCM7-positive epithelial cells in this area presented small and flattened nucleus suggestive of basal cells (arrowheads in B_1). C, VDR staining in areas of the senile lateral prostate with stromal inflammatory foci and acini with normal epithelium or showing proliferative inflammatory atrophy (PIA) or intraepithelial proliferation (IP). As highlighted by the magnification of panel C, the positive epithelial cells in the normal epithelium (arrow in C_1) presented higher VDR staining intensity than those in PIA and IP areas (arrowheads in C_2). Note that the epithelium in PIA displayed cells with reduced height and flattened nucleus while some VDR-positive cells in IP areas presented globose and large nucleus. These altered areas also showed proliferating cells (arrowheads in C_3) as determined by serial sectioning and MCM7 Labeling. The image analysis confirmed a significant reduction in VDR staining intensity in all these altered areas of the senile lateral prostate nearby inflammatory foci, in comparison with positive cells in the adjacent normal epithelium. S: stroma. Scale bar = 50 μm. * = $P < 0.05$

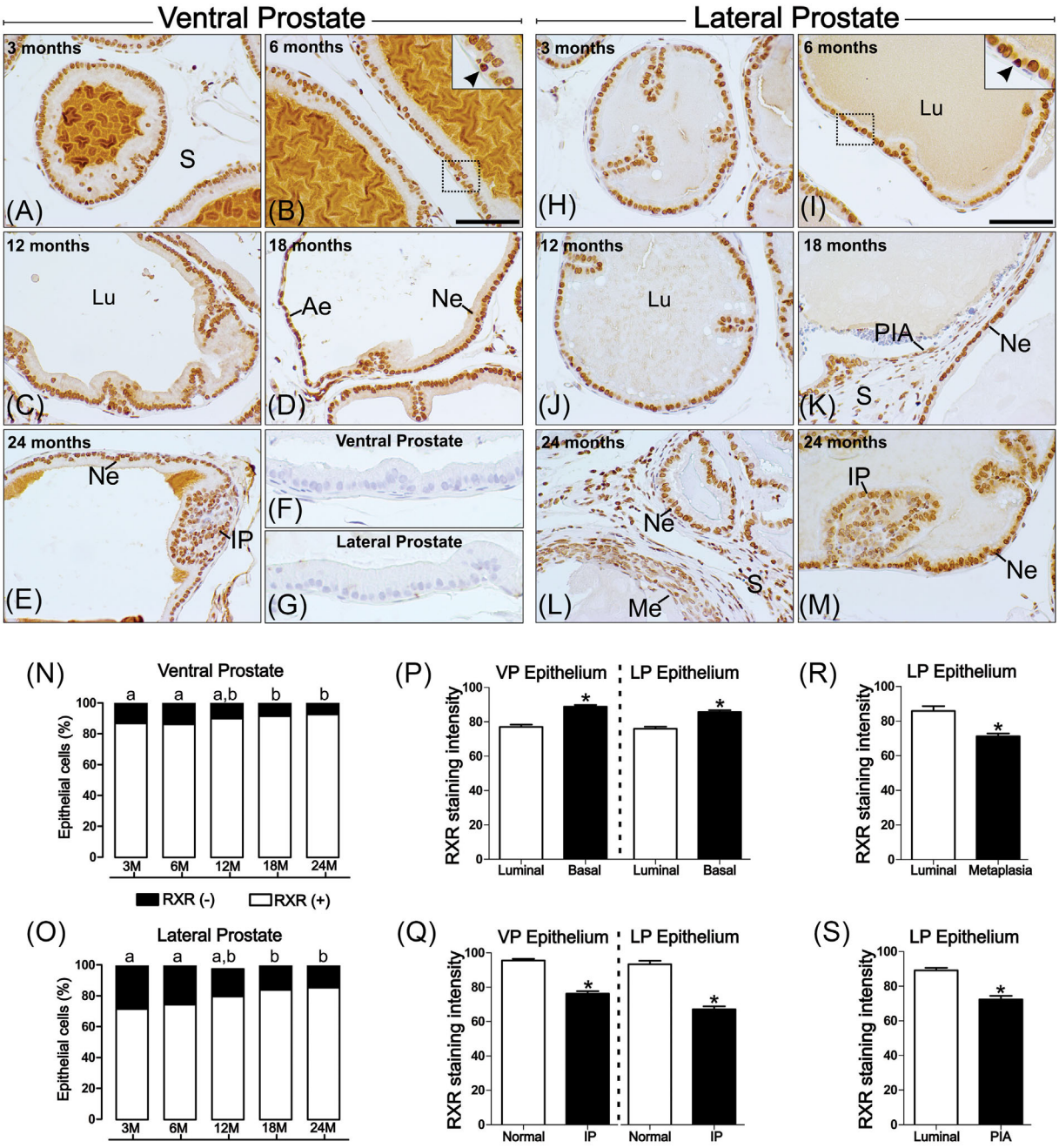

FIGURE 7 Expression pattern of RXR in the aging prostate is similar to that found for VDR. Distribution of RXR in the ventral (A-E) and lateral (H-M) prostates of rats at different ages. Inserts in (B) and (I), as well as the quantification represented in (P) highlight the stronger nuclear staining displayed by basal cells (arrowheads) in comparison with luminal epithelial cells. Note that the percentage of RXR-positive cells in the normal epithelium of the ventral (N) and lateral (O) prostates increased at 12 months of age onwards. However, there was a significant reduction in RXR staining intensity restricted to punctual lesions areas showing intraepithelial proliferation (E, M, and Q), metaplasia (L and R), and proliferative inflammatory atrophy (K and S), which are the same lesions that presented reduced VDR expression. Negative controls in (F) and (G). Ne: normal epithelium. IP: intraepithelial proliferation. Me: metaplasia. PIA: proliferative inflammatory atrophy. S: stroma. Lu: lumen. VP: ventral prostate. LP: lateral prostate. 3, 6, 12, 18, and 24M = age of the animals expressed in months. Scale bars = 50 µm. Mean values with different letters, as well as * represent statistically significant differences ($P < 0.05$)

cells while senile animals presented reduced expression of this receptor restricted to punctual areas of epithelial lesions, a pattern also seen for its partner RXR. The changes in VDR expression occurred concomitantly to reduced plasma 25(OH)D levels, the major circulating form of vitamin D, and were not correlated with testosterone level. It is noteworthy that the data presented herein were obtained under natural aging conditions, without the use of surgical, drug, or genetic interferences in the experimental animals.

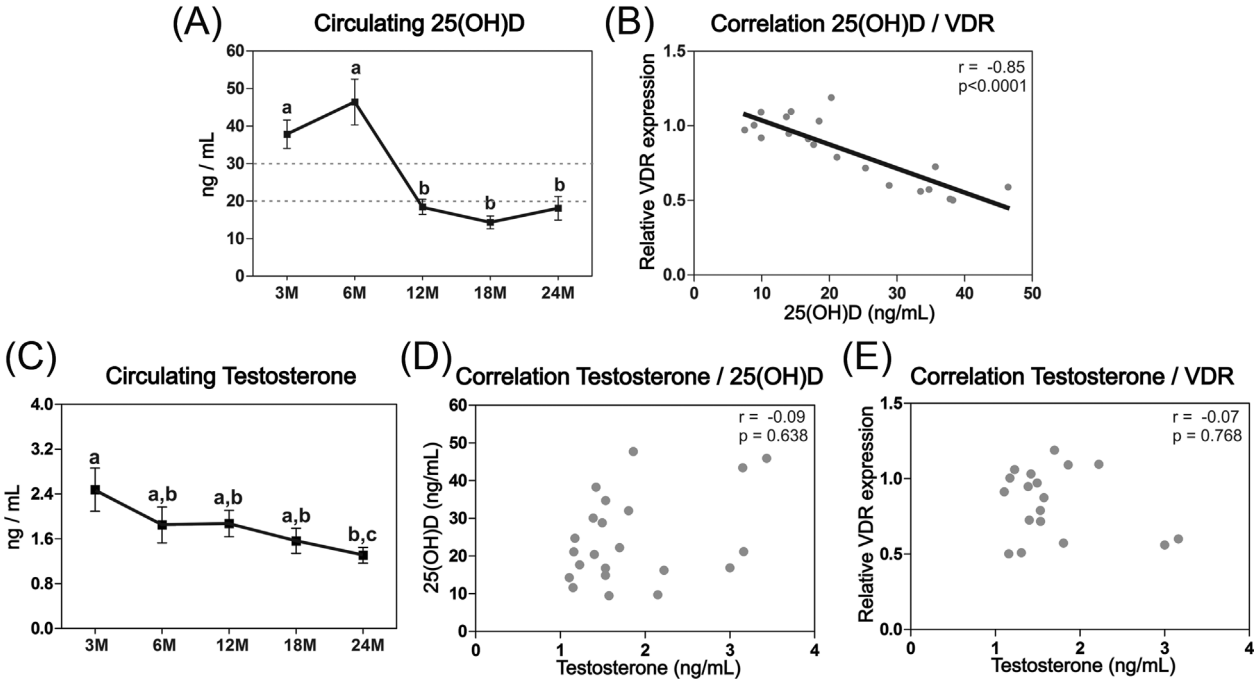

FIGURE 8 Reduction in Plasma 25(OH)D levels with aging is inversely correlated with total VDR protein content in the rat prostate. A, Circulating levels of vitamin D in its major circulating form, the 25(OH)D, decline from 12 months of age onwards. B, Strong negative correlation between plasma 25(OH)D concentrations and the total VDR levels in the prostatic tissue of rats at different ages. C, Circulating levels of testosterone declined gradually from 3 months of age onwards. D, Testosterone levels were not correlated to the 25(OH)D concentrations and E, total VDR levels in the prostatic tissue of rats at different ages. 3, 6, 12, 18, and 24M = age of the animals expressed in months. Mean values with different letters represent significant differences ($P < 0.05$). *r* = Pearson correlation coefficient

In all prostate lobes and ages, intense positivity for VDR was detected in the nucleus of most epithelial cells as well as in some stromal cells. This distribution pattern of VDR follows that previously showed for rat and human prostates,[21,22] and support the evidence that VDR and, therefore, most probably vitamin D signaling, occurs mainly in the epithelium but may also occur in the stromal compartment of the prostate.[7,37,38]

An intriguing observation reported herein is that many of the basal cells had higher nuclear VDR immunoreactivity than luminal cells. Other basal cells, but at a much lower number, presented moderate staining or were unreactive to VDR, thus pointing out that this cell population may present different degrees of response to vitamin D. Previous studies hinted at prostate basal cells as a target for vitamin D, but did not confirm the suggestion.[39,40] Other investigations described immunopositivity for VDR only in luminal cells[21,22] or did not formally distinguish the staining pattern of VDR among the epithelial cell types of the prostate.[39,41]

It is well known that, following binding to 1,25-dihydroxyvitamin D, which is the active metabolite of vitamin D, VDR forms heteromeric complexes with RXR subtypes to mediate most of the vitamin D effects on target cells.[42] Interestingly, Mao et al[43] showed that, compared to luminal cells, the nucleus of human basal cells expresses more intensely RXRα, the main RXR isoform acting in the prostate. Therefore, by using an antibody that binds with a high affinity to RXRα, but that also detects the other isoforms (RXRβ and RXRγ), we found that many basal epithelial cells of the rat prostate express RXR more intensely than adjacent luminal cells, a pattern matched by the VDR expression data presented herein. Taken together, the above-discussed data support a hypothesis that basal cells may be a primary target for vitamin D and may be, therefore, important protagonists in mediating the effects of the active metabolite of vitamin D on the prostate epithelium. Further studies are needed to confirm this hypothesis and to characterize the vitamin D signaling pathways taking place in prostate basal cell populations.

As the animals aged, there was a significant increase in VDR expression in all prostate lobes. The only other work analyzing the expression pattern of VDR with age was Krill et al,[22] which partially corroborates our findings. The study was conducted in normal prostate tissue and revealed that VDR expression was lowest in the prostate epithelium of young organ donors aged 10-19 years, then increased at 20-59 years of age and reduced thereafter, although this reduction was not statistically significant.

One of the main effects of the vitamin D signaling pathway on the prostate is the inhibition of cell proliferation, either by blocking the G1 to S phase cell cycle transition or by attenuating cell growth stimulating factors.[7,9,44,45] Accordingly, the observed increase in VDR expression at 12 months onwards corroborates previous works from our laboratory showing that the normal prostate epithelium of older rats presents lower rates of cell proliferation than the prostate epithelium of young animals.[26,27] In addition, the rat ventral prostate, which is the

lobe less affected by spontaneous age-related or androgen-induced proliferative disorders,[46] is also the region where we observed the highest VDR expression. These data support a role for VDR signaling pathway in the anti-proliferative mechanisms taking place in the prostate.

Importantly, while total protein extracts and the normal prostate epithelium of senile rats showed increased VDR expression, punctual areas of proliferative lesions in the prostatic complex of these animals presented a significant reduction of VDR expression. Similar observations were made in proliferative inflammatory atrophy and metaplasia of the lateral prostate. These lesions presented increased cell proliferation and many VDR-negative cells corresponded to proliferating cells, as well demonstrated in the intraepithelial proliferation. Moreover, expression of RXR was also significantly reduced in these prostate lesions. It is noteworthy that the punctual changes described above were only possible to detect because we used a combination of immunohistochemical and computer-assisted image analyses. Our work suggests that decreased presence of VDR and its partner RXR and, therefore, decreased anti-proliferative effects of vitamin D signaling mediated by the VDR/RXR complex, may be impaired in the altered areas of the aging prostate, which include premalignant lesions.

There is evidence that the anti-proliferative effect of 1,25-dihydroxyvitamin/VDR in prostate cells is positively influenced by testosterone and dihydrotestosterone (DHT) levels, being blocked by androgen withdrawal or anti-androgenic compounds.[28–31] Herein, the VDR expression in the prostate was not affected by castration, a finding that corroborates previous results.[31] Furthermore, the VDR occurred at high levels in basal cells, which presented low or undetectable expression of androgen receptor. Moreover, it was observed a gradual reduction in plasma testosterone concentrations from 3 months of age onwards, which reached statistical significance just at 24 months. This data is in agreement with the decrease of circulating androgens with aging,[27,46] but was not correlated with the changes observed for 25(OH)D and VDR levels at 12, 18, and 24 months of age. However, we have shown that compared to young animals (3 and 6 months), Wistar rats aged 12 months and older presented lower intraprostatic concentrations of DHT, the main androgen acting upon the prostate.[27] Therefore, it is possible that the reduced VDR expression in punctual prostate lesions associated with a tissue environment containing low DHT, impairs even more the anti-proliferative effect mediated by the vitamin D signaling pathway on the aging prostate.

The occurrence of prostate lesions and the turning-off of anti-proliferative factors are thought to precede cancer development.[25–27] Studying a transgenic mouse model of prostate cancer, Banach-Petrosky et al[11] showed that the administration of active vitamin D to animals reduced the development of precancerous lesions in a VDR expression dependent fashion. We found that although reduced, VDR-positive cells were still present in the prostate lesions analyzed herein. Therefore, it is plausible to think that administration of VDR agonists at early stages of age-related prostatic alterations might prevent the development of prostate diseases, including cancer. The non-encouraging results reported by a study investigating the protective effects of vitamin D in men with premalignant lesions and prostate cancer could put off future efforts to explore this idea.[47] However, other experimental conditions using different VDR agonists at different concentrations and length of treatment, among other factors, may yet have some effect on the prevention or reversal of aging-related prostatic alterations. We believe that further research is needed to clarify this matter.

Increased VDR expression in the aging prostates was matched by a significant reduction of plasma 25(OH)D levels. Reduced circulating levels of vitamin D metabolites with aging have been found for other studies, and may be a consequence of age-related decline in vitamin D production, enzymatic activity and/or intestinal absorption.[48] The 25(OH)D is the vitamin D metabolite precursor of the VDR ligand 1,25-dihydroxyvitamin D which, in turn, depending on its concentration, negatively regulates VDR expression in prostate cells.[38] Thus, low 25(OH)D levels may impact the 1,25-dihydroxyvitamin D synthesis and limit the protective effects that this hormone exerts via VDR not only in the prostate but also in several other target organs. Our results support the notion that the aging prostate can suffer from an imbalance on the intricate mechanism of tissue regulation by the vitamin D responsive system.

While some epidemiological studies associated low circulating levels of 25(OH)D with an increased risk to develop prostate cancer,[4,5,13,14] others did not support this association (see the meta-analyses by Yin et al[15] and Xu et al[49]). Hendrickson et al[23] examined VDR expression in 841 patients with prostate cancer and found a significant association between high VDR expression in prostate tumors and a reduced risk of advanced cancer or even lethal tumors, irrespective of plasma 25(OH)D levels. We found a strong inverse correlation between 25(OH)D levels and total VDR content in the prostate tissue. Considering the conflicting data about circulating 25(OH)D and prostate cancer development, the results presented herein, and those of Hendrickson et al,[23] we argue that vitamin D response should not be based on the levels of 25(OH)D and its respective metabolite alone, but also on VDR expression in the target cells.

5 | CONCLUSIONS

Our results indicate that VDR is widely distributed in the prostatic complex of Wistar rats, with the highest immunoexpression found in basal epithelial cells. As the animals age, VDR levels is increased, except in lesion areas associated with intraepithelial proliferation, metaplasia, and proliferative inflammatory atrophy, which presented reduced expression of this receptor and its partner RXR. The observed changes coincided with a decline in plasma 25(OH)D levels. We conclude that declined circulating levels of vitamin D and flaws in VDR expression and therefore on the vitamin D pathway may be an important element in the development of histopathological alterations in the aging prostate. We argue that the status of the receptor expression in the target cells should not be ignored in future research on the relationship between vitamin D and prostate disorders.

ACKNOWLEDGMENTS

We are grateful to the financial support provided to this study by the Conselho Nacional de Desenvolvimento Científico e Tecnológico – CNPq/Brazil (Grant and research fellowship to C.A.O and PIBIC scholarship to B.T.M); the Fundação de Amparo a Pesquisa do Estado de Minas Gerais-FAPEMIG/Brazil (Grant to C.A.O.); the Coordenação de Aperfeiçoamento de Pessoal de Nível Superior-CAPES/Brazil (Doctoral fellowship to G.H.C.S.); and the Pró-Reitoria de Pesquisa-PRPq/UFMG.

CONFLICTS OF INTEREST

The authors have nothing to disclose.

ORCID

Gabriel H. Campolina-Silva http://orcid.org/0000-0002-4473-3340

Cleida A. Oliveira http://orcid.org/0000-0001-9610-7846

REFERENCES

1. Holick MF. The vitamin D deficiency pandemic: approaches for diagnosis, treatment and prevention. *Rev Endocr Metab Disord*. 2017;18:153–165.
2. Wang H, Chen W, Li D, et al. Vitamin D and chronic diseases. *Aging Dis*. 2017;8:346–353.
3. Schwartz GG, Hulka BS. Is vitamin D deficiency a risk factor for prostate cancer? (Hypothesis). *Anticancer Res*. 1990;10:1307–1311.
4. Ahonen MH, Tenkanen L, Teppo L, et al. Prostate cancer risk and prediagnostic serum 25-hydroxyvitamin D levels (Finland). *Cancer Causes Control*. 2000;11:847–852.
5. Deschasaux M, Souberbielle JC, Latino-Martel P, et al. A prospective study of plasma 25-hydroxyvitamin D concentration and prostate cancer risk. *Br J Nutr*. 2016;115:305–314.
6. Torre LA, Bray F, Siegel RL, et al. Global cancer statistics, 2012. *CA Cancer J Clin*. 2015;65:87–108.
7. Peehl DM, Skowronski RJ, Leung GK, et al. Antiproliferative effects of 1,25-dihydroxyvitamin D3 on primary cultures of human prostatic cells. *Cancer Res*. 1994;54:805–810.
8. Hsu JY, Feldman D, Mcneal JE, Peehl DM. Reduced 1alpha-hydroxylase activity in human prostate cancer cells correlates with decreased susceptibility to 25-hydroxyvitamin D3-induced growth inhibition. *Cancer Res*. 2001;61:2852–2856.
9. Moreno J, Krishnan AV, Swami S, Nonn L, Peehl DM, Feldman D. Regulation of prostaglandin metabolism by calcitriol attenuates growth stimulation in prostate cancer cells. *Cancer Res*. 2005;65:7917–7925.
10. Swami S, Krishnan AV, Wang JY, et al. Dietary vitamin D(3) and 1,25-dihydroxyvitamin D(3) (calcitriol) exhibit equivalent anticancer activity in mouse xenograft models of breast and prostate cancer. *Endocrinology*. 2012;153:2576–2587.
11. Banach-Petrosky W, Ouyang X, Gao H, et al. Vitamin D inhibits the formation of prostatic intraepithelial neoplasia in Nkx3.1;Pten mutant mice. *Clin Cancer Res*. 2006;12:5895–5901.
12. Ajibade AA, Kirk JS, Karasik E, et al. Early growth inhibition is followed by increased metastatic disease with vitamin D (calcitriol) treatment in the TRAMP model of prostate cancer. *PLoS ONE*. 2014;9:e89555.
13. Tretli S, Hernes E, Berg JP, et al. Association between serum 25(OH)D and death from prostate cancer. *Br J Cancer*. 2009;100:450–454.
14. Xie DD, Chen YH, Xu S, et al. Low vitamin D status is associated with inflammation in patients with prostate cancer. *Oncotarget*. 2017;8:22076–22085.
15. Yin L, Raum E, Haug U, Arndt V, Brenner H. Meta-analysis of longitudinal studies: Serum vitamin D and prostate cancer risk. *Cancer Epidemiol*. 2009;33:435–445.
16. Park SY, Cooney RV, Wilkens LR, et al. Plasma 25-hydroxyvitamin D and prostate cancer risk: the multiethnic cohort. *Eur J Cancer*. 2010;46:932–936.
17. Barnett CM, Nielson CM, Shannon J, et al. Serum 25-OH vitamin D levels and risk of developing prostate cancer in older men. *Cancer Causes Control*. 2010;21:1297–1303.
18. Albanes D, Mondul AM, Yu K, et al. Serum 25-hydroxy vitamin D and prostate cancer risk in a large nested case-control study. *Cancer Epidemiol Biomarkers Prev*. 2011;20:1850–1860.
19. Holt SK, Kolb S, Fu R, et al. Circulating levels of 25-hydroxyvitamin D and prostate cancer prognosis. *Cancer Epidemiol*. 2013;37:666–670.
20. Jackson MD, Tulloch-Reid MK, Lindsay CM, et al. Both serum 25-hydroxyvitamin D and calcium levels may increase the risk of incident prostate cancer in Caribbean men of African ancestry. *Cancer Med*. 2015;4:925–935.
21. Kivineva M, Blauer M, Syvala H, Tammela T, Tuohimaa P. Localization of 1,25-dihydroxyvitamin D3 receptor (VDR) expression in human prostate. *J Steroid Biochem Mol Biol*. 1998;66:121–127.
22. Krill D, Deflavia P, Dhir R, et al. Expression patterns of vitamin D receptor in human prostate. *J Cell Biochem*. 2001;82:566–572.
23. Hendrickson WK, Flavin R, Kasperzyk JL, et al. Vitamin D receptor protein expression in tumor tissue and prostate cancer progression. *J Clin Oncol*. 2011;29:2378–2385.
24. Sakr WA, Grignon DJ, Haas GP, et al. Age and racial distribution of prostatic intraepithelial neoplasia. *Eur Urol*. 1996;30:138–144.
25. Di Silverio F, Gentile V, De Matteis A, et al. Distribution of inflammation, pre-malignant lesions, incidental carcinoma in histologically confirmed benign prostatic hyperplasia: a retrospective analysis. *Eur Urol*. 2003;43:164–175.
26. Gonzaga ACR, Campolina-Silva GH, Werneck-Gomes H, et al. Profile of cell proliferation and apoptosis activated by the intrinsic and extrinsic pathways in the prostate of aging rats. *Prostate*. 2017;77:937–948.
27. Morais-Santos M, Nunes AE, Oliveira AG, et al. Changes in Estrogen Receptor ERbeta (ESR2) Expression without Changes in the Estradiol Levels in the Prostate of Aging Rats. *PLoS ONE* 2015;10:e0131901.
28. Zhao X, Peehl D, Navone NM. Feldman, D. 1a,25-Dihydroxyvitamin D_3 inhibits prostate cancer cell growth by androgen-dependent and androgen-independent mechanisms. *Endocrinology*. 2000;141:2548–2556.
29. Murthy S, Agoulnik IU, Weigel NL. Androgen receptor signaling and vitamin D receptor action in prostate cancer cells. *Prostate*. 2005;64:362–372.
30. Leman ES, Demiguel F, Gao AC, Getzenberg RH. Regulation of androgen and vitamin d receptors by 1,25-dihydroxyvitamin D3 in human prostate epithelial and stromal cells. *J Urol*. 2003;170:235–240.
31. Leman ES, Arlotti JA, Dhir R, Getzenberg RH. Vitamin D and androgen regulation of prostatic growth. *J of cell bioc*. 2003;90:138–147.
32. Oliveira AG, Coelho PH, Guedes FD, et al. 5alpha-Androstane-3beta,17beta-diol (3beta-diol), an estrogenic metabolite of 5alpha-dihydrotestosterone, is a potent modulator of estrogen receptor ERbeta expression in the ventral prostrate of adult rats. *Steroids*. 2007;72:914–922.
33. Hollis BW. Circulating 25-hydroxyvitamin D levels indicative of vitamin D sufficiency: implications for establishing a new effective dietary intake recommendation for vitamin D. *J Nutr*. 2005;135:317–322.
34. Wang Y, Borchert ML, DeLuca HF. Identification of the vitamin D receptor in various cells of the mouse kidney. *Kidney Intern*. 2012;81:993–1001.

35. Morais-Santos M, Werneck-Gomes H, Campolina-Silva GH, et al. Basal cells show increased expression of aromatase and estrogen receptor a in prostate epithelial lesions of male aging rats. *Endocrinology*. 2018;159:723–732.
36. Brawer MK. Prostatic intraepithelial neoplasia: an overview. *Rev Urol*. 2005;7:S11–18.
37. Konety BR, Schwartz GG, Acierno JS, et al. The role of vitamin D in normal prostate growth and differentiation. *Cell Growth Differ*. 1996;7:1563–1570.
38. Giangreco AA, Dambal S, Wagner D, et al. Differential expression and regulation of vitamin D hydroxylases and inflammatory genes in prostate stroma and epithelium by 1,25-dihydroxyvitamin D in men with prostate cancer and an in vitro model. *J Steroid Biochem Mol Biol*. 2015;148:156–165.
39. Blomberg Jensen M, Nielsen JE, Jorgensen A, et al. Vitamin D receptor and vitamin D metabolizing enzymes are expressed in the human male reproductive tract. *Hum Reprod*. 2010;25:1303–1311.
40. Schleicher G, Privette TH, Stumpf WE. Distribution of soltriol [1,25 (OH)2-vitamin D3] binding sites in male sex organs of the mouse: an autoradiographic study. *J Histochem Cytochem*. 1989;37:1083–1086.
41. Mahmoudi AR, Zarnani AH, Jeddi-Tehrani M, et al. Distribution of vitamin D receptor and 1alpha-hydroxylase in male mouse reproductive tract. *Reprod Sci*. 2013;20:426–436.
42. Haussler MR, Jurutka PW, Mizwicki M, Norman AW. Vitamin D receptor (VDR)-mediated actions of 1alpha,25(OH)(2)vitamin D(3): genomic and non-genomic mechanisms. *Best Pract Res Clin Endocrinol Metab*. 2011;25:543–559.
43. Mao GE, Reuter VE, Cordon-Cardo C, et al. Decreased retinoid X receptor-alpha protein expression in basal cells occurs in the early stage of human prostate cancer development. *Cancer Epidemiol Biomarkers Prev*. 2004;13:383–390.
44. Skowronski RJ, Peehl DM, Feldman D. Vitamin D and prostate cancer: 1, 25 dihydroxyvitamin D3 receptors and actions in human prostate cancer cell lines. *Endocrinology*. 1993;132:1952–1960.
45. Yang ES, Burnstein KL. Vitamin D inhibits G1 to S progression in LNCaP prostate cancer cells through p27Kip1 stabilization and Cdk2 mislocalization to the cytoplasm. *J Biol Chem*. 2003;278:46862–46868.
46. Banerjee PP, Banerjee S, Lai JM, et al. Age-dependent and lobe-specific spontaneous hyperplasia in the brown Norway rat prostate. *Biol Reprod*. 1998;59:1163–1170.
47. Gee J, Bailey H, Kim K, et al. Phase II open label, multi-center clinical trial of modulation of intermediate endpoint biomarkers by 1alpha-hydroxyvitamin D2 in patients with clinically localized prostate cancer and high grade pin. *Prostate*. 2013;73:970–978.
48. Gallagher JC. Vitamin D and aging. *Endocrinol Metab Clin North Am*. 2013;42:319–332.
49. Xu Y, Shao X, Yao Y, et al. Positive association between circulating 25-hydroxyvitamin D levels and prostate cancer risk: new findings from an updated meta-analysis. *J Cancer Res Clin Oncol*. 2014;140:1465–1477.

How to cite this article: Campolina-Silva GH, Maria BT, Mahecha GA, Oliveira CA. Reduced vitamin D receptor (VDR) expression and plasma vitamin D levels are associated with aging-related prostate lesions. *The Prostate*. 2018;1–15. https://doi.org/10.1002/pros.23498

ARTIGO 2: Altered expression of the vitamin D metabolizing enzymes CYP27B1 and CYP24A1 under the context of prostate aging and pathologies. *Under Review.*

Journal of Steroid Biochemistry and Molecular Biology

Altered expression of the vitamin D metabolizing enzymes CYP27B1 and CYP24A1 under the context of prostate aging and pathologies

--Manuscript Draft--

Manuscript Number:	
Article Type:	Full Length Article
Keywords:	aging, prostate, prostate lesions, Vitamin D, CYP24A1, CYP27B1
Corresponding Author:	Cleida Oliveira, Ph.D UFMG BRAZIL
First Author:	Gabriel Henrique Campolina-Silva
Order of Authors:	Gabriel Henrique Campolina-Silva
	Maria Clara Barata
	Hipácia Werneck-Gomes
	Bruna Toledo Maria
	Germán Arturo Bohórquez Mahecha
	Clémence Belleannée
	Cleida Oliveira, Ph.D
Abstract:	Low circulating levels of vitamin D are common at older ages and have been linked to an increased risk of prostate disease, including cancer. However, it has not yet been determined whether aging affects the ability of prostate cells to locally metabolize vitamin D into its active metabolite calcitriol and thus mediate the vitamin D signaling in autocrine and paracrine ways. By using a powerful rat model to interrogate spontaneous prostatic modifications over the course of aging, here we showed that both CYP27B1 and CYP24A1 enzymes, which are key players respectively involved with calcitriol synthesis and deactivation, were highly expressed in the prostate epithelium. Furthermore, as the animals aged, a drastic reduction of CYP27B1 levels was detected in total protein extracts and especially in epithelial areas of lesions, including tumors. On the other hand, CYP24A1 expression significantly increased with aging and remained elevated even in altered epithelia. Such intricate unbalance in regard to vitamin D metabolizing enzymes was strongly associated with reduced bioavailability of calcitriol in the senile prostate, which in addition to decreased expression of the vitamin D receptor, further limits the protective actions mediated by vitamin D signaling. This evidence was corroborated by the increased proliferative activity exactly at sites of lesions where the factors implicated with calcitriol synthesis and responsiveness had its expression inhibited. Taken together, our results emphasize a set of modifications over the course of aging with a high potential to hamper vitamin D signaling on the prostate. These findings highlight a crosstalk between vitamin D, aging, and prostate carcinogenesis, offering new potential targets in the prevention of malignancies and other aging-related disorders arising in the gland.
Suggested Reviewers:	Catarina Segreti Porto, Ph.D Full Professor, Universidade Federal de São Paulo (UNIFESP) csporto@unifesp.br
	Amado A. Quintar, Ph.D Professor, National University of Cordoba aquintar@cmefcm.uncor.edu

May 14, 2020

Jerzy Adamski
Editor-In-Chief – The Journal of Steroid Biochemistry and Molecular Biology

Dear Dr. Jerzy Adamski

Please find enclosed the manuscript titled **"Altered expression of the vitamin D metabolizing enzymes CYP27B1 and CYP24A1 under the context of prostate aging and pathologies"** to be considered for publication as original article in The Journal of Steroid Biochemistry and Molecular Biology.

This is a pioneering study showing that aging, the main risk factor linked to prostate disorders including cancer, plays significative effects on the three classes of components related to the vitamin D signaling: (i) hormone; (ii) metabolizing enzymes; and (iii) receptors. The changes presently found provide strong evidence that vitamin D signaling and, consequently, its protective effect is attenuated in the aging prostate, thereby favoring the development of histopathological alterations that disrupt tissue homeostasis and may even progress to cancer. These unprecedented findings highlight crosstalk between vitamin D, aging, and prostate carcinogenesis, offering new perspectives for the design of vitamin D-based therapies targeting malignancies and other aging-related prostate disorders.

This original study has not been submitted, accepted or published either in part or as a whole. The authors declare that it will not be submitted for publication elsewhere until the Editorial board of The Journal of Steroid Biochemistry and Molecular Biology has decided whether to publish the paper. We appreciate your time considering our manuscript and look forward to receiving your editorial decision.

Sincerely,

Prof. Dr. Cleida Aparecida Oliveira

Altered expression of the vitamin D metabolizing enzymes CYP27B1 and CYP24A1 under the context of prostate aging and pathologies

Gabriel Henrique Campolina-Silva[1], Maria Clara Barata[1], Hipácia Werneck-Gomes[1], Bruna Toledo Maria[1], Germán Arturo Bohórquez Mahecha[1], Clémence Belleannée[2], Cleida Aparecida Oliveira[1]

[1]Department of Morphology, Universidade Federal de Minas Gerais, Cx. Postal 486, CEP 31.270-901, Belo Horizonte, MG, Brazil

[2] Faculty of Medicine, Department of Obstetrics, Gynecology and Reproduction, Université Laval, CHU de Québec Research Center (CHUL), Quebec City, QC, Canada

To whom correspondence should be addressed:
Cleida Aparecida Oliveira
Av. Antônio Carlos, 6627
31270-901, Belo Horizonte, MG - Brasil.
Phone: +55.31.3409-2795
E-mail: cleida@icb.ufmg.br

Keywords: aging, prostate, prostate lesions, Vitamin D, CYP24A1, CYP27B1

ABSTRACT

Low circulating levels of vitamin D are common at older ages and have been linked to an increased risk of prostate disease, including cancer. However, it has not yet been determined whether aging affects the ability of prostate cells to locally metabolize vitamin D into its active metabolite calcitriol and thus mediate the vitamin D signaling in autocrine and paracrine ways. By using a powerful rat model to interrogate spontaneous prostatic modifications over the course of aging, here we showed that both CYP27B1 and CYP24A1 enzymes, which are key players respectively involved with calcitriol synthesis and deactivation, were highly expressed in the prostate epithelium. Furthermore, as the animals aged, a drastic reduction of CYP27B1 levels was detected in total protein extracts and especially in epithelial areas of lesions, including tumors. On the other hand, CYP24A1 expression significantly increased with aging and remained elevated even in altered epithelia. Such intricate unbalance in regard to vitamin D metabolizing enzymes was strongly associated with reduced bioavailability of calcitriol in the senile prostate, which in addition to decreased expression of the vitamin D receptor, further limits the protective actions mediated by vitamin D signaling. This evidence was corroborated by the increased proliferative activity exactly at sites of lesions where the factors implicated with calcitriol synthesis and responsiveness had its expression inhibited. Taken together, our results emphasize a set of modifications over the course of aging with a high potential to hamper vitamin D signaling on the prostate. These findings highlight a crosstalk between vitamin D, aging, and prostate carcinogenesis, offering new potential targets in the prevention of malignancies and other aging-related disorders arising in the gland.

1. INTRODUCTION

The prostate is regulated by a complex interplay of endocrine, paracrine and autocrine signals, including vitamin D that carry out multiple roles in the body other than regulation of mineral homeostasis [1], such as anti-inflammatory, anti-carcinogenic and metabolic actions [2-6]. Accumulating in vitro and in vivo experimental studies have shed light on the mechanisms by which vitamin D signaling plays beneficial actions in the prostate. This includes attenuation of cellular proliferation, angiogenesis and synthesis of pro-inflammatory mediators, as well as induction of cellular differentiation, apoptosis and control of energy metabolism [7-12]. Such actions are corroborated in part by epidemiological data showing a positive correlation between vitamin D deficiency and increased risk of prostate cancer [13-16], one of the most diagnosed malignancies worldwide [17]. However, clinical trials enrolling patients with prostatic adenocarcinoma and administration of vitamin D or its bioactive metabolite, known as $1,25(OH)_2D$ or calcitriol, have provided limited antitumor benefits, especially in those patients with hormone-refractory prostate cancer [18-24]. This intriguing issue draws attention to the urgent need for understanding factors hampering the vitamin D signaling in the gland.

The classic paradigm for vitamin D signaling is that prior to binding to the vitamin D receptor (VDR), vitamin D molecules produced in the skin upon exposure to sunlight (cholecalciferol, vitamin D_3) or supplied as a component of the diet (ergocalciferol, vitamin D_2 as well as vitamin D_3) need to be first converted to an intermediate metabolite called 25(OH)D and then metabolized into calcitriol [25]. Therefore, some players other than VDR are critical to ensure this signaling, including the enzymes 1α-hydroxylase CYP27B1 and 24-hydroxylase CYP24A1, which play antagonistic roles in vitamin D metabolism. While CYP27B1 is responsible for synthesizing calcitriol from its precursor 25(OH)D, the CYP24A1 acts reducing calcitriol into less active metabolites, thereby controlling the bioavailability of

the VDR ligand [25]. Thus, the levels of VDR, as well as calcitriol and its metabolizing enzymes are thought to dictate the action spectrum of the vitamin D signaling in target tissues. In line, evidence has demonstrated that the growth-inhibitory action of vitamin D supplementation in prostate cells correlates positively with the endogenous amounts and/or activity of CYP27B1 and VDR, and inversely with CYP24A1 expression [26-29]. However, the status of these potential predictive factors of vitamin D response has been overlooked in the clinical outcome of vitamin D-based therapies, and very little is known about their spatial-temporal distributions in the prostate gland.

In this scenario, a recent study reported that VDR, as well as its heterodimeric partner, the retinoid X receptor (RXR), are downregulated specifically in aging-related prostate lesions that exhibited pronounced proliferative activity and include tumor initiation sites [30]. Such lesions appeared in the prostatic epithelium at the same advanced ages in which plasma 25(OH)D drastically declined, pointing to a plausible relationship between vitamin D, aging, and prostate disorders. However, little is known about the vitamin D metabolizing enzymes under the context of prostate aging and pathologies. Moreover, most investigations targeting such enzymes in the gland employed cell cultures, so that a comprehensive study describing their distribution in the prostatic tissue is still needed. Therefore, in the present study, we systematically examined the expression pattern of the vitamin D metabolizing enzymes CYP27B1 and CYP24A1 in the prostates of young adults, middle-aged and senile Wistar rats, a valuable *in vivo* model for studying aging-related prostatic disorders including cancer.

2. MATERIALS AND METHODS

2.1 Experimental animals

The investigation was undertaken in the prostate of young adults (3 and 6 months), middle-aged (12 months), and senile (18 and 24 months) Wistar rats kept in the absence of surgical and chemical interference. The animals (n= 10 per age) were housed in a proper animal facility at the Universidade Federal de Minas Gerais (UFMG), receiving *ad libitum* access to water and standard pelleted chow (Nuvilab CR1, Nuvital Nutrientes S.A, Colombo, Brazil) containing 2.000 IU vitamin D_3/Kg [30]. No changes in food consumption were observed among the groups.

Complementarily, prostate tissues from a previous cohort of senile Wistar rats chronically treated with testosterone and estradiol to induce prostate carcinogenesis [31] were also employed. Animal experiments received the approval of the Ethical Committee for Animal Experimentation of the UFMG (CEUA licenses 286/2008 and 344/2018).

2.2 Sample collection and processing

Prostate samples were obtained from rats under deep anesthesia (i.p injection of 87 mg ketamine/Kg and 13 mg xylazine/Kg) and perfused transcardially with Ringer's solution followed by 10% neutral buffered formalin (NBF). The prostatic complex consisting of the ventral (VP), lateral (LP), dorsal (DP), and anterior (AP) prostate lobes was harvested from 5 animals per group, dissected, immersed in NBF solution, and then processed for paraffin embedding (FFPE samples). Otherwise, a similar number of animals per group was perfused only with Ringer's solution and their prostate lobes were harvested, snap-frozen in liquid nitrogen, and stored at -80 ºC. Blood samples were collected immediately before perfusion through cardiac puncture and placed in heparin-coated tubes for plasma separation, by centrifugation at 800 g for 5 min.

2.3 Calcitriol dosage

Liquid-phase extraction of steroids was applied to plasma and tissue samples before calcitriol measurements [32]. Briefly, frozen ventral prostates were macerated in dry ice and 200 mg of the pulverized tissue was solubilized in 1 mL of chilled PBS. Tissue homogenates and plasma samples (200 µL) were then vigorously mixed to diethyl ether at 5:1 (v/v) solvent:sample ratio. After complete phase separation by centrifugation (800 g for 5 min), samples were frozen in dry ice/ethanol bath and the floating solvent fraction was transferred into a new centrifuge tube. Two other rounds of diethyl ether mixing and supernatant collection were performed for every sample. The pooled steroid-enriched solvent fraction was dried in a Savant SpeedVac® Concentrator and stored at -20 ºC. Matched samples spiked with 50 pg/mL of calcitriol were used to assess the hormone recovery rate following steroid extraction.

Circulating and intraprostatic concentrations of calcitriol were determined by using a competitive ELISA assay (Cat. nº OKEH02542, AVIVA Systems Biology), following the manufacture's instruction. To this end, dried extracted samples were resuspended in 100 µL of 1x ELISA buffer immediately prior to assay and measured in duplicate. The sensitivity of the assay was 3.6 pg/mL and proper recovery rates of calcitriol were obtained from plasma (93%) and tissue (88%) samples.

2.4 Histopathology

Histopathological changes arising spontaneously in the prostate parenchyma of aging Wistar rats or those hormonally-induced by testosterone plus estradiol were described according to established parameters [30,33,34]. In this approach, FFPE sections stained with hematoxylin and eosin as well as supportive immunohistochemical preparations were examined.

2.5 Immunohistochemistry

FFPE prostate sections at 5µm thickness were submitted to immunohistochemical detection of targets related to vitamin D metabolism and responsiveness, cell proliferation, and basal cell phenotype, based on our previous protocol [30]. Primary and secondary antibodies used in the assays are listed in Table S1. The immunoreaction was acquired using an Avidin-Biotin Complex (ABC)-based detection system (Cat. nº PK-6100, Vector Laboratories) followed by 3,3'-diaminobenzidine (DAB) reaction. Negative controls received only PBS in place of each primary antibody. To confirm the results, the assays were performed in triplicate.

2.6 Immunofluorescence

Immunofluorescence assays were employed to colocalize CYP27B1 and CYP24A1 with each other or with VDR, RXR, and the basal cell marker CKHMW. For this purpose, 5µm thick FFPE sections were submitted to antigen retrieval and nonspecific binding blockage [30] prior to 40 h incubation at 4 ºC with a solution containing the primary antibodies of interest (Table S1). Negative controls were established by omitting primary antibodies. After several washes in PBS, the tissue sections were exposed for 2 h at RT to Alexa Fluor-conjugated secondary antibodies (Table S1). Monovalent unconjugated Fab fragments of affinity-purified secondary antibodies (Jackson ImmunoResearch) were employed to enable multiple labeling. Cell nuclei were counterstained with 1 µg/mL DAPI. The fluorescent signals were examined in the Zeiss ApoTome.2 microscope equipped with an epi-illumination module and specific filters for suitable detection of the Alexa Fluor dyes presently used.

2.7 Western blotting

Total protein levels of CYP27B1 and CYP24A1 in rat prostates were evaluated by Western blotting. For this purpose, protein extracts from VP and LP frozen samples of rats at different ages (3, 6, 12, 18, and 24 months, n= 5) were first obtained using 8M urea buffer, electrophoretically separated and transferred to nitrocellulose membranes [30]. After blocking nonspecific bindings with 10% normal goat serum, the membranes were incubated overnight at 4ºC with primary antibodies raised against CYP27B1, CYP24A1, or β-actin protein, washed in PBS, and then exposed (for 1h at RT) to biotinylated secondary antibodies followed by ABC incubation. The list of antibodies used is provided in Table S1. The correspondent immunoreactive bands of rat CYP27B1 (54 kDa), CYP24A1 (55 kDa), and β-actin (42 kDa) were visualized following enhanced chemiluminescence (ECL detection) and quantified by densitometric analysis [35]. β-actin was used for data normalization. The assays were performed in triplicate to confirm the results.

2.8 Computer-assisted image analysis

To estimate the positivity rates of CYP27B1 and CYP24A1 in the prostate epithelium at different ages, pictures at 400x magnification were randomly taken in each immunofluorescence section of the VP and LP. The number of cells positive or negative for each or both enzymes was determined in 6 distal acini with normal morphology, totalizing approximately 765 cells counted per animal. The expression of CYP27B1 and CYP24A1 was also compared between basal and luminal cells [36]. The epithelial cell types were differentiated based on their positioning within the epithelium, nuclear morphology, and CKHMW staining pattern. Next, we evaluated the number and staining intensity of both CYP27B1+ and CYP24A1+ cells in immunohistochemistry sections of the ventral and lateral prostate presenting atrophic, metaplastic and proliferative aging-related lesions, and compared with the adjacent normal epithelium, as previously described [30]. The number of

MCM7+ proliferating cells was also established in epithelial lesions and normal adjacent epithelium.

2.9 Statistical analyses

GraphPad Prism 7 software (GraphPad Software, La Jolla, CA) was used for statistical analyses. After normality assessment using Q-Q plot and Shapiro-Wilk test, comparisons between two or more parametric datasets were performed by Student's *t*-test or one-way ANOVA plus Tukey post hoc test, respectively. Otherwise, the Wilcoxon matched-pairs signed rank test or Kruskal-Wallis plus Dunn's post hoc test were used to compare nonparametric data between two or more groups, respectively. Statistical dependence between two variables was assessed by Spearman’s correlation. The significance level used for all tests was $p < 0.05$.

3. RESULTS

3.1 Immunolocalization of CYP27B1 and CYP24A1 in the prostate

Although there is some evidence that prostate cells express vitamin D metabolizing enzymes [37,38], a detailed characterization of the cellular and subcellular distribution of CYP27B1 and CYP24A1 in the gland is still needed. Hence, we first sought to determine the expression pattern of such enzymes in the prostatic complex of adult Wistar rats (Fig. 1A).

As shown by Western blot assays, molecular weight compatible bands for CYP27B1 (54 kDa) and CYP24A1 (55 kDa) were specifically detected throughout the adult rat prostate (Fig. 1B). However, the levels of each enzyme varied according to the prostate lobe. The CYP24A1 expression was significantly higher in the VP, whereas the CYP27B1 signal was more pronounced in both VP and LP and occurred at comparable levels to that from whole kidney extracts (Fig. 1B), one of the main organs fully competent in metabolizing and responding to vitamin D [39,40].

Concerning the spatial distribution of the enzymes within the adult prostate, immunoreactivity for CYP27B1 and CYP24A1 were primarily found in the cytoplasm of epithelial cells (Fig. 1C) and did not vary between luminal (CKHMW-) and basal (CKHMW+) epithelial cells (Fig. 1D, E). Interestingly, few cells unreactive for CYP27B1 or CYP24A1 were observed in colocalized areas within the normal-appearing epithelium. These epithelial cells usually exhibited a slightly enlarged rounded nucleus with a prominent nucleolus (Fig. 1F). Therefore, we next checked whether the prostate epithelium could harbor a small population of atypical cells lacking the machinery necessary to locally produce and deactivate calcitriol. Multiple labeling immunofluorescence assay showed that 98% of all epithelial cells displayed cytoplasmic staining for both CYP27B1 and CYP24A1, whereas 1.1% and 0.9% of the cells did not express any of these enzymes or only had the CYP27B1, respectively (Fig. 1G,H). Although such epithelial cells appear to be unable to locally

metabolize calcitriol, they still retain the ability to mediate the vitamin D signaling as they express VDR and its partner RXR (Fig. 1I).

3.2 An intricate imbalance between CYP27B1 and CYP24A1 limits calcitriol bioavailability in the aging prostate

It is well known that advancing age sharply raises the risk of prostate disorders including cancer [41,42]. This relationship likely reflects an exacerbation of environmental interferences throughout life including changes in the vitamin D status, since vitamin D deficiency is a common condition in older adults [43-45].To gain insights into the plausible link between vitamin D, aging and prostate health, we next evaluated the expression of CYP24A1 and CYP27B1 as well as calcitriol levels over the course of aging.

Through Western blotting assays, we observed higher CYP27B1 expression in the prostate gland of young rats (3 and 6 months) in comparison with those aged 12 or more months, opposing that observed for CYP24A1, whose expression markedly increased as the animals aged (Fig. 2B). The measurements were performed in total protein extracts from more than one prostate lobe (VP and LP) to confirm the result. Strikingly, additional analysis of transcriptomic data annotated in 79 non-pathological prostate samples contemplated by the GTEx project [46] showed a very similar aging-related change regarding the expression of CYP27B1 and CYP24A1 in the human prostate (Fig. 2C). These results prompted us to investigate whether such intricate unbalance between the vitamin D metabolizing enzymes could limit the availability of calcitriol in the aged prostate. Indeed, the intraprostatic concentrations of calcitriol determined in the VP, the prostatic lobe exhibiting pronounced expression of both CYP27B1 and CYP24A1, was significantly lower in middle-aged and senile rats compared to young ones (Fig. 2D). Plasma calcitriol levels, despite presenting a gradual and subtle decline over aging, remained statistically similar at all ages evaluated (Fig. 2D). Correlation analysis confirmed that the age-related reduction of calcitriol levels

within the prostate was inversely correlated to CYP24A1 expression (Spearman r= -0.45, p=0.039) and mainly positively correlated to CYP27B1 expression (Spearman r= 0.61, p= 0.0035) (Fig. 2E).

3.3 Altered expression of CYP27B1 but not CYP24A1 occurred restricted to sites of histopathological lesions

To further investigate the changes observed in total protein extracts, the vitamin D metabolizing enzymes were immunohistochemically evaluated in the prostate gland of Wistar rats at different ages. As previously described [30,31,47], one advantage of using such experimental model takes into account the spontaneous development of age-related prostatic alterations, which include atrophic, metaplastic, and proliferative lesions. These altered areas are more frequent in the LP and VP of senile animals, being adjacent to unaltered epithelia, and also exhibit reduced expression of VDR and RXR [30].

Regardless the animals' age, nearly all epithelial cells lining normal-appearing ducts and acini of the prostate expressed CYP27B1 (Fig. 3B). The few CYP27B1-negative epithelial cells (~1%) present in areas devoid of morphological changes occurred isolated or forming small groups, as shown in Fig. 1F-I. However, lower and heterogenous CYP27B1 expression was found in areas of epithelial lesions that arose in the prostate of rats aged 12 months and older, as numerous unstained cells were found alongside cells barely or moderately stained (Fig. 3B and Fig. S1). These histopathological lesions include focal epithelial atrophies, hyperplasia and squamous metaplasia (Fig. S1), all alterations of benign nature, as well as the two recognized precursor lesions of prostate cancer [48]: the proliferative inflammatory atrophy (PIA) and prostatic intraepithelial neoplasia (PIN) (Fig. 3B). Moreover, some lesioned areas histopathologically-compatible with adenocarcinomas were also observed in the prostate gland of rats aged 18 and 24 months (Fig. 3B), albeit at lower frequencies than other alterations (Table S2). The malignant sites were actively

proliferative, similarly to that observed for their precursor lesions PIN and PIA, and displayed an abnormal growth pattern where crowded, basophilic, and dysplastic-appearing cells arranged in a microacinar architecture, in which the CYP27B1 expression appeared to be downregulated (Fig. 3B). The computer-assisted image analyses confirmed that both the number and staining intensity of CYP27B1+ cells significantly reduced in all lesions evaluated, compared to the adjacent normal epithelium (Fig. 3C,E and Fig. S1). Such a specific decrease of CYP27B1 expression goes in line with the aging-related changes detected from 12 months onwards by Western blotting assays (Fig. 2B).

Unlike CYP27B1, no difference existed when the CYP24A1 expression was compared between aging-related epithelial lesions and the adjacent normal epithelium (Fig. 3B,D and Fig. S1). However, it was noteworthy that CYP24A1+ epithelial cells from VP and LP of rats aged 12 months and older had stronger cytoplasmic immunoreactivity than those from younger animals (Fig. 3B, F). This finding points to an increased abundance of CYP24A1 per cell with advancing age, thus corroborating the Western blotting results (Fig. 2B).

3.4 Age-related reduction of CYP27B1 expression strongly correlates with epithelial cell proliferation

In vitro experiments have shown that endogenous 1α-hidroxilase activity of CYP27B1 and, consequently, the local production of calcitriol functions as an important mitosis inhibitor in normal, hyperplastic and tumor cells of the prostate [27,29]. Herein, by using serial sections from the ventral and lateral prostate of middle-aged and senile rats, we also showed that high number of MCM7+ proliferating cells occurred exactly in the altered areas presenting significant reduction in CYP27B1 expression (Fig. 3B). Correlation analysis confirmed the existence of a strong inverse correlation between cell proliferation and the

number (r= -0.96, p <0.0001) and staining intensity (r= -0.89, p < 0.0001) of CYP27B1+ cells in the aging prostate epithelium (Fig. 3E).

Complementary to the natural aging model, we also investigate the expression status of components implicated in the synthesis and response to calcitriol in proliferative prostate lesions of 18-month-old Wistar rats chronically treated with testosterone plus estradiol. The use of this additional experimental model, in which 100% of animals develop prostate adenocarcinomas [31], was important to confirm the changes presently observed in those few malignant lesions that arose spontaneously in the senile prostate. As expected, the expression of CYP27B1, VDR and RXR but not CYP24A1 was downregulated at sites of adenocarcinomas, concomitantly with an enhanced cell proliferation activity (Fig. 4). Furthermore, similar changes were observed in non-cancerous prostate lesions that also arose in this model of hormonally-induced prostate tumorigenesis, such as PIN, PIA, hyperplasia, and squamous metaplasia (Table S3).

4. DISCUSSION

The present study describes the spatial-temporal expression of CYP27B1 and CYP24A1 in the prostate gland, the two major enzymes responsible, respectively, for the synthesis and deactivation of calcitriol, the vitamin D active metabolite. Our results show that both enzymes are highly expressed in the prostate epithelium and had their expression markedly changed over the course of aging, with significant consequences for the bioavailability of calcitriol and its downstream beneficial effects on the gland (outlined in Fig. 5).

Regardless the animals' age, positivity for CYP27B1 and CYP24A1 were mainly observed in the cytoplasm of cells localized in the epithelial compartment, which includes both luminal and basal epithelial cells. Previous studies evaluating non-pathological human prostates have also detected the expression of such enzymes primarily in the epithelium, despite the authors have not distinguished the different epithelial cell types [37,49]. These data place the glandular epithelium as the main prostate compartment competent for metabolizing vitamin D. Circulating in the bloodstream, calcitriol acts in an endocrine way at sites of VDR expression, a ligand-induced transcription factor found in nearly every tissue and that acts in cooperation with RXR receptors [50]. It was recently shown [30] and presently reaffirmed that both VDR and RXR are highly expressed in the prostatic epithelium. Together with the possibility that prostate cells locally synthesizing calcitriol from its precursor 25(OH)D by the 1α-hydroxylase action of CYP27B1, our findings evidence *in vivo* that vitamin D signaling can be autocrinally and/or paracrinally triggered in the gland. Although the kidney has long been thought to be the central source of circulating calcitriol (reviewed by Bikle et al. [51]), the finding that some regions of the rat prostate express CYP27B1 at comparable levels to kidneys opens perspectives to further investigate the relevance of the prostate gland for contributing to the body levels of calcitriol in males.

One of the most explored therapeutic potential of calcitriol against prostate cancer is its growth-inhibitory effect, which occurs in a dose-dependent manner and involves downregulation of cell growth stimulating factors, thereby triggering G1/S cell cycle arrest [6,7,9,10]. However, a significant antitumor effect may be difficult to achieve *in vivo*, given that exogenous calcitriol can potentially cause extreme hypercalcemia and thus, the administration of calcitriol is only considered safe at low doses, since exogenous calcitriol has high potential to cause dangerous hypercalcemia [52]. The present finding that the majority of prostate epithelial cells express CYP27B1 raises the possibility that supplementation with the precursor 25(OH)D or even vitamin D, which hardly cause side effects because of their low binding affinity to VDR, could potentially increase intraprostatic levels of calcitriol and therefore inhibits the growth of prostate cancer cells. In line with this interpretation, Hsu et al. [29] showed that 25(OH)D was capable to block the growth of different primary epithelial cell strains derived from normal and pathologic human prostates. However, the growth-inhibitory effect played by 25(OH)D was higher in normal than hyperplastic and tumor cells, which was ascribed to differences in the CYP27B1 activity concerning epithelial cells derived from normal and altered prostates [29].

An important observation reported herein was that the prostatic expression of CYP27B1 drastically reduced with advancing age in altered areas exhibiting atrophies, hyperplasia, metaplasia, premalignant lesions and tumors. Paradoxically, the CYP24A1 expression significantly increased in both normal and altered epithelia of the aged prostate. This aging-related shift concerning the major enzymes involved in calcitriol synthesis and deactivation played a significant role in limiting the local availability of calcitriol, since the intraprostatic concentration of this hormone also decreased with age, paralleling changes in the enzymatic expression. Taken together, these results provide solid evidence that the prostatic synthesis of calcitriol from its precursor 25(OH) coming from the bloodstream is affected by aging. Based on the fact that circulating 25(OH)D is commonly found at low

levels in older adults [30,43-45] and that age-related declines in CYP27B1 expression has also been reported for kidney, bone, small intestine, and parathyroid glands [53-55], it is likely that local synthesis of calcitriol might be compromised at advanced ages in numerous other tissues other than the prostate.

Importantly, we have recently shown [30] and presently reaffirmed that, similar to CYP27B1, the expression of VDR and RXR, both transcript factors required to form the vitamin D signaling complex, is specifically attenuated in the aging-related prostate lesions. Altogether, these data suggest that, while maintaining a normal CYP24A1 expression and thereby the basal ability to inactivate calcitriol, the altered areas of the aging prostate epithelium, which includes sites of premalignant lesions and tumors, exhibited reduced capability not only to synthesize calcitriol but also to transduce its local protective effects. In line with this, the cell proliferation rates in the prostates of aging Wistar rats were inversely correlated with the CYP27B1 levels, as well as with the expression previously portrayed for VDR and RXR [30]. *In vitro* experiments have also showed that the anti-proliferative effect played by vitamin D signaling in prostate cells is positively dependent on the CYP27B1 activity and VDR expression [29,56], and can be enhanced by pharmacological inhibition of CYP24A1 [28]. Therefore, individual differences on these components could explain the limited antitumor effect provided by administration of vitamin D or calcitriol in patients diagnosed with prostate cancer [18-24], as well as shed light on the conflicting epidemiological data concerning the circulating levels of vitamin D metabolites and prostate cancer risk or progression [57,58]. We argue that future studies on the administration of calcitriol or a less calcemic VDR agonist, in association with strategies to regulate the expression and/or activity of CYP27B1, CYP24A1, VDR, and RXR may open new avenues concerning the use of vitamin D-based therapies against prostate diseases including cancer.

Nonetheless, we emphasize that our results were unable to establish a cause-effect relationship between the modifications involving the components of the vitamin D system

and the onset of histopathological lesions in the prostate, even though both events were observed in experimental animals at the same ages (from 12 months onwards). However, it is plausible to consider that reduced capacity of response to calcitriol and, consequently, the maintenance of a high proliferative activity in the senile prostate, might contribute significantly to prostate carcinogenesis. Reinforcing this point of view, Banach-Petrosky et al. [59] demonstrated that the administration of calcitriol was able to inhibit cellular proliferation and suppress the progression of premalignant lesions into tumors by using mice mutant for Nkx3.1 and Pten, which recapitulate stages of prostatic carcinogenesis from PIN to adenocarcinoma.

In summary, our work highlights a combinatory modification over the course of aging with a high potential to impair the protective effects mediated by the vitamin D signaling on the prostate, and thereby favoring the appearance of histopathological alterations in the aging prostate that may disrupt tissue homeostasis and even progress to cancer.

ACKNOWLEDGMENTS

We thank the Conselho Nacional de Desenvolvimento Científico e Tecnológico – CNPq (Grant and Research fellowship to C.A.O and PIBIC scholarship to M.C.B), Fundação de Amparo a Pesquisa do Estado de Minas Gerais - FAPEMIG (Grant to C.A.O), Coordenação de Aperfeiçoamento de Pessoal de Nível Superior-CAPES/Brazil (Doctoral fellowship to G.H.C·S and Masters fellowship to B.T.M and H.W.G) for their financial support. We are also grateful to Dr. Gustavo Menezes and Center for Acquisition and Processing of Images of the UFMG for providing some reagents and access to the ApoTome.2 microscope.

AUTHOR CONTRIBUTIONS

Gabriel H. Campolina-Silva: Conceptualization; Investigation; Formal analysis; Validation; Writing-Original draft preparation. **Maria C. Barata, Hipácia Werneck-Gomes, and Bruna T. Maria:** Formal analysis; Visualization. **Germán A. B. Mahecha and Clémence Belleannée:** Resources; Writing- Reviewing and Editing. **Cleida A. Oliveira:** Supervision; Visualization; Writing- Reviewing and Editing; Funding acquisition.

CONFLICTS OF INTEREST

All the authors have nothing to disclose

MAIN FILES

Legends followed by their respective figures

Figure 1: Expression pattern of CYP27B1 and CYP24A1 in the prostatic complex of adult Wistar rats. (A) Experimental strategy. (B) Representative Western blotting comparing the levels of CYP27B1 and CYP24A1 among different prostate lobes and kidney, as control tissue. Mean values accompanied by standard error bars with different letters represent statistically significant differences ($p < 0.05$) assessed by Kruskal-Wallis plus Dunn's post hoc test. n= 5 per tissue. (C) Immunofluorescence showing that CYP27B1 and CYP24A1 are primarily expressed in the prostatic epithelium. (D) Double labeling assay showing that both enzymes are expressed by basal (CKHMW+) and luminal (CKHMW-) epithelial cells. (E) Quantification of the mean fluorescence signals represented in (D) between basal cells and the adjacent luminal cells. $p > 0.05$ by paired *t* test. n= 10 per lobe. (F) Serial sections immunostained for CYP27B1 and CYP24A1 showing a group of unreactive epithelial cells occurring in colocalized areas. (G, H) Double labeling evidencing that most epithelial cells expressed both vitamin D metabolizing enzymes (arrowhead 1), while few cells presented neither enzyme (arrowhead 2) or only CYP27B1 (arrowhead 3). (I) Multiple labeling immunofluorescence showing that the cells unreactive for CYP27B1 and CYP24A1 express the VDR and RXR transcription factors. The images were taken in the ventral prostate of rats aged 3 to 6 months and are representative of all prostate lobes. VP: ventral prostate. DP: dorsal prostate. LP: lateral prostate. AP: anterior prostate. Lu: lumen. S: stroma. IHC: immunohistochemistry. IF: immunofluorescence. WB: Western blotting.

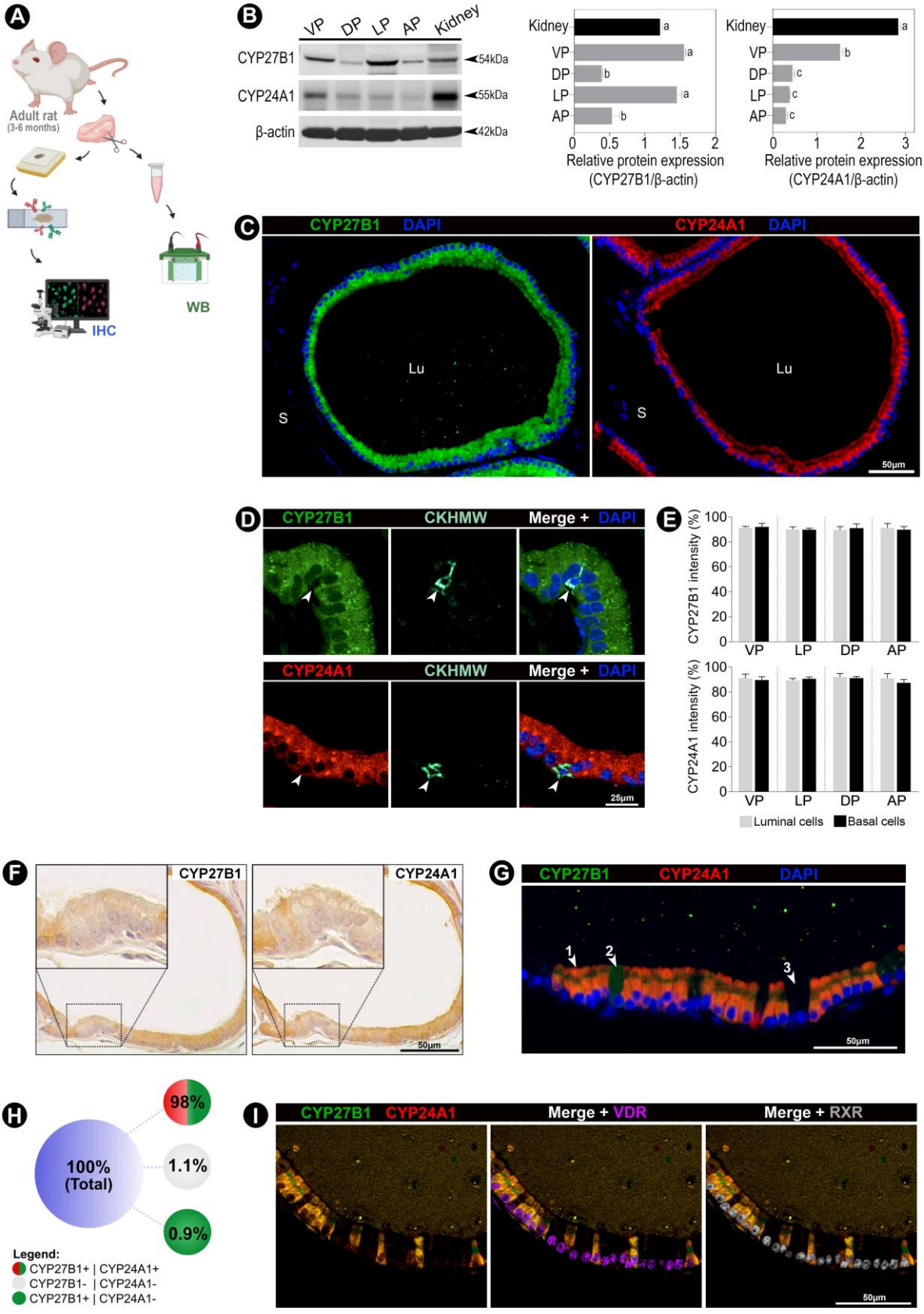
A
Adult rat
(3-6 months)
WB
IHC
B
VP
DP
LP
AP
Kidney
CYP27B1
CYP24A1
β-actin
54kDa
55kDa
42kDa
Kidney
VP
DP
LP
AP
Relative protein expression
(CYP27B1/β-actin)
Relative protein expression
(CYP24A1/β-actin)
C
CYP27B1 DAPI
CYP24A1 DAPI
Lu
S
50μm
D
CYP27B1 CKHMW Merge + DAPI
CYP24A1 CKHMW Merge + DAPI
25μm
E
CYP27B1 intensity (%)
CYP24A1 intensity (%)
VP LP DP AP
Luminal cells
Basal cells
F
CYP27B1
CYP24A1
50μm
G
CYP27B1 CYP24A1 DAPI
1
2
3
50μm
H
98%
1.1%
0.9%
100%
(Total)
Legend:
CYP27B1+ | CYP24A1+
CYP27B1- | CYP24A1-
CYP27B1+ | CYP24A1-
I
CYP27B1 CYP24A1
Merge + VDR
Merge + RXR
50μm

Figure 2: Aging-related unbalance between CYP27B1 and CYP24A1 with consequences in the intraprostatic concentration of calcitriol. (A) Experimental strategy. (B) Western blotting comparing the total protein levels of CYP27B1 and CYP24A1 in the ventral and lateral prostates of rats at different ages. Mean values accompanied by standard error bars with different letters represent statistically significant differences ($p < 0.05$) assessed by one-way ANOVA plus Tukey post hoc test. n= 5 per age. (C) Transcriptional activity of CYP27B1 and CYP24A1 genes in non-pathological prostate samples from young (<40 years old, n= 35) and elderly (>60 years old, n= 44) men contemplated by the GTEX consortium. $p < 0.05$, unpaired *t* test. (D) Calcitriol concentrations determined by ELISA in the plasma and VP samples of rats at different ages. Box plots with different letters represent statistically significant differences ($p < 0.05$) assessed by one-way ANOVA plus Tukey post hoc test. n= 5 per age. The whiskers go from each the 25^{th} to 75^{th} percentiles to the minimum or maximum value. (E) Spearman correlation analysis between individual values obtained for calcitriol levels and the ventral prostate expression of CYP27B1 and CYP24A1. VP: ventral prostate. LP: lateral prostate. 3, 6, 12, 18, and 24M = age of the animals expressed in months.

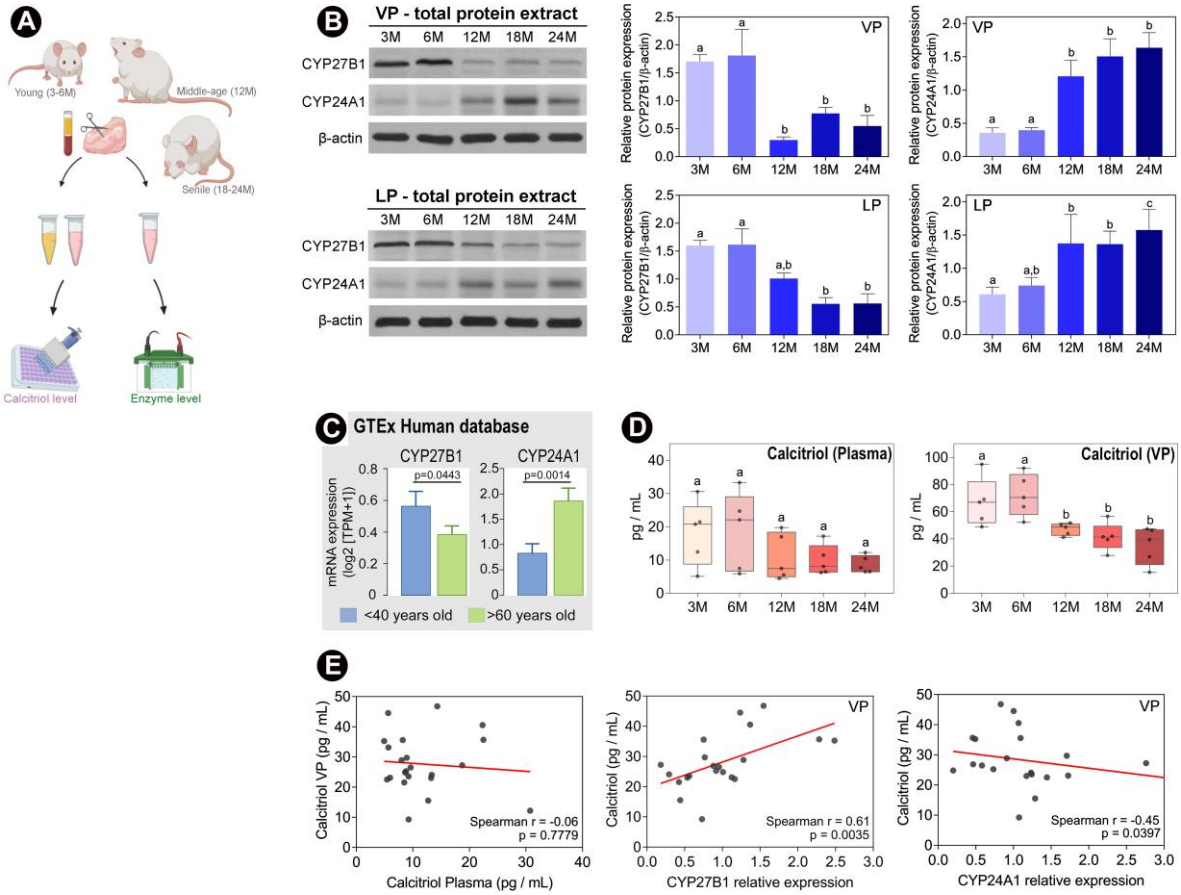
A
Young (3-6M)
Middle-age (12M)
Senile (18-24M)
Calcitriol level
Enzyme level
B
VP - total protein extract
3M 6M 12M 18M 24M
CYP27B1
CYP24A1
β-actin
LP - total protein extract
3M 6M 12M 18M 24M
CYP27B1
CYP24A1
β-actin
Relative protein expression (CYP27B1/β-actin)
VP
Relative protein expression (CYP24A1/β-actin)
VP
Relative protein expression (CYP27B1/β-actin)
LP
Relative protein expression (CYP24A1/β-actin)
LP
C
GTEx Human database
CYP27B1
CYP24A1
p=0.0443
p=0.0014
mRNA expression (log2 [TPM+1])
<40 years old
>60 years old
D
Calcitriol (Plasma)
pg / mL
Calcitriol (VP)
pg / mL
E
Calcitriol VP (pg / mL)
Spearman r = -0.06
p = 0.7779
Calcitriol Plasma (pg / mL)
Calcitriol (pg / mL)
VP
Spearman r = 0.61
p = 0.0035
CYP27B1 relative expression
Calcitriol (pg / mL)
VP
Spearman r = -0.45
p = 0.0397
CYP24A1 relative expression

Figure 3: CYP27B1 expression but not CYP24A1 is affected in histopathological altered areas of the aging prostate epithelium. (A) Experimental strategy. (B) Representative images taken from unaltered and altered regions of the lateral prostate highlighting a reduction of CYP27B1 expression specifically at proliferative sites (MCM7+) of premalignant and malignant nature that arose in the prostate epithelium of rats aged 12 months and older and exhibit prominent expression of CYP24A1. Details on the incidence of lesions were provided in table S1. Arrowhead: indicates cells unreactive or barely stained for CYP27B1, as well as epithelial cells expressing CYP24A1 or MCM7 localized in alteration sites. #: indicates inflammatory foci located within the lumen and surrounding the atrophic epithelium, an important diagnostic factor for PIA lesions. *: indicates microacinar formations. (C and D) Quantification of the number and staining intensity of epithelial cells positive for CYP27B1 according to the epithelial lesion. Values obtained in areas of alteration (right circles; pseudocolored orange and red lines) were compared with those determined in the matched adjacent normal areas (left circles; pseudocolored black line) by the Wilcoxon matched-pairs signed rank test (C) or paired *t* test (D). n.s: not statistically significant. (E) Spearman correlation analysis evidencing the significant inverse relationship between cell proliferation and the number and staining intensity of CYP27B1+ positive cells in the prostate epithelium of aging rats. (F) Quantification of the overall signal determined in the cytoplasm of CYP24A1+ epithelial cells according to age. Normal and altered areas of the ventral and lateral aging prostate were considered together, as they showed similar staining pattern as depicted in (B). Mean values accompanied by standard error bars with different letters represent statistically significant differences ($p < 0.05$) assessed by one-way ANOVA plus Tukey post hoc test. n= 5 per age. H&E: hematoxylin-eosin staining. Ne: normal epithelium. PIA: proliferative inflammatory atrophy. PIN: prostatic intraepithelial neoplasia. PCa: prostate cancer. 3, 6, 12, 18, and 24M = age of the animals expressed in months.

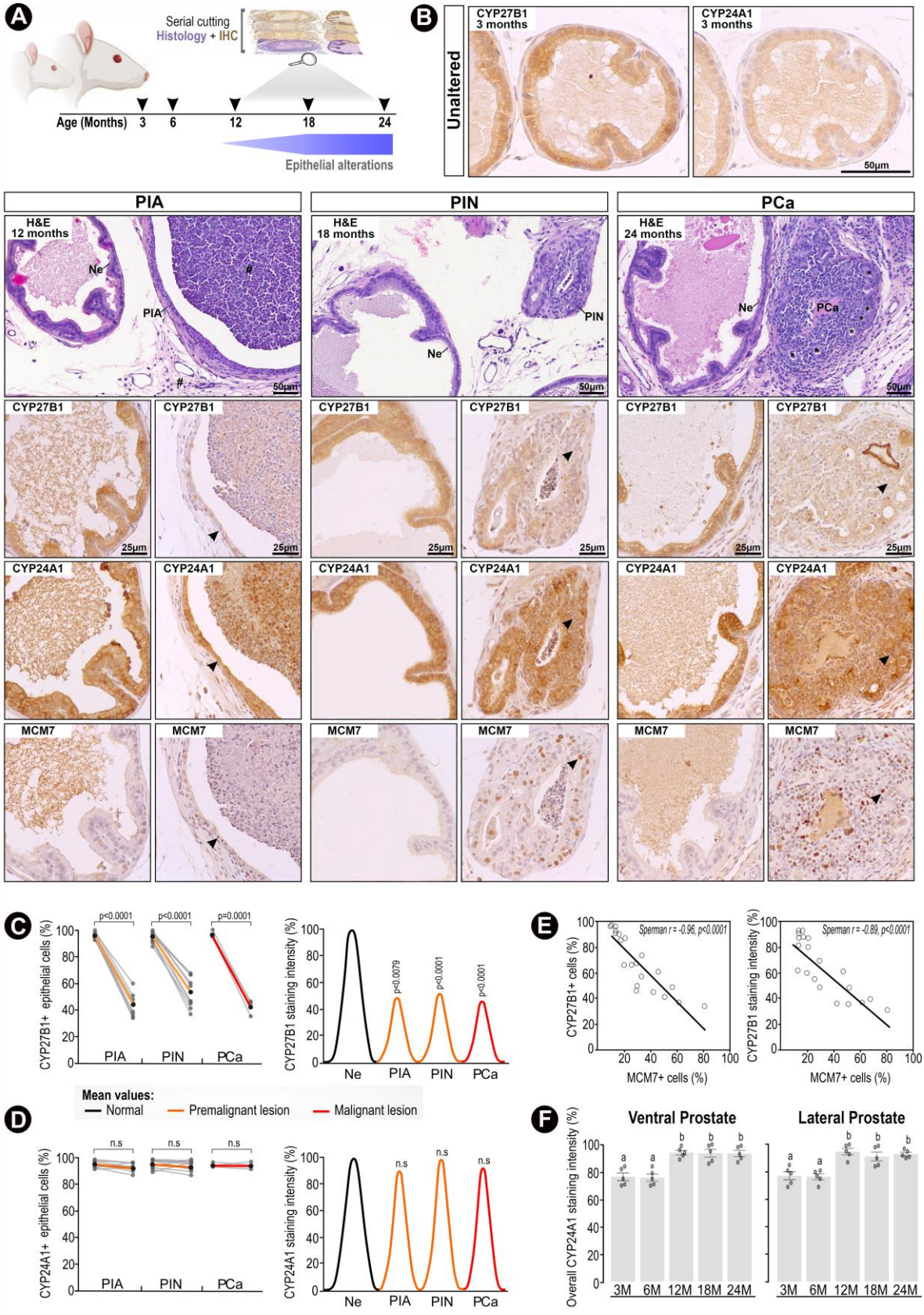
A
Serial cutting
Histology + IHC
Age (Months) 3 6 12 18 24
Epithelial alterations
B
Unaltered
CYP27B1
3 months
CYP24A1
3 months
50µm
PIA
PIN
PCa
H&E
12 months
H&E
18 months
H&E
24 months
Ne
PIA
PIN
PCa
#
50µm
CYP27B1
CYP24A1
MCM7
25µm
C
CYP27B1+ epithelial cells (%)
p<0.0001
p<0.0001
p=0.0001
PIA
PIN
PCa
CYP27B1 staining intensity (%)
p<0.0079
p<0.0001
p<0.0001
Ne
PIA
PIN
PCa
D
Mean values:
Normal
Premalignant lesion
Malignant lesion
CYP24A1+ epithelial cells (%)
n.s
CYP24A1 staining intensity (%)
E
CYP27B1+ cells (%)
Sperman r = -0.96, p<0.0001
MCM7+ cells (%)
CYP27B1 staining intensity (%)
Sperman r = -0.89, p<0.0001
F
Overall CYP24A1 staining intensity (%)
Ventral Prostate
Lateral Prostate
3M 6M 12M 18M 24M

Figure 4: Expression pattern of components involved in the metabolism and response to calcitriol in prostate tumors of aging Wistar rats treated with testosterone plus estradiol. (A) Histology and immunohistochemistry showing differential expression of the target proteins in malignant epithelial sites compared to adjacent normal ones. The images are representative of a tumor arising in the ventral prostate. (B) Comparison of the cell proliferation rate as well as the number and immunoreactivity of epithelial cells expressing CYP27B1, CYP24A1, VDR, or RXR in the tumors and the matched adjacent normal areas by using paired *t* test. n= 10 per lesion. n.s: not statistically significant. Ne: normal epithelium. PCa: prostate cancer.

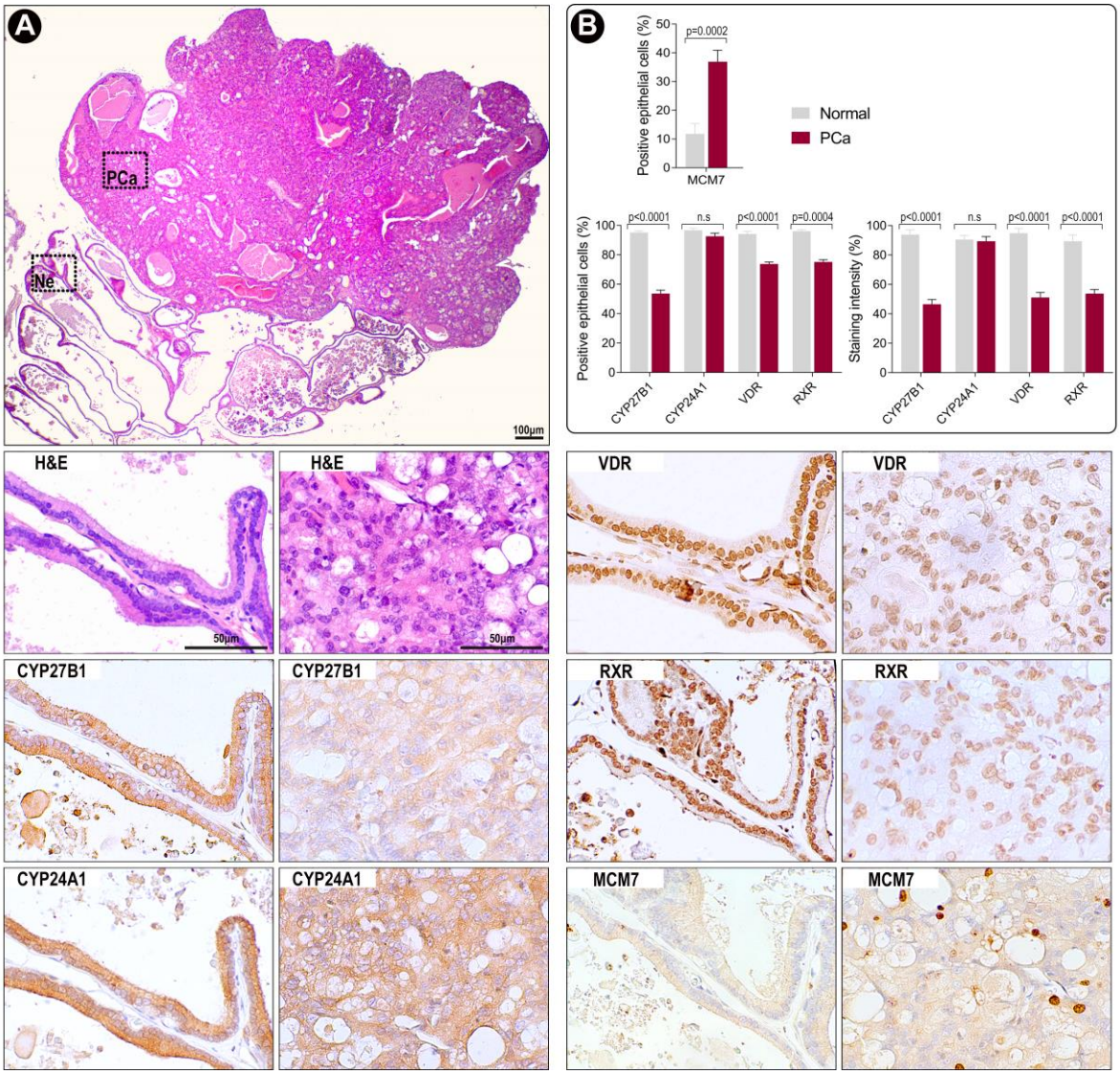
A
PCa
Ne
100μm
B
Positive epithelial cells (%)
p=0.0002
MCM7
Normal
PCa
Positive epithelial cells (%)
p<0.0001
n.s
p<0.0001
p=0.0004
CYP27B1
CYP24A1
VDR
RXR
Staining intensity (%)
p<0.0001
n.s
p<0.0001
p<0.0001
CYP27B1
CYP24A1
VDR
RXR
H&E
50μm
H&E
50μm
VDR
VDR
CYP27B1
CYP27B1
RXR
RXR
CYP24A1
CYP24A1
MCM7
MCM7

Figure 5: Schematic representation of the main findings of this study. (A) Calcitriol metabolism and mechanism of action evidencing the participation of the target enzymes and receptors involved. The multiple actions mediated by the transcriptional VDR/RXR complex result in protective effects on the prostate, and the abrogation of this signaling pathway leads to aberrant cellular proliferation. (B) Summary of the results highlighting that aging, the main risk factor linked to prostate disorders including cancer, plays significative effects on the three classes of components related to the vitamin D signaling: (i) hormone; (ii) metabolizing enzymes; and (iii) receptors. The changes presently found provide strong evidence that vitamin D signaling and, consequently, its protective effect is attenuated in the aging prostate and may be important for development of benign, pre-malignant and malignant epithelial changes.

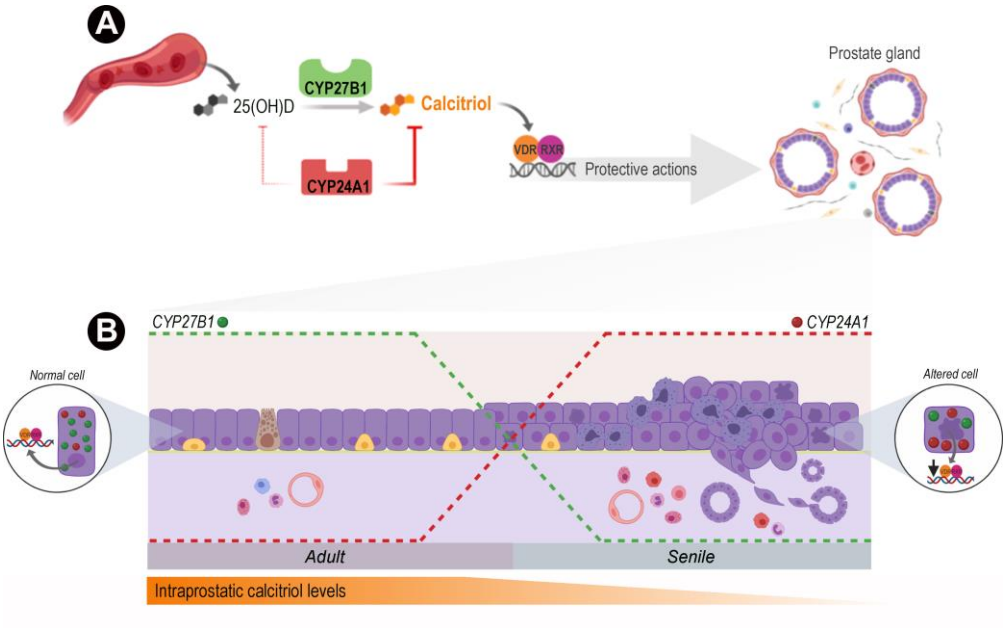
A
25(OH)D
CYP27B1
Calcitriol
CYP24A1
VDR
RXR
Protective actions
Prostate gland
B
CYP27B1
CYP24A1
Normal cell
Altered cell
Adult
Senile
Intraprostatic calcitriol levels

SUPLEMENTARY DATA

Following the order cited in the text

Table S1: List of antibodies used in this study.

Antigen	Type	Manufacturer, Cat. No.	[a] Dilution (technique)	Conjugation
CYP27B1	Rabbit mAB	Invitrogen, PA5-26065	1:800(IHC),1:400(IF), 1:500 (WB)	none
CYP24A1	Rabbit mAB	Invitrogen, PA5-21704	1:200(IHC, IF), 1:500 (WB)	none
VDR	Rat pAB	Thermo Scientific,	1:1500 (IHC), 1:500 (IF)	none
RXRα/β/γ	Mouse mAB	Santa Cruz,	1:400 (IHC)	none
CKHMW	Mouse mAB	DAKO, M0630	1:250 (IHC)	none
MCM7	Mouse mAB	Neomarkers, MS-862-P0	1:600 (IHC)	none
β-actin	Mouse mAB	Sigma-Aldrich, A5316	1:5.000 (WB)	none
mouse IgG	Goat pAB	DAKO, E0433	1:200 (IHC), 1:1000 (WB)	Biotin
Rabbit IgG	Goat pAB	DAKO, E0432	1:200 (IHC), 1:1000 (WB)	Biotin
Rat IgG	Rabbit pAB	DAKO, E0468	1:200 (IHC)	Biotin
Rabbit IgG	Goat pAB	Invitrogen, A-11008	1:200 (IF)	AlexaFluor™488
Rabbit IgG	Goat pAB	Invitrogen, A-11035	1:200 (IF)	AlexaFluor™546
Mouse IgG	Goat pAB	Invitrogen, A-11045	1:200 (IF)	AlexaFluor™350
Rat IgG	Goat pAB	Invitrogen, A-21247	1:200 (IF)	AlexaFluor™647

[a] Antibodies were diluted in PBS (pH 7.4).
IHC: immunohistochemistry. IF: immunofluorescence. WB: Western blotting.

Table S2: Incidence of spontaneous epithelial lesions in the ventral and lateral prostate of young adult to senile Wistar rats.

Experimental group	**[a] Epithelial lesion (No. animals)**					
	Atrophy	Hyperplasia	Squamous metaplasia	PIA	PIN	PCa
3 months	0/0	0/0	0/0	0/0	0/0	0/0
6 months	0/0	0/0	0/0	0/0	0/0	0/0
12 months	4/5	3/5	1/5	1/5	2/5	0/0
18 months	5/5	4/5	4/5	3/5	3/5	1/5
24 months	5/5	4/5	5/5	4/5	5/5	2/5

[a] Ventral and lateral prostates were considered together. PIA: proliferative inflammatory atrophy. PIN: prostatic intraepithelial neoplasia. PCa: prostate cancer (adenocarcinomas). n= 5 per age.

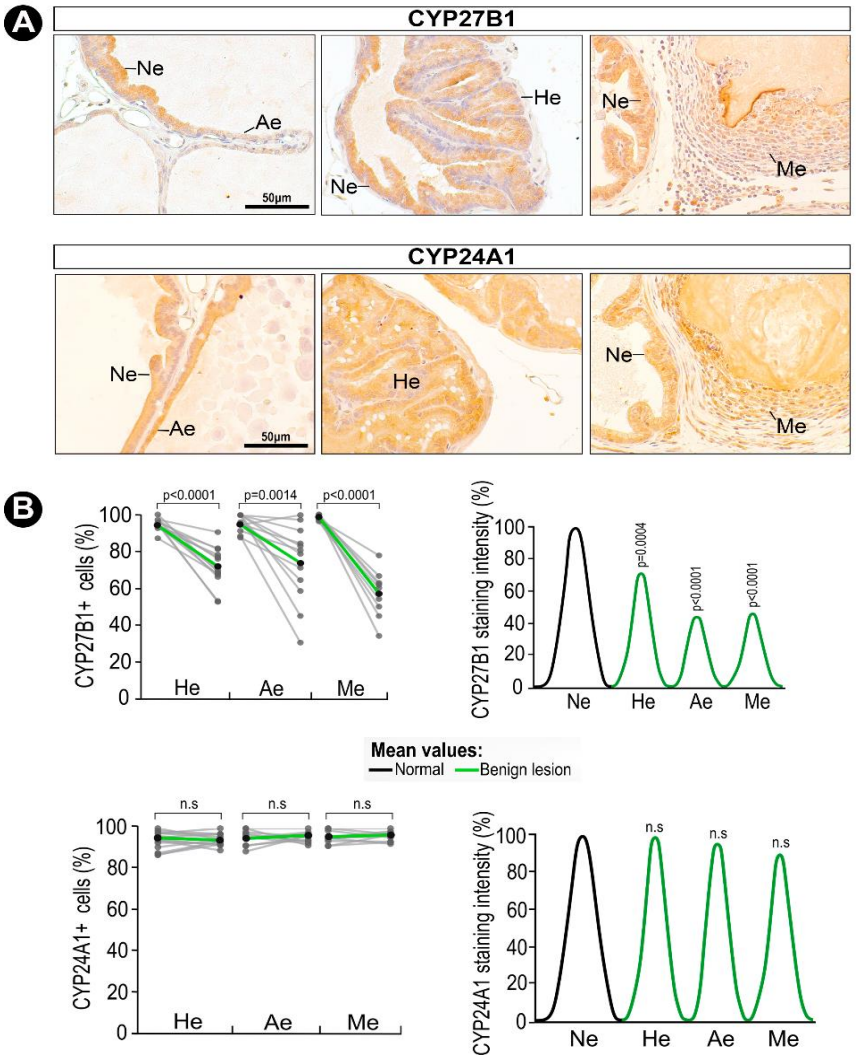

Figure S1: Immunolocalization of vitamin D metabolizing enzymes in aging-related prostate lesions of benign nature. (A) Representative images from immunohistochemistry highlighting the staining for CYP27B1 and CYP24A1 in atrophic (Ae), hyperplastic (He) and metaplastic (Me) epithelium. (B) Quantification of the number and staining intensity of CYP24A1+ cells according to the epithelial lesion. Values obtained in areas of alteration (right circles; pseudocolored green lines) were compared with those determined in the matched adjacent normal areas (left circles; pseudocolored black line) by paired *t* test. n.s: not statistically significant (p>0.05). n= 14 (atrophy), 11 (hyperplasia), 10 (squamous metaplasia). Ne: normal epithelium. He: hyperplastic epithelium. Ae: atrophic epithelium. Me: metaplastic epithelium.

Table S3: Expression of components implicated with the metabolism and response to calcitriol as well as cell proliferation in non-cancerous epithelial lesions diagnosed in the prostate of senile Wistar rats treated with testosterone plus estradiol.

Epithelial Lesion	Target	Positive Cells (% ± S.E.M)			Staining intensity (% ± S.E.M)		
		Normal	Altered	[a] p value	Normal	Altered	[a] p value
Prostatic intraepithelial neoplasia (PIN)	CYP27B1	98.6 ± 1.3	55.4 +2.0	<0.0001	89.5 ± 2.8	50.8 ± 2.9	<0.0001
	CYP24A1	95.1 ± 1.1	94.3 ± 0.7	0.8370	91.7 ± 3.1	90.0 ± 2.9	0.6935
	VDR	90.3 ± 1.8	73.1 ± 1.4	<0.0001	88.2 ± 3.9	58.2 ± 4.1	<0.0001
	RXR	92.4 ± 1.7	70.4 ± 0.9	<0.0001	90.7 ± 3.0	59.1 ± 2.9	<0.0001
	MCM7	12.4 ± 3.2	35.0 ± 5.9	0.0003	N/A	N/A	N/A
Proliferative inflammatory atrophy (PIA)	CYP27B1	97.5 ± 1.2	48.8 ± 0.7	<0.0001	91.2 ± 3.4	42.8 ± 3.6	<0.0001
	CYP24A1	95.4 ± 1.0	95.6 ± 0.7	0.9271	94.1 ± 2.5	89.6 ± 2.8	0.2461
	VDR	91.2 ± 1.9	60.0 ± 1.5	<0.0001	90.3 ± 2.9	62.2 ± 2.8	<0.0001
	RXR	90.7 ± 1.7	66.5 ± 1.9	<0.0001	91.8 ± 3.2	55.0 ± 3.2	<0.0001
	MCM7	10.1 ± 3.4	31.7 ± 3.7	0.0004	N/A	N/A	N/A
Squamous Metaplasia	CYP27B1	97.2 + 0.9	51.8 ± 2.0	<0.0001	89.3 ± 3.6	40.7 ± 4.4	<0.0001
	CYP24A1	95.7 ± 1.0	96.1 ± 0.8	0.6359	90.8 ± 2.4	90.5 ± 2.7	0.9347
	VDR	89.6 ± 2.4	56.6 ± 1.9	<0.0001	89.0 ± 3.4	43.1 ± 3.5	<0.0001
	RXR	91.4 ± 1.1	63.0 ± 1.4	<0.0001	90.2 ± 4.0	58.5 ± 3.6	<0.0001
	MCM7	10.8 ± 3.5	37.1 ± 4.0	0.0001	N/A	N/A	N/A
Hyperplasia	CYP27B1	95.3 ± 1.4	69.4 ± 3.3	<0.0001	89.3 ± 2.8	45.2 ± 4.6	0.0004
	CYP24A1	96.3 ± 1.1	95.2 ± 1.3	0.4203	92.3 ± 2.9	91.2 ± 2.8	0.7881
	VDR	90.9 ± 1.7	72.5 ± 1.9	<0.0001	88.4 ± 3.6	80.2 ± 4.0	0.1449
	RXR	90.4 ± 1.5	61.8 ± 2.2	<0.0001	91.1 ± 2.8	61.4 ± 2.5	<0.0001
	MCM7	13.4 ± 3.3	25.6 ± 3.4	0.0191	N/A	N/A	N/A

[a] Paired *t* test or Wilcoxon matched-pairs signed rank test taking into account individual values determined in epithelial lesions and the matched adjacent normal epithelium. N/A: not assessed. n = 10 per lesion.

REFERENCES

[1] A. Gil, J. Plaza-Diaz, M.D. Mesa, Vitamin D: Classic and Novel Actions, Ann Nutr Metab, 72 (2018) 87-95.

[2] V. Rai, N.E. Dietz, M.F. Dilisio, M.M. Radwan, D.K. Agrawal, Vitamin D attenuates inflammation, fatty infiltration, and cartilage loss in the knee of hyperlipidemic microswine, Arthritis Res Ther, 18 (2016) 203.

[3] J.J. Cannell, W.B. Grant, M.F. Holick, Vitamin D and inflammation, Dermatoendocrinol, 6 (2014) e983401.

[4] M. El-Boshy, M.A. BaSalamah, J. Ahmad, S. Idris, A. Mahbub, A.H. Abdelghany, R.A. Almaimani, H. Almasmoum, M.M. Ghaith, M. Elzubier, B. Refaat, Vitamin D protects against oxidative stress, inflammation and hepatorenal damage induced by acute paracetamol toxicity in rat, Free Radic Biol Med, 141 (2019) 310-321.

[5] S. Swami, A.V. Krishnan, J.Y. Wang, K. Jensen, R. Horst, M.A. Albertelli, D. Feldman, Dietary vitamin D(3) and 1,25-dihydroxyvitamin D(3) (calcitriol) exhibit equivalent anticancer activity in mouse xenograft models of breast and prostate cancer, Endocrinology, 153 (2012) 2576-2587.

[6] D. Feldman, A.V. Krishnan, S. Swami, E. Giovannucci, B.J. Feldman, The role of vitamin D in reducing cancer risk and progression, Nat Rev Cancer, 14 (2014) 342-357.

[7] D.M. Peehl, R.J. Skowronski, G.K. Leung, S.T. Wong, T.A. Stamey, D. Feldman, Antiproliferative effects of 1,25-dihydroxyvitamin D3 on primary cultures of human prostatic cells, Cancer Res, 54 (1994) 805-810.

[8] C.C. Blajszczak, L. Nonn, Vitamin D regulates prostate cell metabolism via genomic and non-genomic mitochondrial redox-dependent mechanisms, J Steroid Biochem Mol Biol, 195 (2019) 105484.

[9] T.C. Chen, M.F. Holick, Vitamin D and prostate cancer prevention and treatment, Trends Endocrinol Metab, 14 (2003) 423-430.

[10] J. Moreno, A.V. Krishnan, S. Swami, L. Nonn, D.M. Peehl, D. Feldman, Regulation of prostaglandin metabolism by calcitriol attenuates growth stimulation in prostate cancer cells, Cancer Res, 65 (2005) 7917-7925.

[11] P. Zhang, A. Schatz, B. Adeyemi, D. Kozminski, J. Welsh, M. Tenniswood, W.W. Wang, Vitamin D and testosterone co-ordinately modulate intracellular zinc levels and energy metabolism in prostate cancer cells, J Steroid Biochem Mol Biol, 189 (2019) 248-258.

[12] A.A. Giangreco, S. Dambal, D. Wagner, T. Van der Kwast, R. Vieth, G.S. Prins, L. Nonn, Differential expression and regulation of vitamin D hydroxylases and inflammatory genes in prostate stroma and epithelium by 1,25-dihydroxyvitamin D in men with prostate cancer and an in vitro model, J Steroid Biochem Mol Biol, 148 (2015) 156-165.

[13] M.H. Ahonen, L. Tenkanen, L. Teppo, M. Hakama, P. Tuohimaa, Prostate cancer risk and prediagnostic serum 25-hydroxyvitamin D levels (Finland), Cancer Causes Control, 11 (2000) 847-852.

[14] S. Tretli, E. Hernes, J.P. Berg, U.E. Hestvik, T.E. Robsahm, Association between serum 25(OH)D and death from prostate cancer, Br J Cancer, 100 (2009) 450-454.

[15] A.B. Murphy, Y. Nyame, I.K. Martin, W.J. Catalona, C.M. Hollowell, R.B. Nadler, J.M. Kozlowski, K.T. Perry, A. Kajdacsy-Balla, R. Kittles, Vitamin D deficiency predicts prostate biopsy outcomes, Clin Cancer Res, 20 (2014) 2289-2299.

[16] M. Deschasaux, J.C. Souberbielle, P. Latino-Martel, A. Sutton, N. Charnaux, N. Druesne-Pecollo, P. Galan, S. Hercberg, S. Le Clerc, E. Kesse-Guyot, K. Ezzedine, M. Touvier, A prospective study of plasma 25-hydroxyvitamin D concentration and prostate cancer risk, Br J Nutr, 115 (2016) 305-314.

[17] F. Bray, J. Ferlay, I. Soerjomataram, R.L. Siegel, L.A. Torre, A. Jemal, Global cancer statistics 2018: GLOBOCAN estimates of incidence and mortality worldwide for 36 cancers in 185 countries, CA Cancer J Clin, 68 (2018) 394-424.

[18] J.L. Osborn, G.G. Schwartz, D.C. Smith, R. Bahnson, R. Day, D.L. Trump, Phase II trial of oral 1,25-dihydroxyvitamin D (calcitriol) in hormone refractory prostate cancer, Urol Oncol, 1 (1995) 195-198.

[19] G. Liu, G. Wilding, M.J. Staab, D. Horvath, K. Miller, A. Dresen, D. Alberti, R. Arzoomanian, R. Chappell, H.H. Bailey, Phase II study of 1alpha-hydroxyvitamin D(2) in the treatment of advanced androgen-independent prostate cancer, Clin Cancer Res, 9 (2003) 4077-4083.

[20] T.M. Beer, A. Myrthue, M. Garzotto, F. O'Hara M, R. Chin, B.A. Lowe, M.A. Montalto, C.L. Corless, W.D. Henner, Randomized study of high-dose pulse calcitriol or placebo prior to radical prostatectomy, Cancer Epidemiol Biomarkers Prev, 13 (2004) 2225-2232.

[21] N.M. Tiffany, C.W. Ryan, M. Garzotto, E.M. Wersinger, T.M. Beer, High dose pulse calcitriol, docetaxel and estramustine for androgen independent prostate cancer: a phase I/II study, J Urol, 174 (2005) 888-892.

[22] T.W. Flaig, A. Barqawi, G. Miller, M. Kane, C. Zeng, E.D. Crawford, L.M. Glode, A phase II trial of dexamethasone, vitamin D, and carboplatin in patients with hormone-refractory prostate cancer, Cancer, 107 (2006) 266-274.

[23] T.M. Beer, C.W. Ryan, P.M. Venner, D.P. Petrylak, G.S. Chatta, J.D. Ruether, C.H. Redfern, L. Fehrenbacher, M.N. Saleh, D.M. Waterhouse, M.A. Carducci, D. Vicario, R. Dreicer, C.S. Higano, F.R. Ahmann, K.N. Chi, W.D. Henner, A. Arroyo, F.W. Clow, A. Investigators, Double-blinded randomized study of high-dose calcitriol plus docetaxel compared with placebo plus docetaxel in androgen-independent prostate cancer: a report from the ASCENT Investigators, J Clin Oncol, 25 (2007) 669-674.

[24] D.T. Marshall, S.J. Savage, E. Garrett-Mayer, T.E. Keane, B.W. Hollis, R.L. Horst, L.H. Ambrose, M.S. Kindy, S. Gattoni-Celli, Vitamin D3 supplementation at 4000 international units per day for one year results in a decrease of positive cores at

repeat biopsy in subjects with low-risk prostate cancer under active surveillance, J Clin Endocrinol Metab, 97 (2012) 2315-2324.

[25] I. Schuster, Cytochromes P450 are essential players in the vitamin D signaling system, Biochim Biophys Acta, 1814 (2011) 186-199.

[26] R.J. Skowronski, D.M. Peehl, D. Feldman, Vitamin D and prostate cancer: 1,25 dihydroxyvitamin D3 receptors and actions in human prostate cancer cell lines, Endocrinology, 132 (1993) 1952-1960.

[27] M. Banks, M.F. Holick, Molecular Mechanism(s) Involved in 25-Hydroxyvitamin D's Antiproliferative Effects in CYP27B1-transfected LNCaP Cells, Anticancer Res, 35 (2015) 3773-3779.

[28] M. Tannour-Louet, S.K. Lewis, J.F. Louet, J. Stewart, J.B. Addai, A. Sahin, H.V. Vangapandu, A.L. Lewis, K. Dittmar, R.G. Pautler, L. Zhang, R.G. Smith, D.J. Lamb, Increased expression of CYP24A1 correlates with advanced stages of prostate cancer and can cause resistance to vitamin D3-based therapies, FASEB J, 28 (2014) 364-372.

[29] J.Y. Hsu, D. Feldman, J.E. McNeal, D.M. Peehl, Reduced 1alpha-hydroxylase activity in human prostate cancer cells correlates with decreased susceptibility to 25-hydroxyvitamin D3-induced growth inhibition, Cancer Res, 61 (2001) 2852-2856.

[30] G.H. Campolina-Silva, B.T. Maria, G.A.B. Mahecha, C.A. Oliveira, Reduced vitamin D receptor (VDR) expression and plasma vitamin D levels are associated with aging-related prostate lesions, Prostate, 78 (2018) 532-546.

[31] G.H. Campolina-Silva, H. Werneck-Gomes, B.T. Maria, M.C. Barata, M.J. Torres, H.R. Contreras, G.A.B. Mahecha, C.A. Oliveira, Targeting Wistar rat as a model for studying benign, premalignant and malignant lesions of the prostate, Life Sci, 242 (2020) 117149.

[32] J. Hany, H. Lilienthal, A. Sarasin, A. Roth-Harer, A. Fastabend, L. Dunemann, W. Lichtensteiger, G. Winneke, Developmental exposure of rats to a reconstituted PCB mixture or aroclor 1254: effects on organ weights, aromatase activity, sex hormone levels, and sweet preference behavior, Toxicol Appl Pharmacol, 158 (1999) 231-243.

[33] S.B. Shappell, G.V. Thomas, R.L. Roberts, R. Herbert, M.M. Ittmann, M.A. Rubin, P.A. Humphrey, J.P. Sundberg, N. Rozengurt, R. Barrios, J.M. Ward, R.D. Cardiff, Prostate pathology of genetically engineered mice: definitions and classification. The consensus report from the Bar Harbor meeting of the Mouse Models of Human Cancer Consortium Prostate Pathology Committee, Cancer Res, 64 (2004) 2270-2305.

[34] D. Creasy, A. Bube, E. de Rijk, H. Kandori, M. Kuwahara, R. Masson, T. Nolte, R. Reams, K. Regan, S. Rehm, P. Rogerson, K. Whitney, Proliferative and nonproliferative lesions of the rat and mouse male reproductive system, Toxicol Pathol, 40 (2012) 40S-121S.

[35] S.C. Taylor, T. Berkelman, G. Yadav, M. Hammond, A defined methodology for reliable quantification of Western blot data, Mol Biotechnol, 55 (2013) 217-226.

[36] M. Morais-Santos, H. Werneck-Gomes, G.H. Campolina-Silva, L.C. Santos, G.A.B. Mahecha, R.A. Hess, C.A. Oliveira, Basal Cells Show Increased Expression of Aromatase and Estrogen Receptor alpha in Prostate Epithelial Lesions of Male Aging Rats, Endocrinology, 159 (2018) 723-732.

[37] M. Blomberg Jensen, J.E. Nielsen, A. Jorgensen, E. Rajpert-De Meyts, D.M. Kristensen, N. Jorgensen, N.E. Skakkebaek, A. Juul, H. Leffers, Vitamin D receptor and vitamin D metabolizing enzymes are expressed in the human male reproductive tract, Hum Reprod, 25 (2010) 1303-1311.

[38] A.R. Mahmoudi, A.H. Zarnani, M. Jeddi-Tehrani, L. Katouzian, M. Tavakoli, H. Soltanghoraei, E. Mirzadegan, Distribution of vitamin D receptor and 1alpha-hydroxylase in male mouse reproductive tract, Reprod Sci, 20 (2013) 426-436.

[39] Y. Wang, M.L. Borchert, H.F. DeLuca, Identification of the vitamin D receptor in various cells of the mouse kidney, Kidney Int, 81 (2012) 993-1001.

[40] L. Kagi, C. Bettoni, E.M. Pastor-Arroyo, U. Schnitzbauer, N. Hernando, C.A. Wagner, Regulation of vitamin D metabolizing enzymes in murine renal and extrarenal tissues by dietary phosphate, FGF23, and 1,25(OH)2D3, PLoS One, 13 (2018) e0195427.

[41] M.F. Leitzmann, S. Rohrmann, Risk factors for the onset of prostatic cancer: age, location, and behavioral correlates, Clin Epidemiol, 4 (2012) 1-11.

[42] K.B. Lim, Epidemiology of clinical benign prostatic hyperplasia, Asian J Urol, 4 (2017) 148-151.

[43] E.S. Orwoll, D.E. Meier, Alterations in calcium, vitamin D, and parathyroid hormone physiology in normal men with aging: relationship to the development of senile osteopenia, J Clin Endocrinol Metab, 63 (1986) 1262-1269.

[44] J.C. Gallagher, Vitamin D and aging, Endocrinol Metab Clin North Am, 42 (2013) 319-332.

[45] L. Elizondo-Montemayor, E.C. Castillo, C. Rodriguez-Lopez, J.R. Villarreal-Calderon, M. Gomez-Carmona, S. Tenorio-Martinez, B. Nieblas, G. Garcia-Rivas, Seasonal Variation in Vitamin D in Association with Age, Inflammatory Cytokines, Anthropometric Parameters, and Lifestyle Factors in Older Adults, Mediators Inflamm, 2017 (2017) 5719461.

[46] G.T. Consortium, The Genotype-Tissue Expression (GTEx) project, Nat Genet, 45 (2013) 580-585.

[47] M. Morais-Santos, A.E. Nunes, A.G. Oliveira, J.D. Moura-Cordeiro, G.A. Mahecha, M.C. Avellar, C.A. Oliveira, Changes in Estrogen Receptor ERbeta (ESR2) Expression without Changes in the Estradiol Levels in the Prostate of Aging Rats, PLoS One, 10 (2015) e0131901.

[48] A.M. De Marzo, M.C. Haffner, T.L. Lotan, S. Yegnasubramanian, W.G. Nelson, Premalignancy in Prostate Cancer: Rethinking What we Know, Cancer Prev Res (Phila), 9 (2016) 648-656.

[49] A.M. Barreto, G.G. Schwartz, R. Woodruff, S.D. Cramer, 25-Hydroxyvitamin D3, the prohormone of 1,25-dihydroxyvitamin D3, inhibits the proliferation of primary prostatic epithelial cells, Cancer Epidemiol Biomarkers Prev, 9 (2000) 265-270.

[50] M.R. Haussler, P.W. Jurutka, M. Mizwicki, A.W. Norman, Vitamin D receptor (VDR)-mediated actions of 1alpha,25(OH)(2)vitamin D(3): genomic and non-genomic mechanisms, Best Pract Res Clin Endocrinol Metab, 25 (2011) 543-559.

[51] D.D. Bikle, S. Patzek, Y. Wang, Physiologic and pathophysiologic roles of extra renal CYP27b1: Case report and review, Bone Rep, 8 (2018) 255-267.

[52] Beer, T. M. and A. Myrthue (2006). Calcitriol in the treatment of prostate cancer. Anticancer Res 26(4A): 2647-2651.

[53] P.H. Anderson, P.D. O'Loughlin, B.K. May, H.A. Morris, Modulation of CYP27B1 and CYP24 mRNA expression in bone is independent of circulating 1,25(OH)2D3 levels, Bone, 36 (2005) 654-662.

[54] A. Gawlik, V. Gepstein, N. Rozen, A. Dahan, D. Ben-Yosef, G. Wildbaum, O. Verbitsky, R. Shaoul, Y. Weisman, D. Tiosano, Duodenal Expression of 25 Hydroxyvitamin D3-1alpha-hydroxylase Is Higher in Adolescents Than in Children and Adults, J Clin Endocrinol Metab, 100 (2015) 3668-3675.

[55] Y. Jiang, L. Liao, J. Li, L. Wang, Z. Xie, Older Age Is Associated with Decreased Levels of VDR, CYP27B1, and CYP24A1 and Increased Levels of PTH in Human Parathyroid Glands, Int J Endocrinol, 2020 (2020) 7257913.

[56] G.J. Miller, G.E. Stapleton, T.E. Hedlund, K.A. Moffat, Vitamin D receptor expression, 24-hydroxylase activity, and inhibition of growth by 1alpha,25-dihydroxyvitamin D3 in seven human prostatic carcinoma cell lines, Clin Cancer Res, 1 (1995) 997-1003.

[57] R.C. Travis, A. Perez-Cornago, P.N. Appleby, D. Albanes, C.E. Joshu, P.L. Lutsey, A.M. Mondul, E.A. Platz, S.J. Weinstein, T.M. Layne, K.J. Helzlsouer, K. Visvanathan, D. Palli, P.H. Peeters, B. Bueno-de-Mesquita, A. Trichopoulou, M.J. Gunter, K.K. Tsilidis, M.J. Sanchez, A. Olsen, H. Brenner, B. Schottker, L. Perna, B. Holleczek, P. Knekt, H. Rissanen, B.B. Yeap, L. Flicker, O.P. Almeida, Y.Y.E. Wong, J.M. Chan, E.L. Giovannucci, M.J. Stampfer, G. Ursin, R.E. Gislefoss, T. Bjorge, H.E. Meyer, R. Blomhoff, S. Tsugane, N. Sawada, D.R. English, D.W. Eyles, A.K. Heath, E.J. Williamson, J. Manjer, J. Malm, M. Almquist, L.L. Marchand, C.A. Haiman, L.R. Wilkens, J.M. Schenk, C.M. Tangen, A. Black, M.B. Cook, W.Y. Huang, R.G. Ziegler, R.M. Martin, F.C. Hamdy, J.L. Donovan, D.E. Neal, M. Touvier, S. Hercberg, P. Galan, M. Deschasaux, T.J. Key, N.E. Allen, A Collaborative Analysis of Individual Participant Data from 19 Prospective Studies Assesses Circulating Vitamin D and Prostate Cancer Risk, Cancer Res, 79 (2019) 274-285.

[58] S. Ramakrishnan, S.E. Steck, L. Arab, H. Zhang, J.T. Bensen, E.T.H. Fontham, C.S. Johnson, J.L. Mohler, G.J. Smith, L.J. Su, A. Woloszynska, Association among plasma 1,25(OH)2 D, ratio of 1,25(OH)2 D to 25(OH)D, and prostate cancer aggressiveness, Prostate, 79 (2019) 1117-1124.

[59] W. Banach-Petrosky, X. Ouyang, H. Gao, K. Nader, Y. Ji, N. Suh, R.S. DiPaola, C. Abate-Shen, Vitamin D inhibits the formation of prostatic intraepithelial neoplasia in Nkx3.1;Pten mutant mice, Clin Cancer Res, 12 (2006) 5895-5901.

ARTIGO 3: Targeting Wistar rat as a model for studying benign, premalignant and malignant lesions of the prostate. Life Sciences, 242: 117149.

Life Sciences 242 (2020) 117149

Contents lists available at ScienceDirect

Life Sciences

journal homepage: www.elsevier.com/locate/lifescie

Targeting Wistar rat as a model for studying benign, premalignant and malignant lesions of the prostate

Gabriel H. Campolina-Silva[a,1], Hipácia Werneck-Gomes[a,1], Bruna T. Maria[a], Maria C. Barata[a], María J. Torres[b], Héctor R. Contreras[b], Germán A.B. Mahecha[a], Cleida A. Oliveira[a,*]

[a] Department of Morphology, Universidade Federal de Minas Gerais, Belo Horizonte, Brazil
[b] Department of Basic and Clinic Oncology, Universidad de Chile, Santiago, Chile

ARTICLE INFO

Keywords:
Prostate lesions
Adenocarcinoma
Aging
Androgen:estrogen imbalance
Wistar rat

ABSTRACT

Aims: The purpose of this study was to describe a suitable experimental model for studying aging-related prostate disorders including cancer.
Materials and methods: 12-month old Wistar rats were kept in control conditions ($n = 12$) or treated ($n = 16$) for 6 months with Silastic implants filled with testosterone (T) and estradiol (E_2). After the experiment period (at 18 months of age), animals were euthanized and the prostate and other organs were harvested, dissected, weighed, and processed for morphological, ultrastructural and molecular analyses.
Key findings: We demonstrated that male rats of Wistar strain nicely recapitulate the carcinogenesis process taking place in the aging prostate through the arising of benign, precancerous and malignant lesions, and above all yields a modest incidence of spontaneous PCa (~36%). Moreover, our results highlight that 100% incidence of PCa and precancerous lesions such as prostatic intraepithelial neoplasia and proliferative inflammatory atrophy were achieved in this rat strain after T + E_2 treatment, without changing the broad spectrum of changes that naturally emerge in the prostate at advanced ages. Such enhancement of precancerous lesions and tumors was linked to a decreased expression of E-cadherin and β-catenin in parallel with an increase in Vimentin and N-cadherin, hallmark modifications of epithelial-mesenchymal transition.
Significance: Our findings provide solid evidence that aged Wistar rats may be an excellent model for studies regarding human prostate biology and related disorders including cancer.

1. Introduction

Living long enough, nearly all men will develop some histologically detectable alteration in the prostate. This fact puts the advancing age as the major risk factor for some prostate diseases including the prostate cancer (PCa), one of the most frequently diagnosed neoplasms worldwide and whose incidence raises sharply from the 4th decade of life [1,2]. The relationship between aging and the prostate diseases likely reflects an exacerbation of factors that influence the gland throughout life, particularly the increased androgen:estrogen ratio [3–8]. In this regard, researches conducted in rats have shown that the chronic exposure to androgenic and estrogenic compounds strongly predisposes the prostate gland to develop dysplastic foci and adenocarcinomas at senescence [9–15].

The use of laboratory rodents in experimental research has expressively advanced our comprehension of PCa biology. Since the arising of precancerous lesions and the eventual detection of tumors in the prostate gland is a long and silent process, preclinical investigations performed in spontaneous models of PCa are assumed to be time-consuming and still have to cope with the relatively low incidence of tumors [16]. Furthermore, the incidence of spontaneous PCa varies according to animal strain [3,17,18]. Thus, efforts have been employed over the last decades to design in vivo models capable of yielding a high frequency of prostate tumors in a shorter period of time. These models include rats or mice that undergo chemical, genetic or tissue recombinant interference (reviewed by [16,19]), which have been applied to generate new insights into the initiation, progression, and treatment of PCa. However, the adoption of contrived and highly abnormal conditions to truncate the long latency period needed for PCa development does not precisely provide the ideal properties to mimic the natural history of the disease [20]. Therefore, defining new PCa models that yield a high incidence of malignant lesions spontaneously

* Corresponding author at: Av. Antônio Carlos, 6627, CEP 31270-901 Belo Horizonte, MG, Brazil.
E-mail address: cleida@icb.ufmg.br (C.A. Oliveira).
[1] These authors should be regarded as joint First Authors.

https://doi.org/10.1016/j.lfs.2019.117149
Received 9 October 2019; Received in revised form 29 November 2019; Accepted 6 December 2019
Available online 09 December 2019
0024-3205/

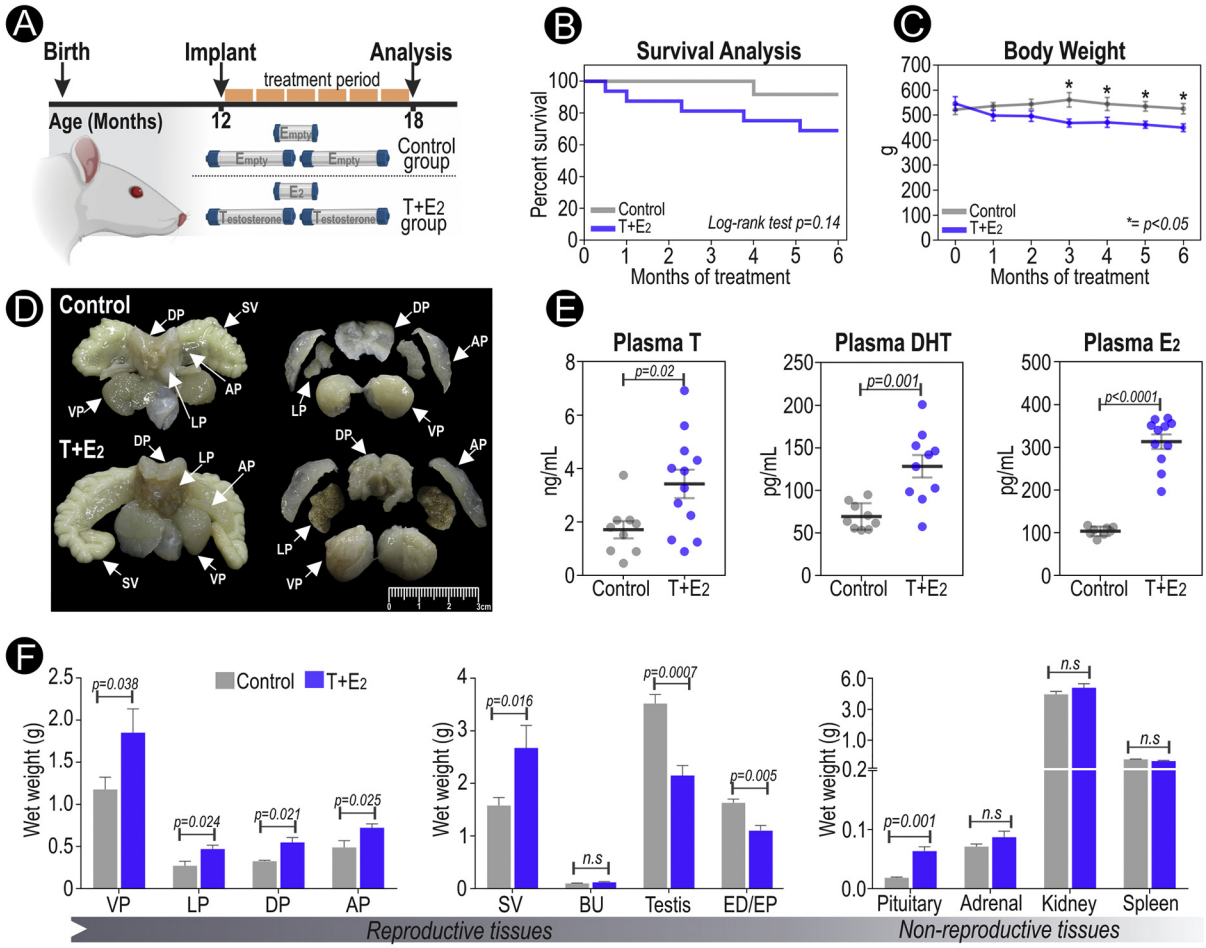

Fig. 1. Testosterone plus E_2 treatment induces significant structural changes in the rat prostate at 18 months of age. (A) Experimental design. (B) Kaplan-Meier plot showing statistically similar survival curves between groups. (C) Progressive weight loss in the T + E_2-treated animals over the experiment course. (D) Gross morphology of whole prostatic complex with seminal vesicles and each dissected prostate lobe highlighting the difference in the size and appearance between groups. (E) Scatter plots showing the circulating level of testosterone, dihydrotestosterone, and estradiol. (F) Wet weights of reproductive and non-reproductive organs. All paired organs were weighted together. AP: anterior prostate. DP: dorsal prostate. LP: lateral prostate. VP: ventral prostate. BU: bulbourethral gland. ED/EP: epididymis containing the efferent ductules. SV: seminal vesicle. n.s: not statistically significant.

or through less drastic interferences could be valuable to proper understand the molecular basis underlying the disease.

In the early 1970s, Morris Pollard showed that male rats of Wistar strain are genetically predisposed to develop prostatic adenocarcinoma at senescence [21]. More recently, we have presented evidence that aged Wistar rats are highly susceptible to the onset of histopathological alterations that mimic most of those affecting the human prostate and include both non-neoplastic and neoplastic lesions [6]. Such data entice attention to the potential use of these animals as a suitable experimental model for studying aging-related prostate disorders including PCa. However, a systematic evaluation of the changes affecting the prostates of Wistar rats as well as their incidence, is still lacking. Moreover, it is not known whether a sex steroid-induced imbalance during the window in which this rat strain becomes more susceptible to the onset (12 months) and intensification (18 months) of prostatic alterations could enhance the development of specific lesions such as adenocarcinomas. Therefore, the aim of the present study was to provide a detailed description of the broad spectrum of changes found in the prostate of Wistar rats at 18 months of age, and compared the incidence of each lesion between control and the age-matched rats treated with testosterone plus estradiol.

2. Materials and methods

2.1. Ethics statement

The experimental procedures involving animals were approved by the Ethical Committee for Animal Experimentation of the UFMG (process No. 344/2018) and conducted in accordance to the ARRIVE (Animal Research: Reporting In Vivo Experiments) guidelines.

2.2. Experimental approach

Male Wistar rats were obtained from the Central Animal House of the Universidade Federal de Minas Gerais (UFMG) and kept in a proper animal facility under controlled environmental conditions (50 ± 10% relative humidity, 22 ± 2 °C, 12 h light/ 12 h dark), with ad libitum access to water and food (Nuvilab CR1, Nuvital Nutrientes S.A, Colombo, Brazil). At 12 months of age, a group of animals (n = 16) received two Silastic capsules (2.0 cm length each) tightly filled with testosterone propionate (Cat. No. T-1875, Sigma-Andrich, USA) and one of 1.0 cm length with estradiol (Cat. No. E-8515, Sigma-Andrich, USA), both hormones in powder form. These animals (referred as T + E_2-treated rats) constituted the treatment group. The hormone-containing implants were constructed from Silastic tubes (Cat. No. 508-009, 1.98 mm inner diameter, 3.18 mm outer diameter, Dow-Corning

Table 1
Microscopic alterations and their incidence in the prostate of control and T + E2-treated Wistar rats at 18 months of age.

Histopathology	Cytological aspects	Differential features (Control vs. T + E_2)	Incidence of epithelial lesions No. (%)			p value
			Entity	Control	T + E_2	
Hydropic vacuolation	Luminal cells with cytoplasmic vacuolation of presumably aqueous appearance. Nuclei often flattened and disposed toward to the periphery.	None.	VP (only)	4 (36,4)	11 (91.7)	0.0094*
Squamous metaplasia	Basal cells undergoing aberrant proliferation that confer to the glandular epithelium a squamous stratified appearance.	None.	LP (only)	3 (27.3)	5 (41.7)	0.6668
Mucinous metaplasia	Luminal cells of globet-like morphology with accumulated mucinous materials in their supranuclear area of the cytoplasm.	None.	VP (only)	1 (9.1)	1 (8.3)	> 0.999
Abscess	Massive inflammatory infiltrate with the predominance of granulocytes closely associated with an injured epithelium	None.	LP (only)	3 (27.3)	11 (91.7)	0.0028
Hyperplasia	Cellularity augmentation leading to epithelium unfoldings.Predominance of proliferating luminal cells with no nuclear atypia.	Epithelial unfolding is more pronounced in T + E_2.	Overall	11 (100)	12 (100)	> 0.999
			LP	11 (100)	6 (50.0)	0.0137*
			VP	10 (90.9)	11 (91.7)	> 0.999
			DP	10 (90.9)	11 (91.7)	> 0.999
			AP	10 (90.9)	12 (100)	0.4783
Simple atrophy	Predominance of luminal cells with reduced height and scant cytoplasm. Cells are often in interphase and non-associated to inflamatory infiltrate.	None.	Overall	11 (100)	12 (100)	> 0.999
			LP	7 (63.6)	12 (100)	0.0373*
			VP	10 (90.9)	8 (66.7)	0.3168
			DP	9 (81.8)	9 (75.0)	> 0.999
			AP	4 (36.4)	3 (25.0)	0.3707
Proliferative inflammatory atrophy (PIA)	Predominance of atrophic luminal cells and normal-appearing basal cells. Cells often proliferate and are neighbored by inflammatory foci.	Widespread in T + E_2 and may be found in continuity with HG-PIN.	LP (only)	4 (36,4)	11 (91.7)	0.0094*
Low grade prostatic intraepithelial neoplasia (LG-PIN)	More than two layers of cells with normal or slightly enlarged nuclei sustained by a preserved basement membrane.	Unifocal in control and multifocal in T + E_2.	Overall	10 (90.9)	12 (100)	0.4783
			LP	9 (81.8)	12 (100)	0.4545
			VP	8 (72.7)	10 (83.3)	0.6404
			DP	8 (72.7)	11 (91.7)	0.3168
			AP	6 (54.5)	11 (91.7)	0.0686
High grade prostatic intraepithelial neoplasia (HG-PIN)	Three or more layers of crowded cells of irregular size and often exhibiting enlarged nuclei with prominent nuclei, sustained by a preserved basement menbrane.	Unifocal and usually present tufted and cribriform architecture in control. Multifocal and mostly of flat pattern in T + E_2.	Overall	7 (63.6)	12 (100)	0.0373*
			LP	6 (54.5)	9 (75.0)	0.4003
			VP	3 (27.3)	6 (50.0)	0.4003
			DP	0	6 (50.0)	0.0137*
			AP	0	10 (83.3)	< 0.0001*
Adenocarcinoma	Predominance of crowded cells exhibiting dysplastic features and undergoing proliferation. Basal cells are often absence in nearly but not all tumors.	Mostly invasive and poorly differentiated in T + E_2.	Overall	4 (36.4)	12 (100)	0.0013*
			LP	4 (36.4)	12 (100)	0.0013*
			VP	1 (9.1)	6 (50)	0.0686
			DP	2 (18.2)	6 (50)	0.1930
			AP	0 (0.0)	1 (8.33)	> 0.999

LP: lateral prostate. VP: ventral prostate. DP: dorsal prostate. AP: anterior prostate.
* Statistically significant difference between control and treated ($p < 0.05$).

Corporation, USA) as previously described [14], and placed subcutaneously under sterile surgical conditions into the flank region of anesthetized rats (ketamine-xylazine in combination at 60 and 8 mg/kg of body weight, respectively). To ensure consistent steroid release over time, the implants were replaced at 15 months and kept until animals reached 18 months of age. Control animals ($n = 12$) received empty Silastic implants. The animals were constantly monitored for changes in food consumption and health appearance.

2.3. Sample collection and processing

After deep intraperitoneal anesthesia (87 mg ketamine/kg and 13 mg xylazine/kg), the animals were perfused through the left ventricle with Ringer's solution followed by 10% neutral buffered formalin (NBF). The ventral, dorsal, lateral, and anterior prostatic lobes were dissected, weighed, immersed for at least 24 h in the NBF fixative solution, and then processed for paraffin embedding. Immediately prior to fixation, a small fragment (~50 mg) of each prostatic lobe was snap frozen in liquid nitrogen and stored at −80 °C. Additionally, other reproductive (seminal vesicle, bulbourethral gland, testis, and epididymis) and non-reproductive (spleen, kidney, adrenal and pituitary gland) tissues were removed, weighed and processed for future studies. Paired organs were weighted together.

2.4. Hormone measurements

Plasma samples were obtained after blood collection in heparin-coated tubes through cardiac puncture and followed by centrifugation (at 800 *g* for 5 min). The concentrations of testosterone, dihydrotestosterone, and estradiol were assessed in the plasma of control and T + E_2-treated rats with commercial ELISA Kits (Cat. No. EIA-5396, EIA-5761, and EIA-1559, DRG Instruments GmbH, DE). The assays were performed in duplicate and followed the manufacturer's instructions.

2.5. Stereology and histopathological assessment

Microscopic alterations between groups were evaluated by using routine histology and stereological analysis. For this, NBF-fixed and paraffin-embedded fragments of the prostates were sectioned at 5 μm, stained with hematoxylin and eosin (HE) or periodic acid-Schiff (PAS), and then scanned in a digital pathology system (Panoramic MIDI II, 3DHISTECH, HU). In addition, cryosections of 12 μm thickness from ventral prostates embedded in OCT compound (Sakura Finetek, USA) were stained with oil red to detect lipid-rich contents.

The relative proportion of each compartment of the gland was determined through stereological assessment. For the measurement, the

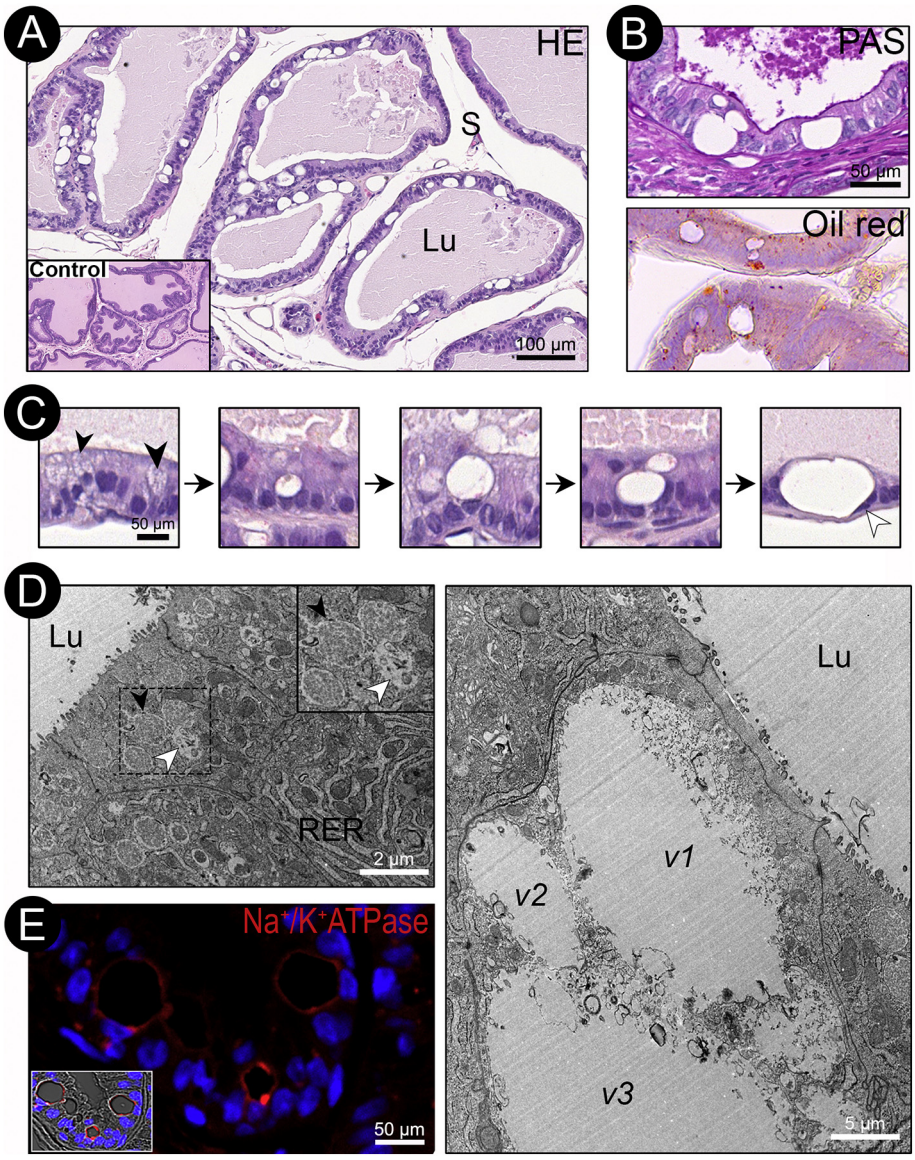

Fig. 2. Hydropic vacuolation in the ventral prostate epithelium of T + E_2-treated Wistar rats. (A) Panoramic view of the ventral prostate epithelium highlighting numerous unstained dilated vacuoles. Insert represents few epithelial vacuolation observed in the control group. (B) PAS and oil red staining showing absence of positive content inside the vacuoles. (C) Cytoplasmic vacuoles in the initial (black arrowhead), intermediate and final (white arrowhead) stages of formation. (D and D′) Ultrastructure of vacuolated epithelial cells. In the supranuclear region, rough endoplasmic reticulum cisternae (RER) and numerous secretory vesicles (black arrowhead) were seen close to small spaces containing residual material that appears to be the initial stage of vacuolation (white arrowhead). As the vacuolation advances, the vacuoles become dilated and merge with each other, as shown in v1, v2, and v3. (E) Confocal microscopy image showing NA+/K+-ATPase expression (red) in the vacuole surface. Cell nucleus was labeled with DAPI (blue). Insert represents an overlap of the image with bright field. Lu: lumen. S: stroma. (For interpretation of the references to color in this figure legend, the reader is referred to the web version of this article.)

prostate compartments were subdivided into epithelium (normal or altered), lumen (with secretion or having sloughed and/or inflammatory cells), and stroma (fibers and connective tissue cells, peri-alveolar smooth muscle layer, blood vessels, and inflammatory foci). For all animals, 10 images were randomly taken (at 40× magnification) from each prostatic lobe and the proportion of compartments was determined by counting the coincident points in a graticulate system with a total of 135 points. The results were expressed as the percentage per constituent.

The histopathological alterations observed in the prostate of control and treated rats were described based on previous investigations [22,23]. In this approach, each prostatic lobe was fragmented into 2 to 4 parts, and at least 8 different sections (stained with HE or PAS) from each fragment were evaluated. The tissue sections were scored for the presence of lesions that include epithelial vacuolation, metaplasia, hyperplasia, atrophy, prostatic intraepithelial neoplasia, and adenocarcinoma. The results were expressed as the incidence of animals affected by each lesion.

2.6. Immunohistochemistry and immunofluorescence

We performed immunohistochemical and immunofluorescence assays to evaluate the epithelial cell type predominant in each prostatic lesion and the expression status of markers implicated with tissue homeostasis and tumorigenesis. For this purpose, tissue sections of NBF-fixed and paraffin-embedded prostate fragments were obtained after serial sectioning at 4 µm and submitted to the protocol previously established [24]. The panel of antibodies used herein is specified in Table S1 and includes markers of basal cells (CK5, CKHMW), cellular proliferation (MCM7), epithelial-mesenchymal transition (E-cadherin, N-cadherin, and Vimentin), and ion transport (NA^+/K^+-ATPase).

After mounting the slides, the immunofluorescence images were acquired using the inverted Nikon Eclipse Ti confocal microscope coupled to an A1 scanning, while those from immunohistochemistry assays were obtained in the 3DHISTECH Panoramic MIDI II slide scanner.

2.7. Transmission electron microscopy (TEM)

Fragments of approximately 1 mm^3 from the ventral prostate were fixed in 2,5% glutaraldehyde for 24 h and post-fixed in 2% osmium tetroxide and then proceeded for standard epoxy resin embedding. Digital images were acquired after examination of ultrathin sections with a Tecnai- G2-Spirit FEI/Quanta electron microscope, operating at

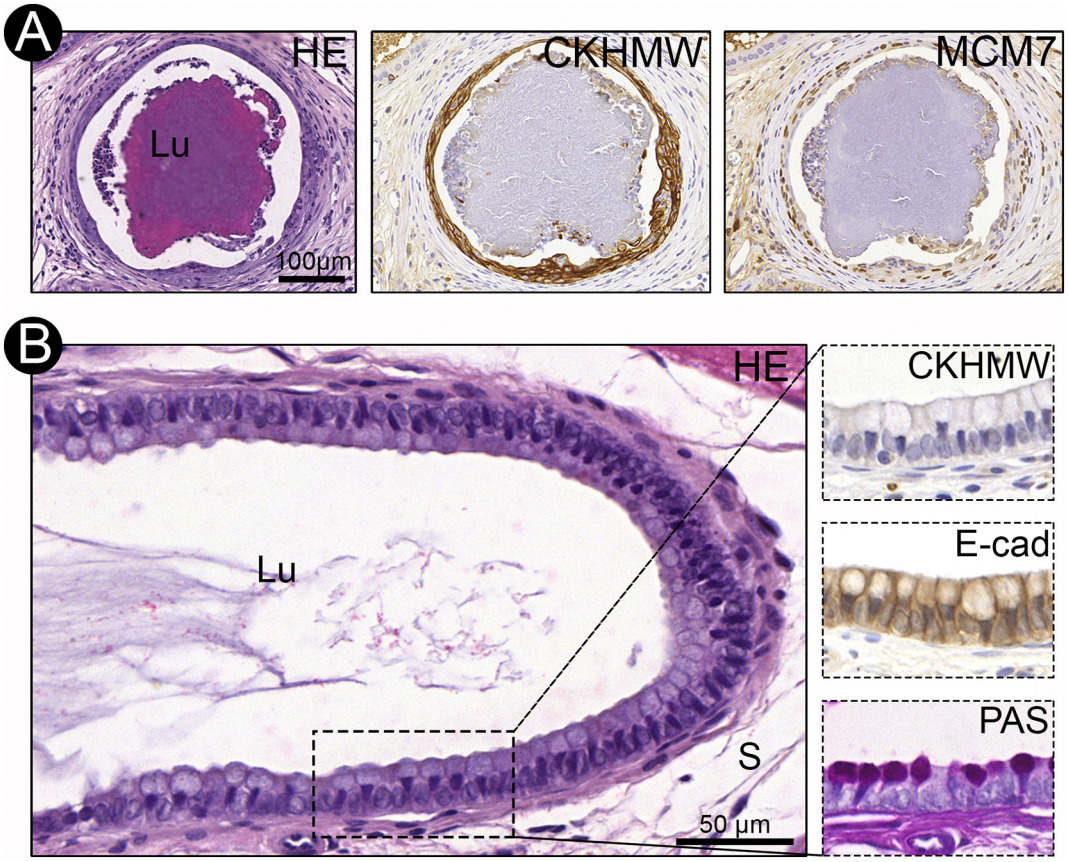

Fig. 3. Metaplastic lesions in the prostate of senile Wistar rat. (A) Lateral prostate acinus exhibiting squamous metaplasia. CKHMW and MCM7 staining were used to identify basal and proliferating cells, respectively. (B) Ventral prostate epithelium undergoing mucinous metaplasia characterized by atypical cells showing a strong PAS positive content and surface well delimited by E-cadherin staining. The figures were taken from control animals. Lu: lumen. S: stroma.

120 kV.

2.8. Protein extraction and Western blotting

Frozen tissues (50 mg) from the ventral and lateral prostates were macerated in dry ice and then solubilized in 150 μL of urea buffer (8 M urea, 20 mM Tris-HCl pH 7.5, 0.5 mM EDTA pH 8.0, 5% protease inhibitors) using a rotor-stator homogenizer. After centrifugation (10 min, 14.000 g, 4 °C), the supernatant fraction was collected from each sample (n = 5 per group) and the protein content was determined by spectrophotometer (NanoDrop 1000, Thermo Scientific, USA).

Western blotting assays were used to evaluate changes in total protein levels of E-cadherin, β-catenin, N-cadherin, and vimentin, recognized markers implicated with epithelial-mesenchymal transition. Initially, 40 μg protein was loaded onto an 8% SDS-PAGE, separated by electrophoresis and then transferred to nitrocellulose membranes. After blocking with 5% BSA/TBST solution, the membranes were incubated *overnight* at 4 °C with the primary antibodies diluted in blocking solution. The immunoreaction was visualized after exposure for 1 h at room temperature to horseradish peroxidase (HRP)-conjugated secondary antibody followed by ECL detection (Cat. No. 20-500-500, Biological Industries, USA). Protein levels were compared between groups by evaluating the signal intensity of target protein bands normalized to that of β-actin (internal control) [25].

2.9. Statistical analyses

Statistical analyses were carried out by using the GraphPad Prism 7 analytical tools. After assessment of normality with the D'Agostino-Pearson test, quantitative variables from control and T + E_2-treated rats were compared by two-tailed unpaired *t*-test or the Mann-Whitney test, when appropriate. The data were presented as mean ± standard error of the mean (SEM). As a categorical data, the incidence of prostatic lesions between groups was presented as frequency and analyzed by Fisher's exact test. Differences were considered significant when obtaining a $p < 0.05$.

3. Results

3.1. Macroscopic and microscopic changes in the rat prostates in parallel to increased levels of testosterone and estradiol

To drive histopathological alterations in the prostate, intact 12-month old Wistar rats were treated for 6 months with Silastic implants containing testosterone plus estradiol. Control animals received empty implants (Fig. 1A). The survival analysis showed that although 5 out of 28 animals died over the experimental course (1/12 controls; 4/16 treated), the long-term hormone exposure was tolerated by the majority (75%) of the animals (Fig. 1B). The treated rats terminated the experiment period in a good health appearance similar to controls, even after undergoing a progressive weight loss of 82 ± 13 g (Fig. 1C). As expected by the hormonal treatment, the concentration of testosterone, dihydrotestosterone, and estradiol was significantly higher in the plasma of T + E_2-treated rats (Fig. 1E).

The treatment induced notorious macroscopic modifications in regard to sizes and appearance of the prostatic complex, especially the lateral prostate, which presented firm and dense bands of yellow-brown tissue (Fig. 1D). In addition, the weight of all the prostate lobes was significantly higher in T + E_2-treated than in control animals (Fig. 1F). The treatment schedule appeared to play primary adverse effects

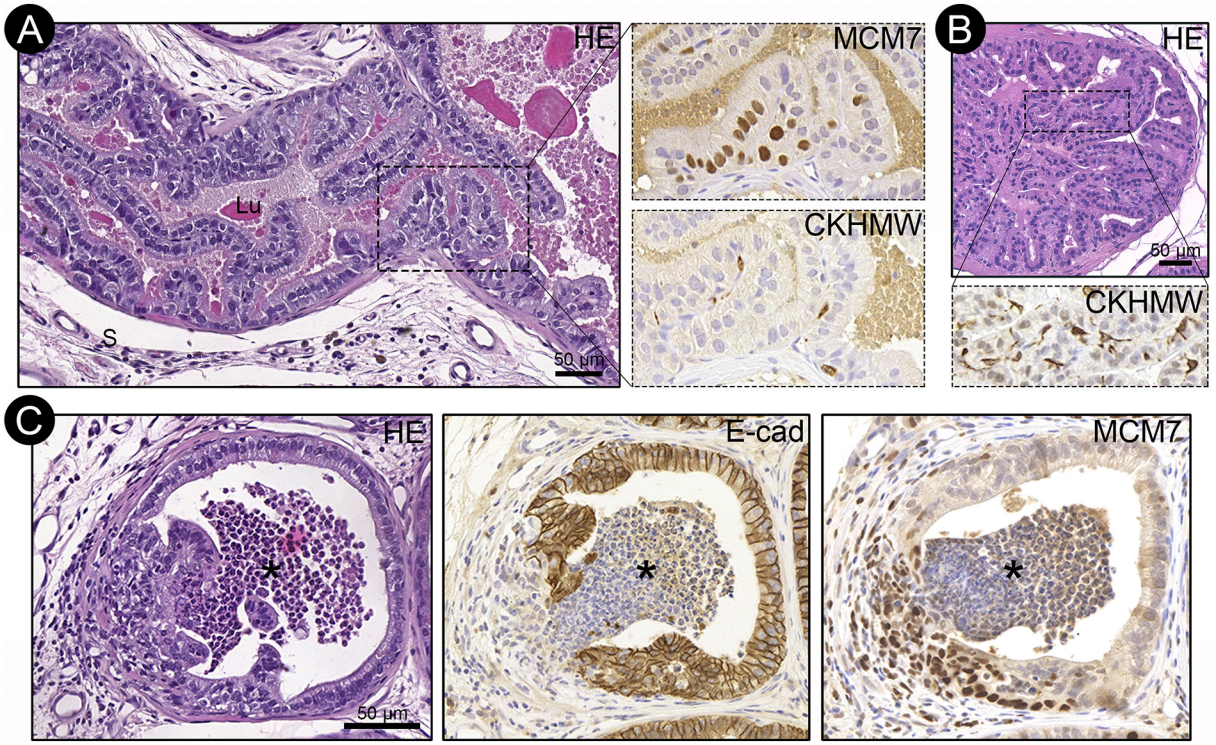

Fig. 4. Hyperplasia and abscess in the prostate of senile Wistar rats. (A) Hyperplastic epithelium from the lateral prostate of T + E_2-treated animals showing cellularity augmentation and projecting moderate unfolding toward the lumen. Hyperplastic foci were actively proliferating as they presented immunoreactivity for MCM7, and showed predominance of luminal cells (CKHMW negative). (B) Occasionally in the treatment group, the anterior prostate also exhibited areas of basal cell hyperplasia, as detected by the high number of CKHMW-positive cells. (C) Prostate abscess in the lateral prostate of a T + E_2-treated rat. This lesion shows focal areas with vast infiltrate of polymorphonuclear cells (*) reaching the lumen and rupture of the associated epithelium, as indicated by the absence of epithelial cells expressing E-cadherin. MCM7-positive proliferating cells were observed in the lesioned epithelium. Lu: lumen. S: stroma.

mainly on the organs most responsive to steroid hormones, since differences in weights and gross morphology were also observed for seminal vesicle, testis, epididymis, and pituitary gland, but not for other organs such as kidney, adrenal gland, and spleen (Fig. 1D, F and Fig. S1A). As previously portrayed in this type of chronic intervention (13–15), testicular atrophy and pituitary adenomas were commonly found in T + E_2-treated rats (Fig. S1A, B).

At the microscopic level, significant modifications were detected in the prostatic tissue after treatment. As evidenced by stereological analysis (Table S2), such modifications were more prominent in the lateral followed by the ventral, dorsal and anterior prostates, and included: (i) marked decrease of acini and ductus with normal features associated with higher prevalence of epithelial sites exhibiting histopathological alterations; (ii) increased density of blood vessels and inflammatory foci in the stroma; (iii) prevalence of leukocytes and sloughed epithelial cells into the lumen; and (iv) lobe-specific variation in the thickness of perialveolar smooth muscle layer.

3.2. Chronic combination of testosterone plus estradiol enhances the incidence of benign, pre-malignant and cancerous lesions in the prostate epithelium

A broad spectrum of lesions was observed in the rat prostate at 18 months of age, in both control and treatment group; however, the changes observed in control animals were punctual and restricted to few epithelial areas randomly distributed alongside acini and ducts with unaltered morphology, whereas a large extent of the prostatic epithelium of T + E_2-treated animals presented some histopathological alteration (for an overview, see Fig. S2). The changes included benign, pre-malignant and tumor lesions, whose incidence and extent varied according to experimental group and prostate lobe (Table 1). For a better understanding, herein we provide a detailed comparative description of each epithelial lesion that arose in the prostates of control and treated rats.

3.2.1. Hydropic vacuolation

Some epithelial cells presenting cytoplasmic vacuoles were observed primarily in the ventral prostate epithelium. They likely correspond to atypical luminal cells, based on the absence of CK5 and CKHMW staining (data not shown). Notably, the treatment with T + E_2 functioned as a potent inducer of epithelial vacuolation, since the number of animals presenting vacuolated epithelial cells was significantly higher in the treatment group (4/11 controls vs. 11/12 treated, $p = 0.0009$, Table 1). The vacuoles were often larger and occupied a space of the epithelium that could fit two or more luminal cells (Fig. 2A and C). After careful histological and ultrastructural analysis, we found that the vacuolation appeared to involve a progressive ballooning of vesicles in the supranuclear cytoplasm which coalesced to form dilated vacuoles. As the vacuoles increase in size, they merge with each other and usually force the nucleus and residual cytoplasm toward the cell margin (Fig. 2C, D). Thus, it was possible to see within the same epithelial area, cells exhibiting visible cytoplasmic vacuoles at different stages of formation (Fig. 2C). Noteworthy, the vacuoles neither presented electron-dense content nor were stained for HE, PAS or oil red, thereby being structures of presumably aqueous character (Fig. 2B–D). This hypothesis of hydropic vacuolation was corroborated by the intense expression of NA^+/K^+-ATPase located especially in the vacuole surface (Fig. 2E), which is suggestive of hydrolytic imbalance.

3.2.2. Squamous metaplasia

The prostate of aged Wistar rats also displayed areas of squamous metaplasia, a benign lesion in which the aberrant proliferation of basal cells conferred to the prostatic epithelium a squamous stratified appearance (Fig. 3A). The accurate identification of this lesion was

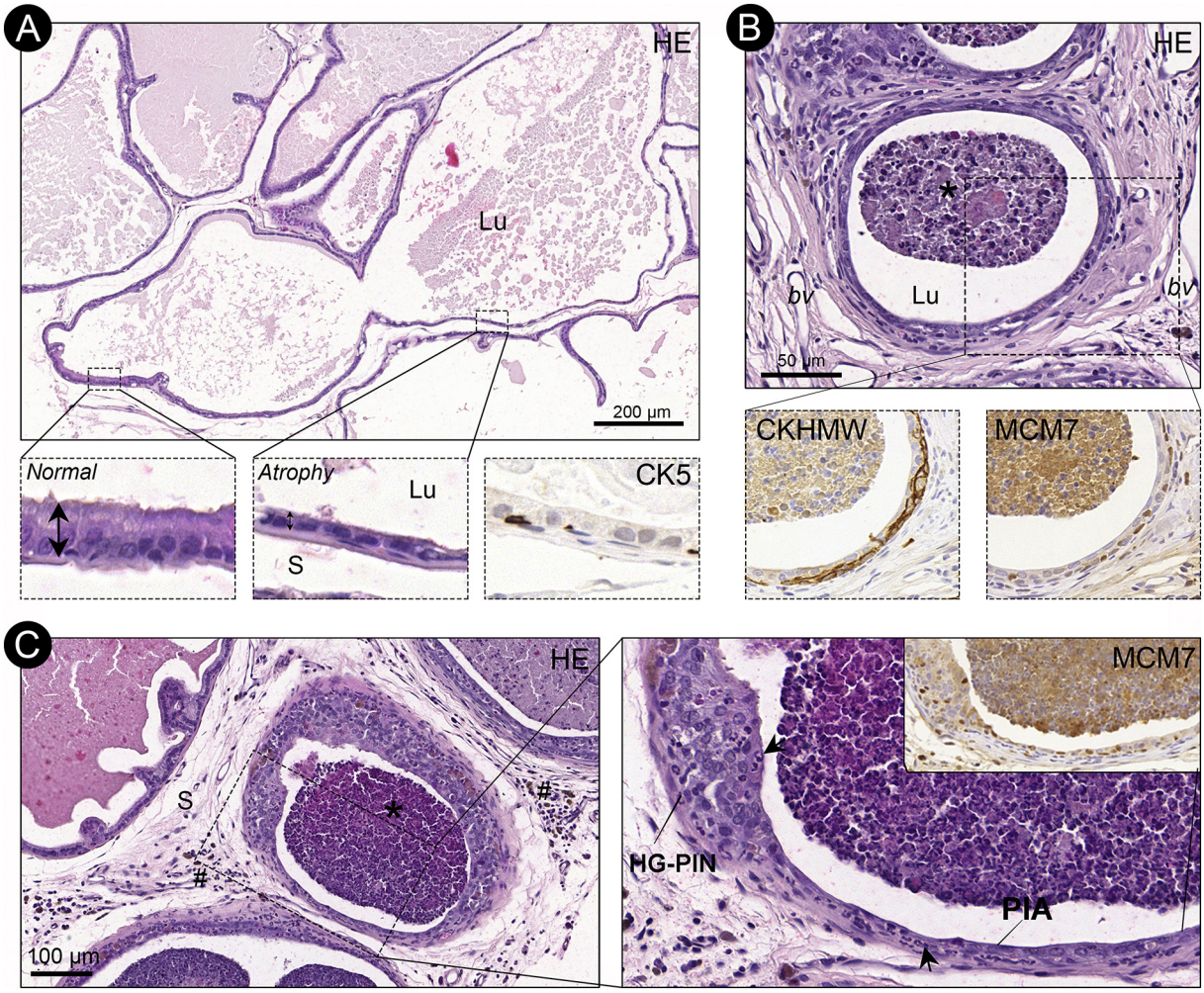

Fig. 5. Atrophic lesions in the prostates of senile Wistar rats. (A) Representative ventral prostate of a control animal exhibiting atrophic luminal cells (CK5 negative). Double arrow highlights the difference in height between normal-appearing and atrophic cells. (B) Atrophic lesion in the lateral prostate of a T + E_2-treated rat showing features of PIA, in which the lesioned acini are actively proliferating (MCM7 positive) and occur in a tight association with inflammatory cells that surround the acini (#) and/or localize within the epithelium (arrowheads) and lumen (*). PIA exhibited a characteristic enrichment of basal cells (CKHMW positive). (C) Some PIA lesions occurred in continuity with HG-PIN. Lu: lumen. S: stroma. bv: blood vessel. PIA: proliferative inflammatory atrophy. HG-PIN: high grade prostatic intraepithelial neoplasia.

performed by using the routine histology in association with immunohistochemical staining for recognized markers of basal cells (CKHMW) and cellular proliferation (MCM7). Acini exhibiting squamous metaplasia were observed only in the lateral prostate. The number of animals having this lesion was quite similar between groups (3/11 control vs. 5/12 treated, p = 0.6668, Table 1).

3.2.3. Mucinous metaplasia

It was characterized by cells displaying goblet-like morphology and that accumulate mucinous materials (strongly positive for PAS) in their supranuclear cytoplasm (Fig. 3B). Based on the absence of CKHMW staining, the mucinous cells likely correspond to luminal cells (Fig. 3B). These metaplastic cells occurred scattered or forming small groups in the ventral prostate epithelium and affected only one animal of each group (Table 1). The atypical cells presented a precise delimitation as indicated by the staining pattern of the membrane-anchored protein E-cadherin (Fig. 3B).

3.2.4. Hyperplasia

Present in the prostate of all control and treated rats (Table 1), hyperplasia was identified by a glandular epithelium showing cellularity augmentation and immunopositivity for MCM7 (Fig. 4A). In the control group, hyperplastic acini were punctual and showed slight to moderate unfolding toward the lumen. Conversely, numerous hyperplastic sites projecting moderate to extensive epithelial unfolding that often occupied a great area of the lumen were found within the prostates of T + E_2-treated rats (Fig. 4A). In most cases, hyperplastic cells corresponded to luminal cells as they did not express CKHMW, except in the anterior prostate of some treated rats, where basal cell hyperplasia was also observed (Fig. 4B).

3.2.5. Abscess

Focal areas presenting a vast inflammatory infiltrate with predominance of polymorphonuclear cells closely associated with a lesioned epithelium were observed in the prostate of few controls but almost all T + E_2-treated rats (3/11 controls vs. 11/12 treated, p = 0.0028, Table 1) (Fig. 4C). These areas were found only in the lateral prostate and correspond to abscesses, in which the acute inflammatory response leads to injury of the associated epithelium. Such tissue damage was easily observed since the epithelium in contact with the inflammatory infiltrate underwent a discontinuity, as confirmed histologically and by the absence of epithelial cells expressing E-cadherin specifically at this site. In addition, it was common to detect MCM7-positive epithelial cells in the lesioned epithelium (Fig. 4C).

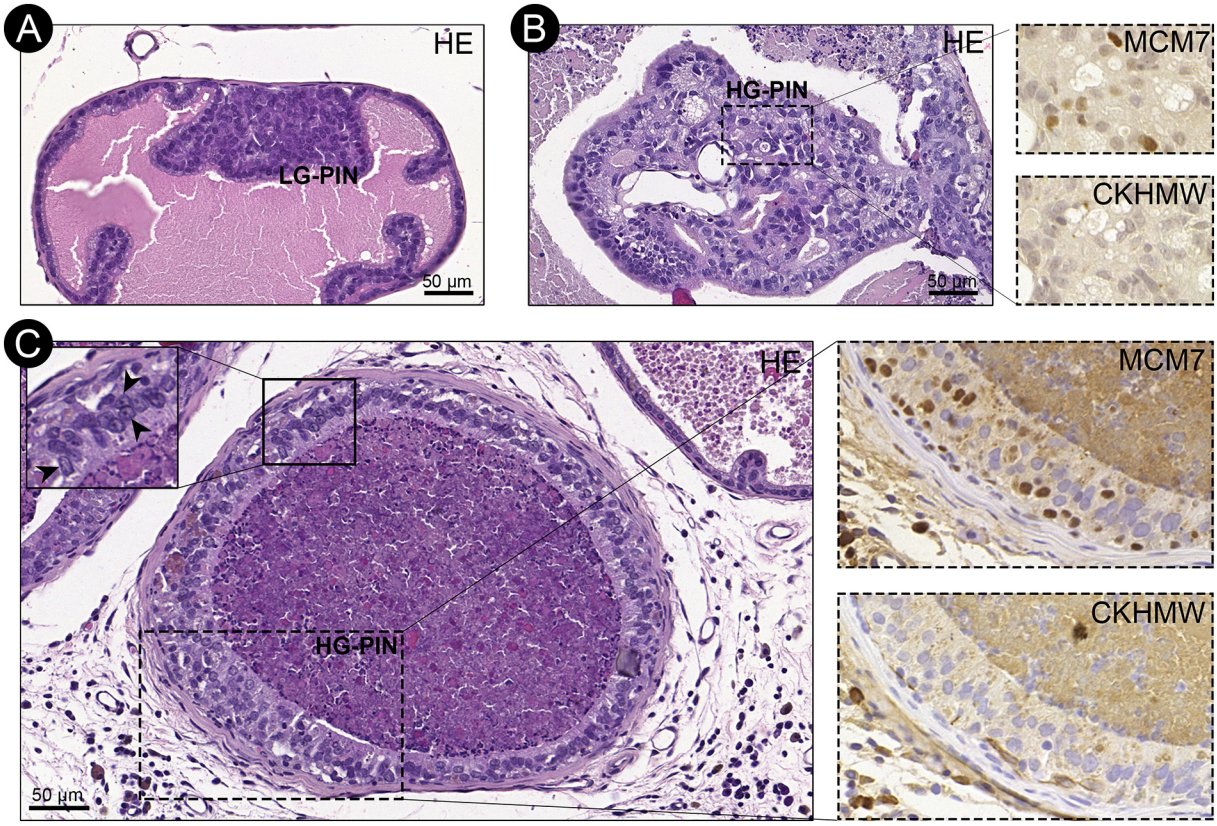

Fig. 6. Prostatic intraepithelial neoplasia in the prostates of senile Wistar rats. (A) Representative HE staining from the lateral prostate of a control animal presenting a LG-PIN. (B) Ventral prostate of a control rat showing a HG-PIN with cribriform pattern and some proliferative MCM7-positive cells. (C) HG-PIN from the lateral prostate after T + E_2 treatment. Layers of epithelial cells with enlarged nuclei and prominent nucleoli (arrowheads), many of them in proliferation, are arranged in a flat architecture. LG-PIN: low-grade prostatic intraepithelial neoplasia. HG-PIN: high-grade prostatic intraepithelial neoplasia.

3.2.6. Atrophies

Another frequently observed prostatic lesion was epithelial atrophy, in which ducts and acini were lined by a cubic to squamous epithelium composed of luminal cells with reduced height and scant cytoplasm, as well as normal-appearing basal cells (Fig. 5). Regardless of experimental group, epithelia undergoing atrophy were observed in the prostate of all animals (Table 1). Despite the majority of atrophies were histologically correspondent to focal simple atrophies, this group of lesions showed to be heterogeneous among prostate lobes and even within the same gland. Accordingly, in the ventral prostate, which was the lobe with the highest extent of atrophic lesions, it was possible to observe glands either partially or completely lined by an atrophic epithelium (Fig. 5A). Particularly in the lateral prostate, glandular atrophy often corresponded to proliferative inflammatory atrophy (PIA), as such lesions were actively proliferative and occurred in a tight association with inflammatory cells surrounding the acini and/or located within the epithelium and lumen (Fig. 5B and C). Differently from simple atrophy, PIA also exhibited a characteristic enrichment of basal cells that usually were arranged beneath or alongside the atrophic luminal cells (Fig. 5B). Importantly, the chronic treatment with T + E_2 potentiated the development of PIA, as these lesions were found widespread in the lateral prostate of almost all treated rats (11/12, ~92%). It is noteworthy that PIA was often found in continuity with prostatic intraepithelial neoplasia, within the same acini (Fig. 5C). In contrast, limited sites containing PIA were found in the lateral prostate epithelium of control animals (36%, 4/11) (Table 1).

3.2.7. Prostatic intraepithelial neoplasia (PIN)

Lesioned areas compatible with PIN were defined through the observation of intraepithelial stratification sustaining luminal cells of varying sizes and nuclear appearance, and a preserved basement membrane (Fig. 6). PIN lesions were classified as low (LG-PIN) or high grade (HG-PIN) according to the predominant morphological features of epithelial cells. LG-PIN was characterized by more than two layers of cells displaying normal or slightly enlarged nuclei with prominent nucleoli (Fig. 6A), whereas the HG-PIN showed three or more layers of crowded cells of irregular size often exhibiting enlarged nuclei with prominent nucleoli and immunopositivity for MCM7 (Fig. 6B and C). Regardless of experimental group, both PIN lesions affected mainly the glands of the lateral prostate. However, LG-PIN and HG-PIN were unifocal within the glands of control animals, since they uniquely affected isolated sites scattered throughout the normal epithelium, whereas in the treatment group, the lesions could be seen in multiple epithelial sites. Noteworthy, as presented in Table 1, the number of animals carrying HG-PIN was significantly higher in the treatment group (7/11 controls vs. 12/12 treated, $p = 0.0373$). The same did not occur for LG-PIN, since this lesion was commonly present in almost all animals (10/11 controls vs. 12/12 treated, $p = 0.4783$). Moreover, the architectural patterns of HG-PIN varied according to the experimental group, as the lesion frequently assumed a tufted or cribriform pattern in the lateral and ventral prostate of controls (Fig. 6A and B), respectively, and a flatter architecture in the prostatic lobes of T + E_2-treated rats (Fig. 6C). It is important to emphasize that, because inflammatory foci were frequently observed close to or associated with HG-PIN in the treatment group (Fig. 5C and 6C), this proliferative lesion could be misidentified as the reactive hyperplasia, a non-neoplastic/inflammatory lesion of the prostate [22,23]. However, the diagnostic features to discriminate these lesions rule out the possibility of reactive hyperplasia [23], as HG-PIN presented many atypical cells and the associated inflammatory infiltrate was not suppurative.

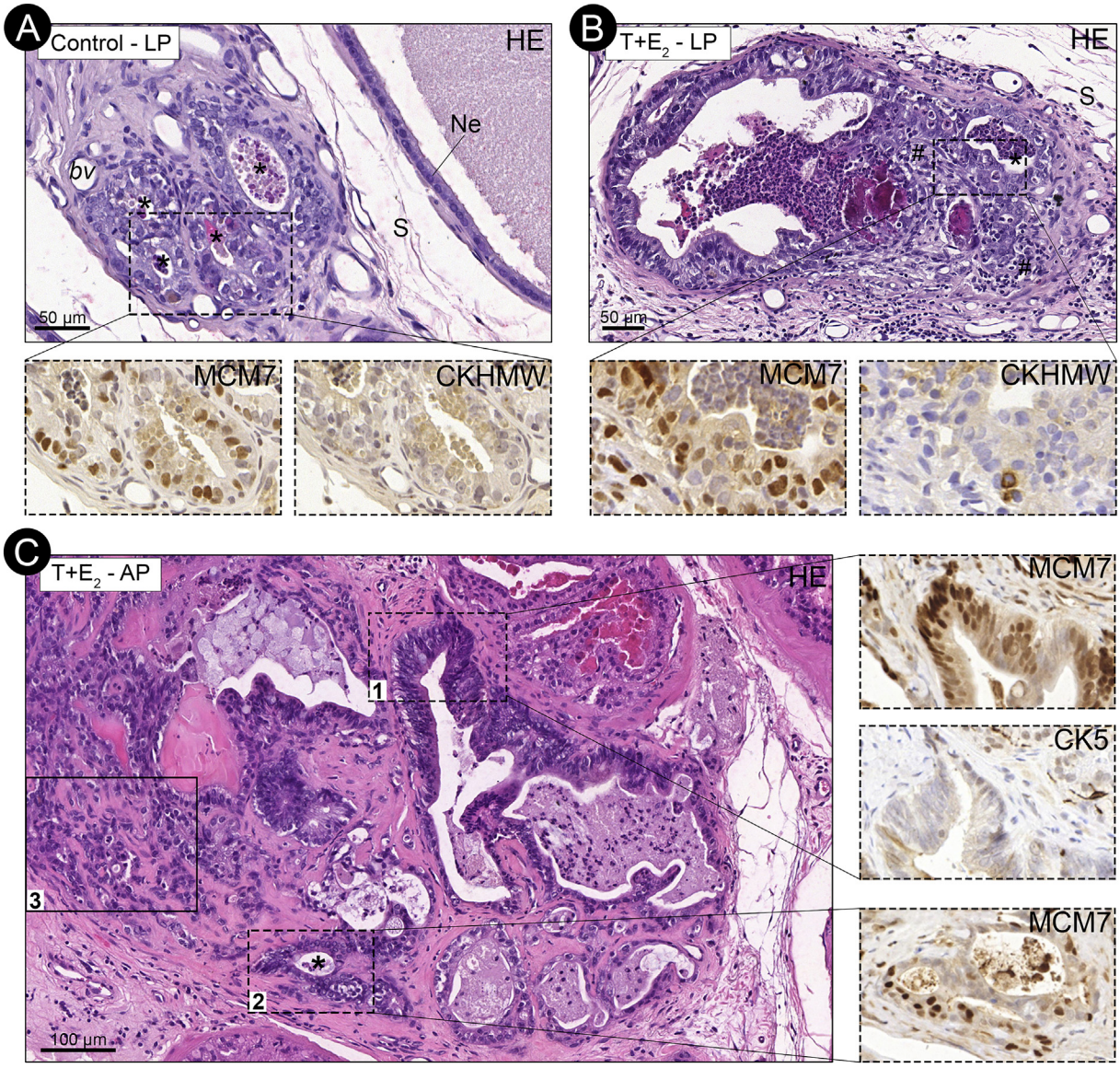

Fig. 7. Adenocarcinoma in the prostates of senile Wistar rats. (A) Ventral prostate of a control animal showing malignant cells forming microacini. (B) Invasive adenocarcinoma in the lateral prostate of a T + E_2-treated rat. Microacini arrangement is present, as well as malignant cells diffused through the stroma in close association with inflammatory infiltrate. (C) Treated anterior prostate in panoramic view, showing different stages of adenocarcinoma: 1 - adenocarcinoma in situ, with dysplastic cells; 2 - microacini formations; 3 - poorly differentiated invasive adenocarcinoma spread through the stroma. Regardless of experimental group, the majority of malignant sites showed high proliferative activity (MCM7-positive) and exhibited predominance of CKHMW-negative cells. S: stroma. Ne: normal epithelium. bv: blood vessels. *: indicates microacini arrangement.

3.2.8. Adenocarcinoma

The occurrence of the premalignant lesions HG-PIN and PIA raised the possibility of detecting tumors in the rat prostate at 18 months of age. After a systematic screening of several histological slides from each prostate lobe, we were able to detect lesions histologically-compatible with adenocarcinomas in the prostates of both groups analyzed. The malignant sites had an abnormal growth pattern with the predominance of crowded, basophilic, dysplastic-appearing cells. The majority of tumors were actively proliferative and did not present positive staining for the basal cell markers CKHMW and CK5 in the epithelium (Fig. 7). One exception was observed in a tumor growing in an intraductal pattern within the lateral prostate of a control animal, where the retention of the basal cell layer, characteristic in this type of adenocarcinoma, was observed (Fig. S3). However, it is important to note that the effects of long-term hormone exposure for inducing prostatic adenocarcinoma surpassed those of physiological aging. Indeed, while a modest incidence of malignant lesions (4/11, 36%) was computed in the control group, 100% (12/12) of T + E_2-treated rats had adenocarcinomas in their prostates. Moreover, unlike the control group in which both in situ and invasive adenocarcinomas were observed, the majority of malignant sites found in the treated animals corresponded to invasive adenocarcinomas arranged in a microacinar architecture or entirely widespread in the stroma (Fig. 7). In consonance with the observation of premalignant lesions, in both control and treated rats, the lateral lobe was the major target for tumors, followed by the dorsal, ventral, and anterior prostates (Table 1).

3.3. The effects of T + E_2 treatment on the rat prostate include induction of epithelial-mesenchymal transition

The epithelial-mesenchymal transition (EMT) is a cellular transdifferentiation program highly implicated with the prostate tumorigenesis, and both androgens and estrogens can modulate EMT-inducing signals [26–28]. Thus, in this study, we sought to investigate whether the

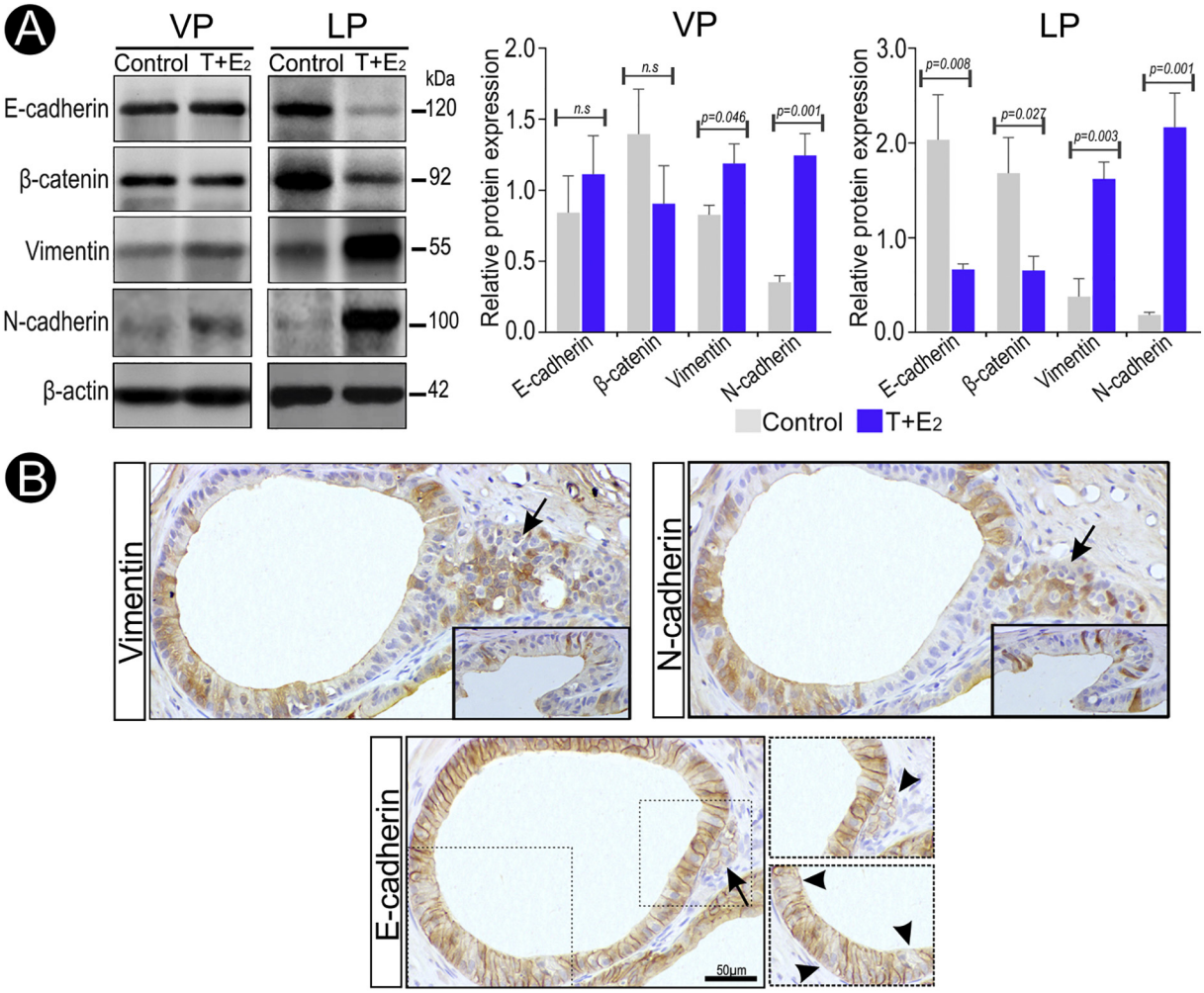

Fig. 8. The effects of T + E_2 treatment on the rat prostate include induction of epithelial-mesenchymal transition. (A) Representative images of Western blotting assays followed by densitometric quantification of immunoreactive bands correspondent to EMT-associated proteins. Note that the changes were more pronounced in the lateral than ventral prostate (B) In line with the main changes observed in total protein extracts, numerous prostate epithelial cells of T + E_2-treated rats became positive for vimentin and N-cadherin while showing flaw in the expression of E-cadherin (arrowheads). Such epithelial cells occurred restricted to areas with altered morphology and portraying lesions such as invasive adenocarcinoma (arrows). Lower inserts highlight the presence of immunoreactive epithelial cells displaying elongated morphology. Pictures were taken from the lateral prostate. VP: ventral prostate. LP: lateral prostate.

enhanced malignant transformation of the prostate epithelium following chronic exposure to T + E_2, such as that observed in the ventral and especially in the lateral prostate, might be associated with changes indicative of EMT.

Western blotting results showed that, while the total level of the cell-cell adhesion molecules E-cadherin and β-catenin remained unchanged in the ventral prostate, their expressions were drastically reduced in the lateral prostate of T + E_2-treated rats (Fig. 8A). On the other hand, the treatment upregulated the expression of vimentin and N-cadherin in the ventral and especially in the lateral prostate (Fig. 8A). Accordingly, in the lateral prostate of treated rats, epithelial cells frequently expressed vimentin and N-cadherin, both mesenchymal proteins that upon physiological conditions are absent in the epithelium. These epithelial cells eventually presented an elongated mesenchymal-like morphology and were found restricted to lesioned areas including HG-PIN and invasive adenocarcinoma, which often showed flaws in expressing epithelial markers such as E-cadherin (Fig. 8B). Altogether, the chronic combination of testosterone plus estradiol affects the expression of epithelial and mesenchymal proteins characteristic of EMT phenotype in a lobe-specific manner. This finding goes in line with the higher incidence of tumors and the pre-malignant lesions HG-PIN and PIA in the lateral prostate of T + E_2 rats (Table 1).

4. Discussion

The present study explored two relevant issues for prostate health: aging and the influence of androgen and estrogen balance. By using the Wistar rat as an experimental model, we showed that at advanced ages, the prostate is targeted by histopathological alterations including benign, premalignant, and malignant lesions, which resemble the aging human prostate in many respects. Strikingly, the incidence of most prostatic alterations including precancerous lesions and adenocarcinomas increased expressively after treatment of middle-aged rats with testosterone plus estradiol, an enhancement that was associated with molecular changes hallmark of epithelial-mesenchymal transition (EMT).

The results presented herein, as well as those from previous investigations [6,21,29,30], demonstrated that aged Wistar rats are highly susceptible to the arising of prostate lesions. Even in the control group, punctual areas exhibiting proliferative, atrophic, metaplastic and inflammatory lesions were observed in the prostate. Since the control animals received empty hormone implants, the changes observed in this group are assumed to be spontaneous and resultant from the aging process. It is important to highlight that, besides the non-neoplastic lesions found in control rats, around 36% of them developed

malignant prostatic tumors. Such tumor rate is close to the 26% previously found for this rat strain at advanced ages [29] and far away exceeds those observed in senescent mouse (< 1%) and hamster (2%) [[31],32]. It also exceeds those reported for other rat strains, such as NBL (0.45%, over 13 months old [9]), F344 (3,4%, at 24 months [33]), Copenhagen (10%, at 36 months [3]), and AXC rats (17%, at 34 to 37 months [17]). Only the ACI/Seg rats aged 33 months and beyond presented a higher incidence of PCa than the presently found, which was reported to reach up to 80% [3,34]. These data suggest that the use of Wistar rats provide advantages over other experimental animals, since they present a modest incidence of spontaneous tumors within a shorter period of time (18 months). Additionally, similar to that commonly found in elderly men, malignant tumors arising in the prostate of aged Wistar rats corresponded to adenocarcinomas, as reported here and by others [21,29].

Besides the animal's age and strain, the detection of naturally occurring PCa is also dependent on the success in sampling the target area. In this study, malignant lesions occurred in punctual areas surrounded by normal-appearing acini and ducts and were not present in the majority of histological slides. Such difficulty in sampling the proper site of prostate lesions had been noticed by others [18,33]. Furthermore, doubts concerning histological discrimination between the precancerous lesion HG-PIN and non-invasive adenocarcinoma have made the diagnosis of PCa and the reliable estimation of its incidence challenging. In this regard, we argue that our approach succeeded in detecting a tumor rate of 36% in untreated Wistar rats due to an exhaustive evaluation of several histological slides taken from different regions of the prostate, in association with key immunohistochemical assays. This fact may explain why we hinted at the possibility but did not confirm previously the occurrence of prostatic adenocarcinomas in aged Wistar rats at that time [6].

The treatment with T + E_2 provided an environment conducive to a greater development of some specific lesions in Wistar rats. One of them was prostatic adenocarcinoma, whose incidence rose from 36% to 100% after the treatment. Such an impressive increment in tumor rate was accompanied by an enhancement of HG-PIN and PIA, recognized precursor lesions of PCa [35]. This data suggests that, like the human disease, PCa development in Wistar rat appears to result from a multistep process involving the onset and progression of premalignant lesions. Intriguingly, it has been thought that a prolonged period of treatment with T + E_2 is needed to effectively induce PCa in rats. For instance, Drago (1984) [12] showed that the incidence of microscopic carcinomas in the prostate of NBL rats jumped from 3.3% to 88% when the treatment period went from 3 to 18 months or longer. Similarly, Bosland et al. (1995) [14] demonstrated that the significant induction of PCa was achieved in NBL and Sprague-Dawley rats after treatment with T + E_2 for approximately 12 months. Conversely, we succeeded in inducing PCa in 100% of middle-aged rats followed by 6 months of treatment. Therefore, it is reasonable to infer that such a high inducement of PCa was not entirely due to the prolonged duration of treatment, but rather the time-life period in which the changes in androgen and estrogen levels occurs. In this line, by evaluating Wistar rats from 3 to 24 months of age, we have recently shown that changes in the circulating and intraprostatic ratio of androgen:estrogen begin at 12 months and intensify at 18 months [6], the time window at which we hereupon performed the treatment.

Recent studies on prostate cells have addressed that key factors involved with EMT can be modulated by androgens and estrogens [22–27,36]. By evaluating the expression of the EMT hallmark proteins E-cadherin, N-cadherin, β-catenin, and vimentin, herein we presented evidence that EMT might be linked to the greater development of precancerous lesions and adenocarcinomas observed after T + E_2 treatment. The EMT-associated modifications were more pronounced in the lateral prostate, which was the prostatic lobe that exhibited the highest incidence of histopathological alterations of premalignant and malignant nature. These data are in agreement with other studies showing that EMT is a putative mechanism of carcinogenesis and tumor progression in the prostate gland [26,27], although they do not exclude the possibility of androgens and estrogens may also be acting via other mechanisms to induce the adverse effects presently observed, as such hormones are well known to have a broad action in the prostatic tissue.

It has been shown that both androgen and estrogen play a role in recruiting inflammatory cells to the prostate [37–39]. This fact entices special attention because it was notorious the presence of neutrophils and mononuclear inflammatory cells in the stroma and within the lumen and epithelium of the prostate of all T + E_2-treated rats, which is indicative of active prostatitis [22]. Moreover, the treatment expressively increased the occurrence of prostate abscess. Although this lesion is often caused by bacterial infections [40], the animals of both groups were maintained under the same environmental conditions and without documentable infections. Thus, the increased frequency of abscesses in the treatment group is likely resulting from a complication of prostatitis. Importantly, besides being the lobe more affected by inflammatory disorders, the lateral prostate was the major site where premalignant lesions and adenocarcinomas arose. Although it was not the focus of the current study, the proper identification of leukocyte subsets as well as their products could be valuable to better understand the crosstalk between inflammation and the enhancement of malignancies in the prostate of T + E_2-treated rats.

Furthermore, the hormonal intervention functioned as a potent inducer of epithelial vacuolation. Vacuolated cells were primarily observed in the ventral prostate epithelium, which has been noticed as the prostatic lobe most susceptible to this alteration [6,18,41,42]. If on the one hand this data highlights the influence of sex steroids triggering vacuolation, on the other there is not yet a consensual term to designate this morphological phenomenon in the prostate [6,18,22,41,42]. Additionally, little is known about the nature of the vacuoles. In the present investigation, we used a combination of light, confocal and transmission electron microscopy to better characterize this alteration. The ultrastructural changes in association with the absence of lipid or glycoprotein rich content within the vacuole led us to propose the hydropic degeneration as the most plausible cause of vacuolation. In line with this piece of evidence, hydropic degeneration followed by vacuolation was also observed in the human prostate epithelium after treatment with the estrogenic compound diethylstilbestrol (DES) [43]. Moreover, it was observed an intense expression of NA^+/K^+-ATPase at the vacuole surface, which can disturb the equilibrium of osmotic pressure and contribute to water inflow into the vacuole.

Given the above background, our results highlight the potential use of aged Wistar rats as a suitable model to study prostatic lesions. Besides its advantages in regard to the higher PCa incidence and shorter latency period over the pre-existent spontaneous and hormonally-induced rodent models [16,44], the proposed animal model could serve as a valuable alternative to identify preventive or therapeutic measures for the prostate gland. Accordingly, a plethora of non-neoplastic and neoplastic lesions was presently described, thereby allowing evaluating, simultaneously, whether a particular target exerts effective actions against one or more histopathological alteration. On the other hand, for researchers who aim to generate preliminary or rapid insights into prostate diseases, the in vitro assays or other animal models such as those established from more drastic conditions (e.g. genetically engineered mice) might be more attractive. Nevertheless, a plausible alternative to circumvent the relatively long period of animal aging presently proposed would be purchasing animals at an advanced age, a service already offered by some animal production facilities. Also, in this study, we did not investigate if the invasive adenocarcinomas could metastasize to other organs. Further investigations are needed to evaluate the potential use of aged Wistar rats to study the metastatic PCa.

5. Conclusion

Taken together, our results provide solid evidence that male Wistar rats may be useful as a suitable preclinical model for studying aging-related prostate disorders including PCa. This statement is based upon the observation that such rat strain nicely recapitulates the prostate carcinogenesis through the arising of benign, precancerous and malignant lesions, and above all naturally yields a modest incidence of PCa that can be increased up to 100% following exposure to testosterone plus estradiol.

Acknowledgments

Funding

This work was supported by the Conselho Nacional de Desenvolvimento Científico e Tecnológico - CNPq/Brazil (Grant and research fellowship to C.A.O and PIBIC scholarship to M.C.B); the Fundação de Amparo a Pesquisa do Estado de Minas Gerais-FAPEMIG/Brazil (Grant to C.A.O.); and the Coordenação de Aperfeiçoamento de Pessoal de Nível Superior-CAPES/Brazil (Doctoral fellowship to G.H.C·S and Masters fellowship to B.T.M and H.W.G).

The authors thank the Center of Microscopy, Center for Acquisition and Processing of Images, and Center for Gastrointestinal Biology of the UFMG for providing the equipment and technical support for experiments involving electron, light, and confocal microscopy. The authors are also grateful to Dr. Enio Ferreira for his contribution in identifying pituitary adenomas and all anonymous referees for their helpful suggestions.

Author contributions

Study design: GHCS HWG CAO. Execution of experiments: GHCS HWG BTM MCB MJT. Data collection and analysis: GHCS HWG BTM CAO. Technical and intellectual support: HRC GABM CAO. Manuscript drafting: GHCS HWG BTM CAO. All the authors have revised and approved the final version of the manuscript.

Declaration of competing interest

The authors declare that there are no conflicts of interest.

Appendix A. Supplementary data

Supplementary data to this article can be found online at https://doi.org/10.1016/j.lfs.2019.117149.

References

[1] C.K. Zhou, D.P. Check, J. Lortet-Tieulent, M. Laversanne, A. Jemal, J. Ferlay, F. Bray, M.B. Cook, S.S. Devesa, Prostate cancer incidence in 43 populations worldwide: an analysis of time trends overall and by age group, Int. J. Cancer 138 (2016) 1388–1400.

[2] F. Bray, J. Ferlay, I. Soerjomataram, R.L. Siegel, L.A. Torre, A. Jemal, Global cancer statistics 2018: GLOBOCAN estimates of incidence and mortality worldwide for 36 cancers in 185 countries, CA Cancer J. Clin. 68 (2018) 394–424.

[3] J.T. Isaacs, The aging ACI/Seg versus Copenhagen male rat as a model system for the study of prostatic carcinogenesis, Cancer Res. 44 (1984) 5785–5796.

[4] M. Krieg, R. Nass, S. Tunn, Effect of aging on endogenous level of 5 alpha-dihydrotestosterone, testosterone, estradiol, and estrone in epithelium and stroma of normal and hyperplastic human prostate, J. Clin. Endocrinol. Metab. 77 (1993) 375–381.

[5] P.P. Banerjee, S. Banerjee, J.M. Lai, J.D. Strandberg, B.R. Zirkin, T.R. Brown, Age-dependent and lobe-specific spontaneous hyperplasia in the brown Norway rat prostate, Biol. Reprod. 59 (1998) 1163–1170.

[6] M. Morais-Santos, A.E. Nunes, A.G. Oliveira, J.D. Moura-Cordeiro, G.A. Mahecha, M.C. Avellar, C.A. Oliveira, Changes in estrogen receptor ERbeta (ESR2) expression without changes in the estradiol levels in the Prostate of aging rats, PLoS One 10 (2015) e0131901.

[7] A. Vermeulen, R. Rubens, L. Verdonck, Testosterone secretion and metabolism in old age, Acta Endocrinol. Suppl. (Copenh) 152 (1971) 23.

[8] Y. Shibata, K. Ito, K. Suzuki, K. Nakano, Y. Fukabori, R. Suzuki, Y. Kawabe, S. Honma, H. Yamanaka, Changes in the endocrine environment of the human prostate transition zone with aging: simultaneous quantitative analysis of prostatic sex steroids and comparison with human prostatic histological composition, Prostate 42 (2000) 45–55.

[9] R.L. Noble, The development of prostatic adenocarcinoma in Nb rats following prolonged sex hormone administration, Cancer Res. 37 (1977) 1929–1933.

[10] R.L. Noble, Production of Nb rat carcinoma of the dorsal prostate and response of estrogen-dependent transplants to sex hormones and tamoxifen, Cancer Res. 40 (1980) 3547–3550.

[11] R.L. Noble, Prostate carcinoma of the Nb rat in relation to hormones, Int. Rev. Exp. Pathol. 23 (1982) 113–159.

[12] J.R. Drago, The induction of NB rat prostatic carcinomas, Anticancer Res. 4 (1984) 255–256.

[13] I. Leav, S.M. Ho, P. Ofner, F.B. Merk, P.W. Kwan, D. Damassa, Biochemical alterations in sex hormone-induced hyperplasia and dysplasia of the dorsolateral prostates of Noble rats, J. Natl. Cancer Inst. 80 (1988) 1045–1053.

[14] M.C. Bosland, H. Ford, L. Horton, Induction at high incidence of ductal prostate adenocarcinomas in NBL/Cr and Sprague-Dawley Hsd:SD rats treated with a combination of testosterone and estradiol-17 beta or diethylstilbestrol, Carcinogenesis 16 (1995) 1311–1317.

[15] N. Ozten, K. Vega, J. Liehr, X. Huang, L. Horton, E.L. Cavalieri, E.G. Rogan, M.C. Bosland, Role of estrogen in androgen-induced prostate carcinogenesis in NBL rats, Horm Cancer 10 (2019) 77–88.

[16] E. Nascimento-Goncalves, A.I. Faustino-Rocha, F. Seixas, M. Ginja, B. Colaco, R. Ferreira, M. Fardilha, P.A. Oliveira, Modelling human prostate cancer: rat models, Life Sci. 203 (2018) 210–224.

[17] S.A. Shain, B. McCullough, A. Segaloff, Spontaneous adenocarcinomas of the ventral prostate of aged A X C rats, J. Natl. Cancer Inst. 55 (1975) 177–180.

[18] T. Suwa, A. Nyska, J.C. Peckham, J.R. Hailey, J.F. Mahler, J.K. Haseman, R.R. Maronpot, A retrospective analysis of background lesions and tissue accountability for male accessory sex organs in Fischer-344 rats, Toxicol. Pathol. 29 (2001) 467–478.

[19] D. Cunningham, Z. You, In vitro and in vivo model systems used in prostate cancer research, J. Biol. Methods 2 (2015).

[20] T.R. Tennant, H. Kim, M. Sokoloff, C.W. Rinker-Schaeffer, The Dunning model, Prostate 43 (2000) 295–302.

[21] M. Pollard, Spontaneous prostate adenocarcinomas in aged germfree Wistar rats, J. Natl. Cancer Inst. 51 (1973) 1235–1241.

[22] S.B. Shappell, G.V. Thomas, R.L. Roberts, R. Herbert, M.M. Ittmann, M.A. Rubin, P.A. Humphrey, J.P. Sundberg, N. Rozengurt, R. Barrios, et al., Prostate pathology of genetically engineered mice: definitions and classification. The consensus report from the Bar Harbor meeting of the Mouse Models of Human Cancer Consortium Prostate Pathology Committee, Cancer Res. 64 (2004) 2270–2305.

[23] D. Creasy, A. Bube, E. de Rijk, H. Kandori, M. Kuwahara, R. Masson, T. Nolte, R. Reams, K. Regan, S. Rehm, et al., Proliferative and nonproliferative lesions of the rat and mouse male reproductive system, Toxicol. Pathol. 40 (2012) 40S–121S.

[24] G.H. Campolina-Silva, B.T. Maria, G.A.B. Mahecha, C.A. Oliveira, Reduced vitamin D receptor (VDR) expression and plasma vitamin D levels are associated with aging-related prostate lesions, Prostate 78 (2018) 532–546.

[25] S.C. Taylor, T. Berkelman, G. Yadav, M. Hammond, A defined methodology for reliable quantification of Western blot data, Mol. Biotechnol. 55 (2013) 217–226.

[26] P. Mak, I. Leav, B. Pursell, D. Bae, X. Yang, C.A. Taglienti, L.M. Gouvin, V.M. Sharma, A.M. Mercurio, ERbeta impedes prostate cancer EMT by destabilizing HIF-1alpha and inhibiting VEGF-mediated snail nuclear localization: implications for Gleason grading, Cancer Cell 17 (2010) 319–332.

[27] M.I. Khan, A. Hamid, V.M. Adhami, R.K. Lall, H. Mukhtar, Role of epithelial mesenchymal transition in prostate tumorigenesis, Curr. Pharm. Des. 21 (2015) 1240–1248.

[28] J. Colditz, B. Rupf, C. Maiwald, A. Baniahmad, Androgens induce a distinct response of epithelial-mesenchymal transition factors in human prostate cancer cells, Mol. Cell. Biochem. 421 (2016) 139–147.

[29] M. Pollard, The Lobund-Wistar rat model of prostate cancer, J. Cell. Biochem. Suppl. 16H (1992) 84–88.

[30] M. Morais-Santos, H. Werneck-Gomes, G.H. Campolina-Silva, L.C. Santos, G.A.B. Mahecha, R.A. Hess, C.A. Oliveira, Basal cells show increased expression of aromatase and estrogen receptor alpha in prostate epithelial lesions of male aging rats, Endocrinology 159 (2018) 723–732.

[31] A. Rivenson, J. Silverman, The prostatic carcinoma in laboratory animals: a bibliographic survey from 1900 to 1977, Investig. Urol. 16 (1979) 468–472.

[32] T. Suwa, A. Nyska, J.K. Haseman, J.F. Mahler, R.R. Maronpot, Spontaneous lesions in control B6C3F1 mice and recommended sectioning of male accessory sex organs, Toxicol. Pathol. 30 (2002) 228–234.

[33] G. Reznik, M.H. Hamlin 2nd, J.M. Ward, S.F. Stinson, Prostatic hyperplasia and neoplasia in aging F344 rats, Prostate 2 (1981) 261–268.

[34] J.M. Ward, G. Reznik, S.F. Stinson, C.P. Lattuada, D.G. Longfellow, T.P. Cameron, Histogenesis and morphology of naturally occurring prostatic carcinoma in the ACI/segHapBR rat, Lab. Investig. 43 (1980) 517–522.

[35] A.M. De Marzo, M.C. Haffner, T.L. Lotan, S. Yegnasubramanian, N.W.G. Premalignancy in Prostate Cancer, Rethinking what we know, Cancer Prev. Res. (Phila.) 9 (2016) 648–656.

[36] S. Gadkar, S. Nair, S. Patil, S. Kalamani, A. Bandivdekar, V. Patel, U. Chaudhari, G. Sachdeva, Membrane-initiated estrogen signaling in prostate cancer: a route to epithelial-to-mesenchymal transition, Mol. Carcinog. 58 (2019) 2077–2090.

[37] S.J. Ellem, H. Wang, M. Poutanen, G.P. Risbridger, Increased endogenous estrogen synthesis leads to the sequential induction of prostatic inflammation (prostatitis)

and prostatic pre-malignancy, Am. J. Pathol. 175 (2009) 1187–1199.
[38] J.A.F. Silva, A. Bruni-Cardoso, T.M. Augusto, D.M. Damas-Souza, G.O. Barbosa, S.L. Felisbino, D.R. Stach-Machado, H.F. Carvalho, Macrophage roles in the clearance of apoptotic cells and control of inflammation in the prostate gland after castration, Prostate 78 (2018) 95–103.
[39] M.V. Scalerandi, N. Peinetti, C. Leimgruber, M.M. Cuello Rubio, J.P. Nicola, G.B. Menezes, C.A. Maldonado, A.A. Quintar, Inefficient N2-like neutrophils are promoted by androgens during infection, Front. Immunol. 9 (2018) 1980.
[40] H. Abdelmoteleb, F. Rashed, A. Hawary, Management of prostate abscess in the absence of guidelines, Int. Braz. J. Urol. 43 (2017) 835–840.
[41] K.M. Lau, N.N. Tam, C. Thompson, R.Y. Cheng, Y.K. Leung, S.M. Ho, Age-associated changes in histology and gene-expression profile in the rat ventral prostate, Lab. Investig. 83 (2003) 743–757.
[42] J.C. Rinaldi, L.A. Justulin Jr., L.M. Lacorte, C. Sarobo, P.A. Boer, W.R. Scarano, S.L. Felisbino, Implications of intrauterine protein malnutrition on prostate growth, maturation and aging, Life Sci. 92 (2013) 763–774.
[43] Heckel NJ, Kretschmer. Carcinoma of the prostate treated with diethylstilbestrol. JAMA 1942; 119: 1087.
[44] M.S. Lucia, D.G. Bostwick, M. Bosland, A.T.K. Cockett, D.W. Knapp, I. Leav, M. Pollard, C. Rinker-Schaeffer, T. Shirai, B.A. Watkins, Workgroup I: rodent models of prostate cancer, Prostate 36 (1998) 49–55.

Supplementary data

Table SI: List of antibodies used in this study

Antigen	Type	Manufacturer, Cat. No.	Dilution (technique)	Conjugation	RRID
HMWCK	Mouse mAB	DAKO, M0630	1:200 (IHC)	none	AB_2335714
Cytokeratin 5	Rabbit pAB	Biolegend, 905501	1:20.000 (IHC)	none	AB_2565050
MCM7	Mouse mAB	Neomarkers, MS-862-P0	1:600 (IHC)	none	AB_145298
NA^+/K^+-ATPase α1	Mouse mAB	Santa Cruz, sc-514614	1:200 (IF)	none	AB_2802165
E-cadherin	Mouse mAB	BD Biosciences, 610181	1:1.000 (IHC and WB)	none	AB_397580
β-catenin	Mouse mAB	BD Biosciences, 610153	1:1.000 (IHC and WB)	none	AB_397554
Vimentin	Mouse mAB	DAKO, M7020	1:400 (IHC); 1:1.000 (WB)	none	AB_2304493
N-cadherin	Mouse mAB	Thermo Scientific, 33-3900	1:1.000 (WB)	none	AB_2313779
β-actin	Mouse mAB	Sigma-Aldrich, A5316	1:5.000 (WB)	none	AB_476743
mouse IgG	Goat pAB	DAKO, E0433	1:100 (IHC)	Biotin	AB_2687905
mouse IgG	Goat pAB	Sigma-Aldrich, A2304	1:5.000 (WB)	Peroxidase	AB_257993
mouse IgG	Goat pAB	Thermo Fischer, A-11003	1:100 (IF)	AlexaFluor®546	AB_2534071
rabbit IgG	Goat pAB	DAKO, E0432	1:100 (IHC)	Biotin	AB_2313609

Table SII: Stereological analysis showing the relative proportions of each component according to prostate lobe

Lateral Prostate (LP)

Group	Lumen		Epithelium		Stroma				∑ of sites
	Secretion	[a] Cells	Normal	Altered	Smooth muscle layer	Blood vessels	Inflammatory foci	Fibers and connective cells	
Control	40.49±1.13	0.12±0.09	14.29±0.41	5.93±0.69	3.12±0.56	1.11±0.14	0.47±0.08	34.48±1.27	100
T+E_2	23.41±1.71	14.26±2.11	1.69±0.63	17.37±1.29	7.59±0.75	2.73±0.25	2.56±0.26	30.39±2.32	100
p	<0.001*	<0.001*	<0.001*	<0.001*	0.0029*	0.0016*	<0.001*	0.2652	-

Ventral Prostate (VP)

Group	Lumen		Epithelium		Stroma				∑ of sites
	Secretion	[a] Cells	Normal	Altered	Smooth muscle layer	Blood vessels	Inflammatory foci	Fibers and connective cells	
Control	59.54±1.58	0	13.84±1.48	1.76±0.44	2.13±0.21	0.97±0.20	0.09±0.07	21.67±0.69	100
T+E_2	56.17±4.13	0	1.61±0.32	15.37±2.61	2.61±0.37	0.78±0.24	0.30±0.03	23.15±1.32	100
p	0.5694	-	<0.001*	0.0040*	0.3821	0.6028	0.0130*	0.4417	-

Dorsal Prostate (DP)

Group	Lumen		Epithelium		Stroma				∑ of sites
	Secretion	[a] Cells	Normal	Altered	Smooth muscle layer	Blood vessels	Inflammatory foci	Fibers and connective cells	
Control	28,80±2,37	0	20,62±1,52	1,75±0,46	8,21±0,67	0,83±0,30	0,36±0,18	39,44±3,35	100
T+E_2	41,35±2,06	0,55±0,25	8,83±1,74	8,62±1,34	5,86±0,42	1,44±0,26	1,36±0,21	31,94±1,99	100
p	0.0026*	0.0935	0.0007*	0.0020*	0.0107*	0.1632	0.0074*	0.0677	-

Anterior Prostate (AP)

Group	Lumen		Epithelium		Stroma				∑ of sites
	Secretion	[a] Cells	Normal	Altered	Smooth muscle layer	Blood vessels	Inflammatory foci	Fibers and connective cells	
Control	26,43±1,03	0	20,77±1,79	5,60±2,08	12,25±1,18	1,66±0,47	0,15±0,05	33,21±2,90	100
T+E_2	32,66±1,98	1,02±0,37	21,38±3,16	8,51±0,94	12,13±1,38	3,41±0,64	0,99±0,28	19,91±1,38	100
p	0.0330*	0.0025*	0.8844	0.1877	0.9506	0.0703	0.0455*	0.0010*	-

Data are presented as mean percentage of each constituent ± SEM. * = $p<0.05$.
[a] Refers to leukocytes and sloughed epithelial cells into the gland lumen.

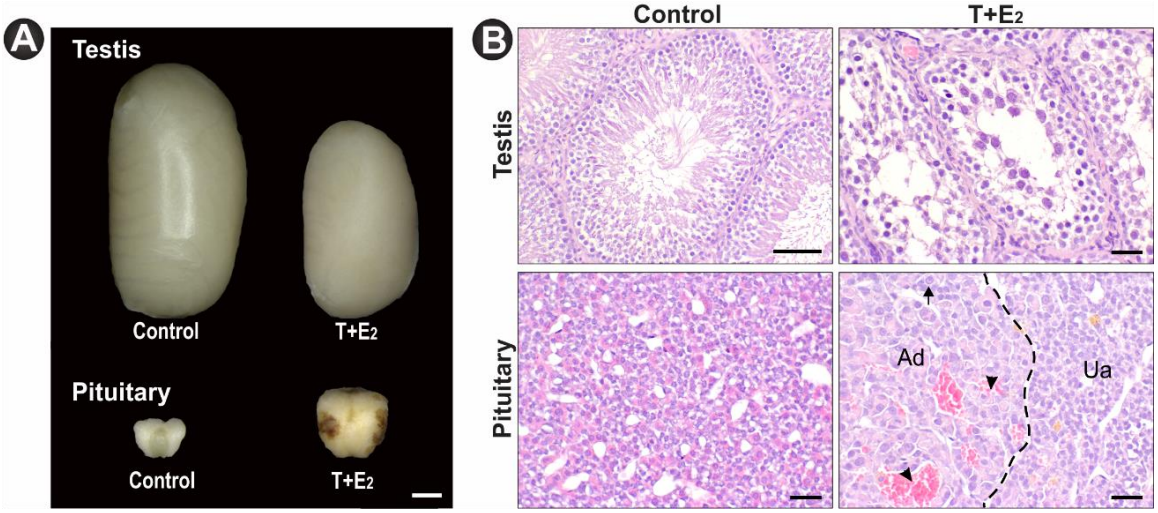

Fig. S1: Testosterone plus estradiol treatment led to macroscopic and microscopic changes in testes and pituitary glands. (A) Reduction of testis size and enlargement of pituitary gland were observed in animals that received T+E_2 treatment, when compared to the control group. Scale bar = 2,5 cm. **(B)** HE staining showing that the treated animals were affected by testicular atrophy (upper right). Moreover, the treatment induced pituitary adenomas (Ad) in the pars distalis, which contained a homogeneous population of enlarged cells showing discreet nuclear pleomorphism and evident nucleolus (arrow), associated with moderate vascular neoformation (arrowheads). An unaffected area (Ua) of pars distalis is shown adjacent to the adenoma. Scale bars = 20 µm.

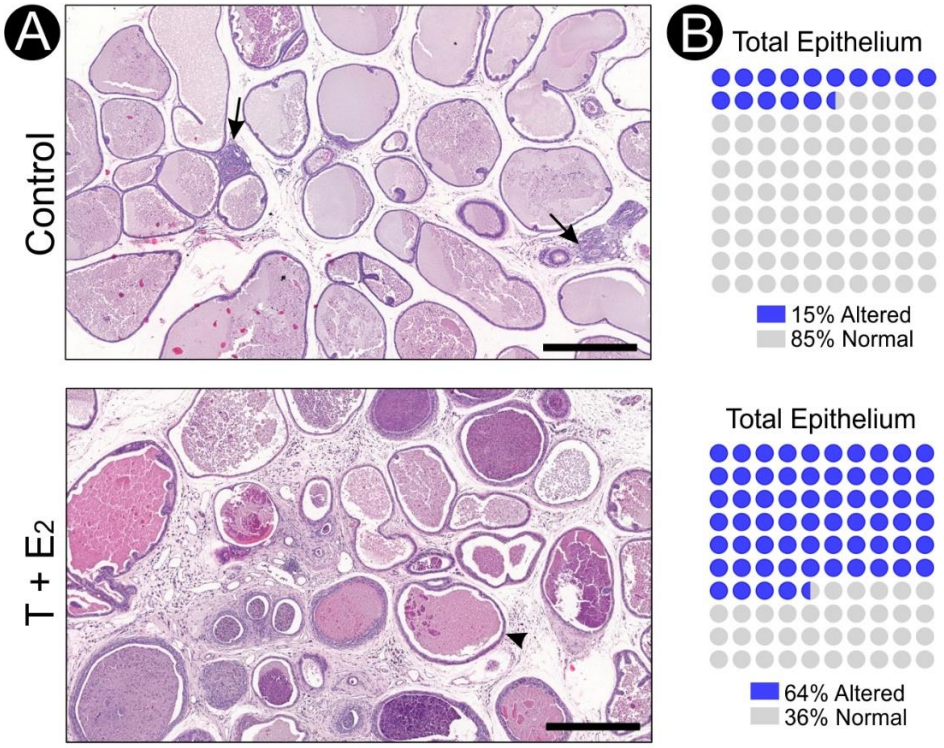

Fig. S2: Overview of the prostatic gland of control and treated animals at 18 months of age. The pictures are representative of the lateral prostate of control and T+E_2-treated Wistar rat. **(A)** Note that in the control group, the changes were observed in punctual sites (arrows) surrounded by normal acini and ducts. Conversely, in the treatment group, a large extent of the prostatic epithelium exhibits altered morphology, and only a few acini with normal-appearing features can be seen (arrowhead). In addition, it is evident the occurrence of inflammatory foci in the stroma and within the lumen of treated animals, which is indicative of prostatitis. **(B)** Diagram representative of the total amount of epithelium (including all prostate lobes) with normal or altered morphology according to experimental groups. The data was extracted from the stereological analysis presented in table S2 and took into account only the coincident points computed in the epithelial compartment. Scale bars = 500 µm.

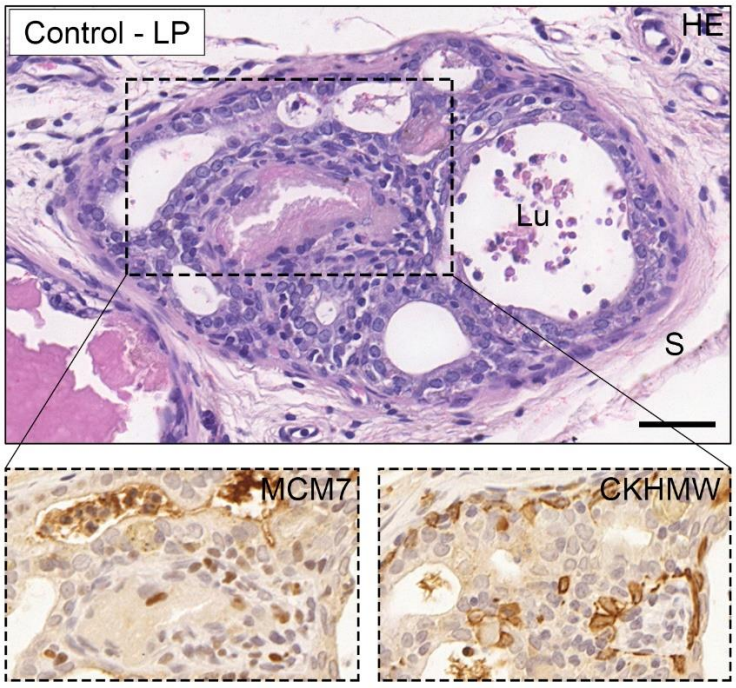

Fig. S3: Intraductal adenocarcinoma from the lateral prostate of a control rat. Retention of the basal cell layer (CKHMW positive) is a common event observed in this type of malignancy. Nuclear positive staining for MCM7 indicates proliferating tumors cells. Lu: lumen. S: stroma. Scale bar = 50µm.

IV. DISCUSSÃO INTEGRADA DOS RESULTADOS

IV. DISCUSSÃO INTEGRADA DOS RESULTADOS

O sistema endócrino vitamina D abrange um conjunto de enzimas, receptores e moléculas precursoras do metabólito ativo da vitamina D, o qual é denominado 1α,25$(OH)_2$D ou calcitriol e cuja ação desencadeia efeitos protetores na maioria – senão em todos – os tecidos corporais (Bikle, 2014). No presente trabalho, a distribuição e abundância de importantes componentes do sistema endócrino vitamina D foram avaliadas no contexto da fisiopatologia da próstata, um dos principais órgãos masculinos alvo de desordens benignas e malignas. Panoramicamente, nossos resultados demonstram que a próstata é um órgão sensível à vitamina D e altamente capaz de metabolizar o calcitriol localmente; e que o envelhecimento, principal fator de risco associado ao desenvolvimento de HPB e câncer de próstata (Leitzmann & Rohrmann, 2012; Lim, 2017), exerce efeitos sobre as três classes de componentes do sistema endócrino vitamina D, sendo elas: (i) ligantes; (ii) enzimas metabolizadoras; e (iii) receptores.

Os resultados apresentados na sessão III desta tese foram obtidos através do emprego de um modelo experimental que consiste na utilização de ratos da linhagem Wistar em diferentes idades, de modo a abranger animais adultos jovens (3 e 6 meses), de meia idade (12 meses) e senis (18 e 24 meses). Esse modelo tem sido adotado para compreender *in vivo* as modificações morfológicas e bioquímicas da próstata em envelhecimento (Morais-Santos et al. 2015; Gonzaga et al. 2017; Morais-Santos et al. 2018; Campolina-Silva et al. 2018; Werneck-Gomes et al. 2020), e tem como principal vantagem o desenvolvimento espontâneo de alterações histopatológicas com o avançar da idade. Tais alterações mimetizam aquelas observadas na próstata humana senil e

incluem tanto lesões benignas e pré-malignas, quanto, em menor frequência, adenocarcinomas (Morais-Santos et al. 2015; 2018; Campolina-Silva et al. 2020). Contudo, vale ressaltar que a baixa constatação de tumores observados nos fragmentos de próstatas avaliados em um primeiro momento e cuja frequência (n=1 tumor entre 25 próstatas) não transmitia confiabilidade para avaliações seguintes nos levou a desenvolver um modelo de indução da carcinogênese prostática nos ratos Wistar, baseado na administração combinatória de testosterona e estradiol dos 12 aos 18 meses de idade (Campolina-Silva et al. 2020). Este modelo induzido configura-se como um valioso modelo pré-clínico de câncer e outras patologias da próstata e foi utilizado para complementar os dados obtidos no modelo de envelhecimento natural.

Por meio da utilização combinatória de técnicas histológicas, de biologia molecular e análise de imagens, foi observado que as células do epitélio prostático expressam os receptores VDR e RXR, bem como as enzimas CYP27B1 e CYP24A1, as quais estão envolvidas respectivamente com a síntese e inativação do calcitriol. Esse achado independe da idade avaliada e indica que a próstata, assim como o rim, pele, osso e intestino (Bikle et al. 2018), é um órgão responsível ao calcitriol e altamente capaz de sintetizá-lo localmente a partir de seu precursor 25(OH)D advindo da circulação sanguínea. No final da década de 80, Dusso e colaboradores comprovaram a existência de produção extra-renal de calcitriol por meio da administração de 25(OH)D à pacientes anéfricos sob hemodiálise (Dusso et al. 1988). Desde então, vários tecidos têm sido identificados como “autossuficientes” em produzir calcitriol, sendo os rins um dos principais órgãos a expressar a enzima CYP27B1 (Bourlon et al. 1997; Li et al. 2002; van Etten & Mathieu, 2005; Liu et al. 2006; Marini et al. 2010; Feldman et al. 2014; Wang et

al. 2017). Apesar de não haver evidências na literatura que denotem importância para a próstata como fonte extra-renal de calcitriol, a constatação de que níveis de CYP27B1 similares aos renais foram observados na VP e LP de ratos adultos abre perspectivas para se investigar a relevância da glândula para manutenção dos níveis corpóreos desse hormônio nos machos. Ainda, vale ressaltar que a atividade 1α-hidroxilase da CYP27B1 nas células da próstata e consequentemente, a síntese local do metabólito ativo da vitamina D, permite que os efeitos mediados pelo complexo transcricional VDR-RXR ativado possam ocorrer também de maneira autócrina e parácrina.

Na próstata, um dos principais efeitos da via de sinalização supracitada é a inibição da proliferação celular, seja pela supressão de fatores de crescimento ou pelo bloqueio do ciclo celular na fase G1 (Peehl et al. 1994; Yang et al. 2003; Moreno et al. 2005; Feldman et al. 2014). É devido a esse conhecido efeito que a vitamina D passou a ser considerada como um potencial agente terapêutico contra o câncer de próstata, uma desordem proliferativa que afeta 1 a cada 6 homens com idade igual ou superior a 65 anos (Pollock et al. 2015; Rawla, 2019). Sabe-se que além das concentrações de calcitriol, a magnitude do efeito mediado pela via de sinalização da vitamina D nas células da próstata depende também dos níveis endógenos dos receptores e enzimas associadas à via (Miller et al. 1992; Skowronski et al. 1993; Peehl et al. 1994; Konety et al. 1996; Hsu et al. 2001; Leman et al. 2003; Moreno et al. 2005; Banach-Petrosky et al. 2006; Tannour-Louet et al. 2014). De forma pioneira, o presente trabalho mostrou que, à medida que os animais envelhecem, o número de células positivas e a imunoreatividade para a enzima CYP27B1 bem como para os receptores VDR e RXR reduzem especificamente em lesões benignas, pré-malignas e malignas que surgem

espontaneamente no epitélio da próstata senil. Adicionalmente, alterações similares também foram observadas restritas às lesões epiteliais induzidas pela exposição prolongada a testosterona e estradiol. Em contraste, a enzima CYP24A1 foi mais expressa no epitélio prostático a partir dos 12 meses de idade e manteve-se inalterada nas lesões histopatológicas. Todas essas modificações ocorreram nas mesmas idades em que os níveis circulantes de 25(OH)D e a concentração intraprostática de calcitriol foram significativamente menores. Juntos, esses dados evidenciam que o envelhecimento exerce um importante efeito sobre os componentes do sistema endócrino vitamina D de forma a limitar sua ação protetora no tecido prostático. Essa evidência é corroborada pelo aumento da atividade proliferativa celular exatamente nas regiões em que a maquinaria de síntese e reposta ao calcitriol teve sua expressão inibida.

Uma limitação do presente estudo é que não foi possível estabelecer uma relação de causa ou efeito entre as modificações envolvendo os componentes do sistema endócrino vitamina D e o surgimento de lesões histopatológicas na próstata, mesmo embora ambas alterações foram observadas exatamente nas mesmas idades experimentais (a partir dos 12 meses). Entretanto, é plausível considerar que a redução da capacidade de resposta ao calcitriol e consequentemente, a sustentação da alta atividade proliferativa na próstata senil, possam contribuir significativamente para a carcinogênese prostática. Reforçando essa ideia, Banach-Petrosky et al. (2006) utilizando camundongos mutantes para Nkx3.1 e Pten, os quais recapitulam estágios da carcinogênese prostática, desde PIN até adenocarcinoma, demonstraram que a administração de calcitriol foi capaz de suprimir a progressão das lesões pré-malignas,

um efeito atrelado à inibição da proliferação celular e aos níveis elevados de VDR no epitélio.

Devido à natureza do modelo experimental utilizado e a ausência de dados sobre o comportamento do sistema endócrino vitamina D na próstata humana ao longo do envelhecimento, estudos futuros serão necessários para confirmar a translacionalidade dos dados aqui apresentados. Entretanto, reduções significativas dos níveis e atividade da CYP27B1, VDR e RXR já foram detectadas restritas às células da próstata humana cometida por HPB, PIN ou câncer (Hsu et al. 2001; Mao et al. 2004; Hendrickson et al. 2011), o que corrobora nossos resultados comparativos entre o epitélio normal e alterado da próstata de ratos. Além disso, é inegável que as constatações aqui realizadas evidenciam a necessidade de se considerar o *status* dos componentes do sistema endócrino vitamina D em investigações futuras que visam avaliar a eficácia terapêutica dos metabólitos da vitamina D no tratamento de patologias da próstata senil. Nesse sentido, evidências *in vitro* e *in vivo* indicam que ação antiproliferativa mediada pela sinalização da vitamina D nas células prostáticas depende positivamente da expressão de CYP27B1 e VDR, e inversamente dos níveis e atividade da CYP24A1 (Skowronski et al. 1993; Hsu et al. 2001; Banach-Petrosky et al. 2006; Tannour-Louet et al. 2014). Portanto, uma expressão diferencial dos receptores VDR e RXR e/ou das enzimas CYP27B1 e CYP24A1 poderia explicar os efeitos anti-tumorais limitados obtidos por ensaios clínicos utilizando a vitamina D_3 ou o calcitriol contra o câncer de próstata (Beer et al. 2004; Flaig et al. 2006; Marshall et al. 2012).

Para explorar esse ponto de vista, a atividade diferencial dos genes que codificam os receptores e enzimas alvo desse estudo em uma coorte de 494 pacientes

diagnosticados com câncer de próstata (TCGA, Pan Cancer Atlas) foi representada na figura 7. Como evidenciado, é notório que os níveis de RNAm para CYP27B1, CYP24A1, VDR e a isoforma α do receptor de retinoide X (RXRα), variam consideravelmente entre as amostras tumorais. Enquanto cerca da metade dos indivíduos possuem níveis de cada RNAm acima da média, a outra metade possui níveis reduzidos. Essa simples comparação evidencia que a atividade transcricional e possivelmente os níveis proteicos dos fatores que ditam o espectro de ação da sinalização de vitamina D são altamente heterogêneos nos tumores prostáticos, inclusive quando considerado a variação intergênica entre as mesmas amostras (Figura 7B). Tal heterogeneidade pode estar atrelada aos relevantes achados feitos por Marshall et al. (2012). Na ocasião, os pesquisadores avaliariam o prognóstico da administração diária de 4.000 UI de vitamina D_3 em homens diagnosticados com câncer de próstata de baixo risco (Escore de Gleason $\leq$ 7; PSA <10; idade entre 49 e 78 anos) e sobre vigilância ativa. Após um ano de intervenção, observou-se que 55% dos pacientes tiveram uma redução no número de biopsias positivas e no escore de Gleason, enquanto 11% e 34% dos pacientes apresentaram, respectivamente, nenhuma melhora ou até mesmo uma piora das variáveis avaliadas. Portanto, além de apresentar evidências de que o envelhecimento afeta a ação do sistema endócrino vitamina D, nós arguimos que o *status* dos componentes desse sistema deve ser considerado tanto no recrutamento de pacientes quanto na interpretação dos resultados obtidos por ensaios clínicos utilizando agonistas naturais ou sintéticos do VDR como estratégia terapêutica para tratar desordens histopatológicas da próstata, incluindo o câncer.

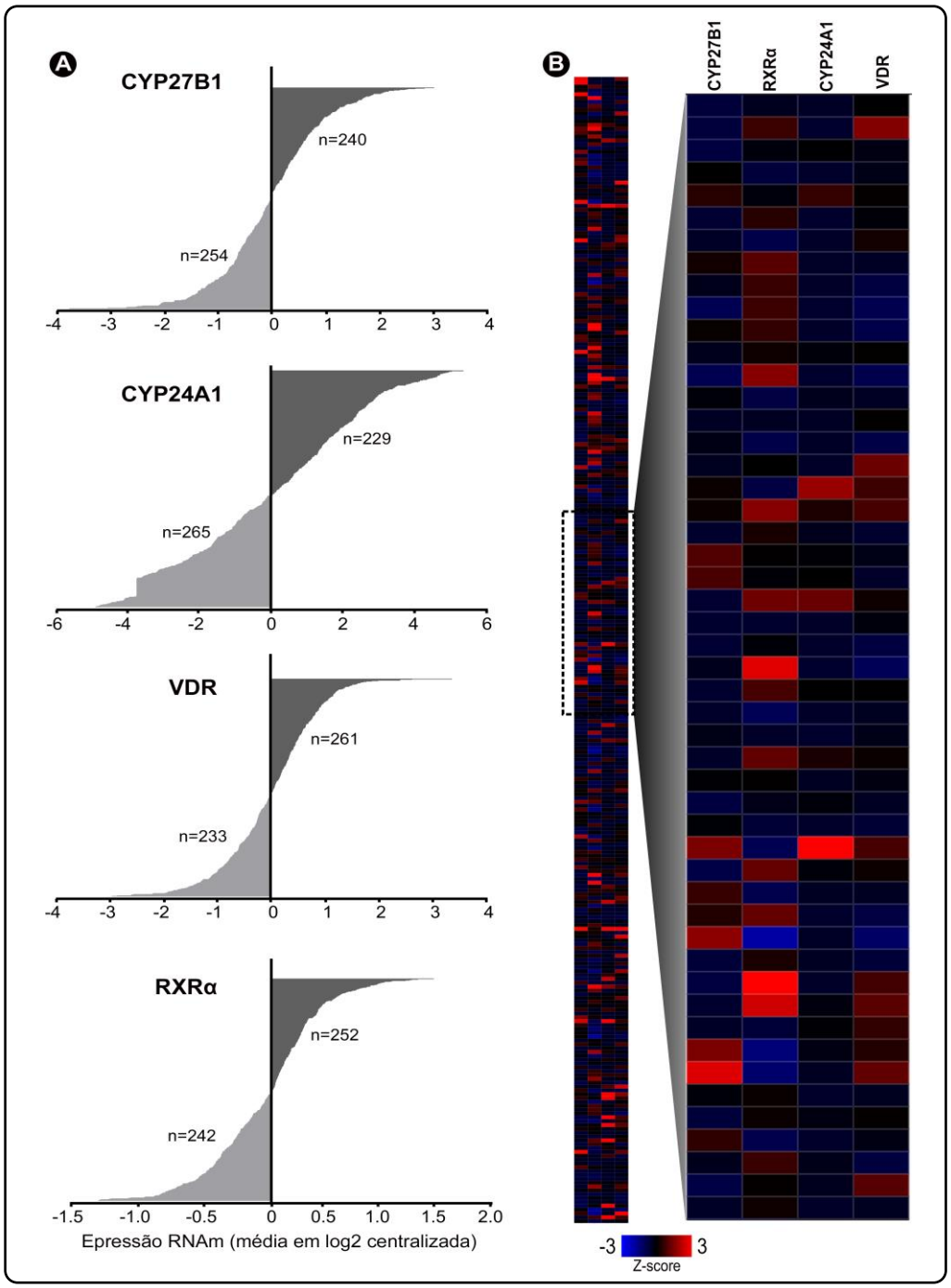

Figura 7 | Heterogeneidade da atividade transcricional dos genes VDR, RXRa, CYP27B1 e CYP24A1 em 494 tumores de próstata humana. (A) Distribuição dos valores individuais em torno da média centralizada para cada RNAm. (B) *Heatmap* representativo mostrando não haver clusterização intergênica de acordo com o produto dos 4 genes avaliados. Esses dados foram extraídos dos transcriptomas anotados para 494 indivíduos da coorte TCGA – Pan Cancer Atlas.

V. CONCLUSÃO

V. CONCLUSÃO

Os resultados do presente trabalho demonstram que a próstata é um órgão alvo da sinalização de vitamina D sendo também capaz de metabolizar o calcitriol localmente, conforme revela a ampla distribuição dos receptores VDR e RXR, bem como das enzimas CYP27B1 e CYP24A1 no tecido prostático. Variações idade-dependentes na expressão desses componentes bem como nos níveis plasmáticos e teciduais dos metabólitos da vitamina provêm fortes evidências de que a sinalização da vitamina D e consequentemente, seus efeitos protetores no local, são atenuados no tecido prostático à medida que os indivíduos envelhecem e alterações benignas, pré-malignas e malignas surgem no local, evidenciando, assim, uma relação entre envelhecimento, fisiopatologia prostática e o sistema endócrino vitamina D.

REFERÊNCIAS BIBLIOGRÁFICAS

Abrahamsson, P. A. (1999). Neuroendocrine cells in tumour growth of the prostate. Endocr Relat Cancer, 6(4), 503-519.

Alipio, M. (2020). Vitamin D Supplementation Could Possibly Improve Clinical Outcomes of Patients Infected with Coronavirus-2019 (COVID-19). SRRN, preprint version, s/n, doi: 10.2139/ssrn.3571484.

Aumuller, G. (1979). Prostate Gland and Seminal Vesicles. II ed. Berlim: Springer.

Aumuller, G. (1989). Morphologic and regulatory aspects of prostatic function. Anat Embryol (Berl), 179(6), 519-531.

Banach-Petrosky, W., Ouyang, X., Gao, H., Nader, K., Ji, Y., Suh, N., et al. (2006). Vitamin D inhibits the formation of prostatic intraepithelial neoplasia in Nkx3.1;Pten mutant mice. Clin Cancer Res, 12(19), 5895-5901.

Banerjee, P. P., Banerjee, S., Lai, J. M., Strandberg, J. D., Zirkin, B. R., & Brown, T. R. (1998). Age-dependent and lobe-specific spontaneous hyperplasia in the brown Norway rat prostate. Biol Reprod, 59(5), 1163-1170.

Banerjee, S., Banerjee, P. P., & Brown, T. R. (2000) Castration-induced apoptotic cell death in the Brown Norway rat prostate decreases as a function of age. Endocrinology, 141,821-832.

Barchette, I., Carotti, S., Labbadia, G., Gentilucci, U. V., Muda, A. O, Angelico, F., et al. (2012). Liver vitamin D receptor, CYP2R1, and CYP27A1 expression: relationship with liver histology and vitamin D3 levels in patients with nonalcoholic steatohepatitis or hepatitis c virus. Hepatol, 56(6), 2180-2187.

Beer, T. M., Myrthue, A., Garzotto, M., O'hara, M. F., Chin, R., Lowe, B.A., Montalto, M. A., Corless, C. L., & Henner, W. D. (2004). Randomized study of high-dose pulse calcitriol or placebo prior to radical prostatectomy. Cancer Epidemiol Biomarkers Prev 13(12), 2225-2232.

Begley, L. A., Kasina, S., MacDonald, J., & Macoska, J. A. (2008). The inflammatory microenvironment of the aging prostate facilitates cellular proliferation and hypertrophy. Cytokine, 43(2), 194-199.

Bikle, D. D. (2009). Extra Renal Synthesis of 1,25-dihydroxyvitamin D and its Health Implications. Clinic Rev Bone Miner Metab, 7, 114-125.

Bikle, D. D. (2014). Vitamin D metabolism, mechanism of action, and clinical applications. Chem Biol, 21(3), 319-329.

Bikle, D. D., Patzek, S., & Wang, Y. (2018). Physiologic and pathophysiologic roles of extra renal CYP27b1: Case report and review. Bone Reports, 8, 255-267.

Blomberg Jensen, M. (2014). Vitamin D and male reproduction. Nat Rev Endocrinol, 10(3), 175-186.

Blomberg Jensen, M., Nielsen, J. E., Jorgensen, A., Rajpert-De Meyts, E., Kristensen, D. M., Jorgensen, N., et al. (2010). Vitamin D receptor and vitamin D metabolizing enzymes are expressed in the human male reproductive tract. Hum Reprod, 25(5), 1303-1311.

Bourlon, P. M., Faure-Dussert, A., & Billaudel, B. (1997). Modulatory role of 1,25 dihydroxyvitamin D3 on pancreatic islet insulin release via the cyclic AMP pathway in the rat. Br J Pharmacol, 121(4), 751-758.

Bray, F., Ferlay, J., Soerjomataram, I., Siegel, R. L., Torre, L. A., & Jemal, A. (2018). Global cancer statistics: GLOBOCAN estimates of incidence and mortality worldwide for 36 cancers in 185 countries. CA Cancer J Clin, 0, 1-31.

Campolina-Silva, G. H. (2016). Mapeamento do receptor de vitamina D (VDR) no complexo prostático de ratos Wistar durante o envelhecimento. Mestrado, Universidade Federal de Minas Gerais.

Campolina-Silva, G.H., Maria, B.T., Mahecha, G.A.B., & Oliveira, C.A. (2018). Reduced vitamin D receptor (VDR) expression and plasma vitamin D levels are associated with aging-related prostate lesions. Prostate,78, 532-546.

Campolina-Silva, G.H., Werneck-Gomes, H., Maria, B.T., Barata, M. C., Torres, M. J., et al. (2020). Wistar rat as a model for studying benign, premalignant and malignant lesions of the prostate. Life Sci, 242, 1-13.

Chaves, M., Aguilera-Merlo, C., Cruceño, A., Fogal, T., & Mohamed, F. (2015). Morphological study of the prostate gland in Viscacha (Lagostomus maximus maximus) during periods of maximal and minimal reproductive activity. Anotom Rec, 298, 1919-1931.

Cheng, J. B., Levine, M. A., Bell, N. H., Mangelsdorf, D. J., & Russel, D. W. (2004). Genetic evidence that the human CYP2R1 enzyme is a key vitamin D 25-hydroxylase. Proc Natl Acad Sci USA, 101(20), 7711-7715.

Cheng, J. B., Motola, D. L., Mangelsdorf, D. J., & Russel, D. W. (2003). De-orphanization of Cytochrome P450 2R1: a microsomal vitamin D 25-hydroxylase. J Biol Chem, 278(39), 38084-38093.

Cooke, P., Nanjappa, M. K., Ko, C., Prins, G. S., & Hess, R. A. (2017). Estrogens in male physiology. Physiol Rev, 97(3), 995-1043.

Danik, J. S., & Manson, J. E. (2012). Vitamin D and cardiovascular disease. Curr Treat Options Cardiovasc Med, 14(4), 414–424.

DeLuca, H. (2004). Overview of general physiologic features and functions of vitamin D. Am J Clin Nutr, 80, 1689-1696.

Desai, K. V., Michalowska, A. M., Kondaiah, P., Ward, J. M., Shih, J. H., & Green, J. E. (2004) Gene expression profiling identifies a unique androgen-mediated inflammatory/immune signature and a PTEN (phosphatase and tensin homolog deleted on chromosome 10)-mediated apoptotic response specific to the rat ventral prostate. Mol Endocrinol 18, 2895-2907.

Dusso, A., Lopez-Hilker, S., Rapp, N., & Slatopolsky, E. (1988). Extra-renal production of calcitriol in chronic renal failure. Kidney Int, 34, 368-375.

Ebadi, M., Montano-Loza, A. J. (2020). Perspective: improving vitamin D *status* in the management of COVID-19. Eur J of Clin Nutr, 74, 856-859.

El-Alfy, M., Pelletier, G., Hermo, L. S., & Labrie, F. (2000). Unique features of the basal cells of human prostate epithelium. Microsc Res Tech, 51(5), 436-446.

Fair, W. R., & Cordonnier, J. J. (1978). The pH of prostatic fluid: a reappraisal and therapeutic implications. Journal of Urology, 120(6), 695-698.

Feldman, D., Krishnan, A. V., Swami, S., Giovannucci, E., & Feldman, B. J. (2014). The role of vitamin D in reducing cancer risk and progression. Nat Rev Cancer 14(5): 342-357.

Flaig, T. W., Barqawi, A., Miller, G., Kane, M., Zeng, C., Crawford, E. D., & Glodé, L. M. (2006). A phase II trial of dexamethasone, vitamin D, and carboplatin in patients with hormone-refractory prostate cancer. Cancer 107, 266-274.

Flanagan J. N., Wang, L., Tangpricha, V., Reichrath, J., Chen, T. C., & Holick, M. F. (2003). Regulation of the 25-hydroxyvitamin D-1alpha-hydroxylase gene and its splice variant. Recent Results Cancer Res,164,157–167.

Fleet, J. C., Eksir, F., Hance, K. W., & Wood, R. J. (2002). Vitamin D-inducible calcium transport and gene expression in three Caco-2 cell lines. Am J Physiol Gastrointest Liver Physiol, 283(3), G618-625.

Flint, T. M., Mcalister, D. A., Agarwal, A., & Plessis, S. (2015) Male Accessory Sex Glands: Structure and Function. In: Mammalian Endocrinology and Male Reproductive Biology. CRC Press, 1st edition, cap. 9.

Gao, X. H., Dwivedi, P. P., Choe, S., Alba, F., Morris, H. A., Omdahl, J. L., et al. (2002). Basal and parathyroid hormone induced expression of the human 25-hydroxyvitamin D 1alpha-hydroxylase gene promoter in kidney AOK-B50 cells: role of Sp1, Ets and CCAAT box protein binding sites. Int J Biochem Cell Biol, 34(8), 921-930.

Giangreco, A. A., Dambal, S., Wagner, D., Van der Kwast, T., Vieth, R., Prins, G. S., et al. (2015). Differential expression and regulation of vitamin D hydroxylases and

inflammatory genes in prostate stroma and epithelium by 1,25-dihydroxyvitamin D in men with prostate cancer and an in vitro model. J Steroid Biochem Mol Biol, 148, 156-165.

Gingrich, J. R., Barrios, R. J., Foster, B. A., & Greenberg N. M. (1999). Pathologic progression of autochthonous prostate cancer in the TRAMP model. Prost Cancer and Prost Diseases, 2, 70-75.

Goncalves, B. F., de Campos, S. G., Zanetoni, C., Scarano, W. R., Falleiros, L. R., Jr., Amorim, R. L., et al. (2013). A new proposed rodent model of chemically induced prostate carcinogenesis: distinct time-course prostate cancer progression in the dorsolateral and ventral lobes. Prostate, 73(11), 1202-1213.

Gonzaga, A. C. R., Campolina-Silva, G. H., Werneck-Gomes, H., Moura-Cordeiro, J. D., Santos, L. C., Mahecha, G. A. B., Morais-Santos, M., & Oliveira, C. A. (2017). Profile of cell proliferation and apoptosis activated by the intrinsic and extrinsic pathways in the prostate of aging rats. Prostate, 77, 937–948.

Grant, W. B., Lahore, H., McDonnell, S. L., Baggerly, C. A., French, C. B., Aliano, J. L., Bhattoa, H. P. (2020). Evidence that vitamin D supplementation could reduce risk of influenza and COVID-19 Infections and deaths. Nutrients, 12, 1-19.

Grossmann, M. E., Huang, H., & Tindall, D. J. (2001). Androgen receptor signaling in androgen-refractory prostate cancer. J Nat Cancer Inst, 93(22), 1687-1697.

Gupta, R. P., Hollis, B. W., Patel, S. B., Patrick, K. S., & Bell, N. H. 2004. CYP3A4 is a human microsomal vitamin D 25-Hydroxylase. J Bone and Mineral Res, 19(4), 680-688.

Halloran, B. P., & DeLuca, H. F. (1980). Effect of vitamin D deficiency on fertility and reproductive capacity in the female rat. J Nutr, 110(8), 1573-1580.

Haussler, M. R., Haussler, C. A., Jurutka, P. W., Thompson, P. D., Hsieh, J. C., Remus, L. S., et al. (1997). The vitamin D hormone and its nuclear receptor: molecular actions and disease states. J Endocrinol, 154 Suppl, S57-73.

Hayashi, N., Sugimura, Y., Kawamura, J., Donjacour, A. A., & Cunha, G. R. (1991). Morphological and functional heterogeneity in the rat prostatic gland. Biol Reprod, 45(2), 308-321.

Hayashi, S., Noshiro, M., & Okuda, K. (1986). Isolation of a Cytochrome P-450 that catalyzes the 25-Hydroxylation of vitamin D3 from rat liver microsomes. J Biochem, 99, 1753-1763.

Hayward, S. W., Baskin, L. S., Haughney, P. C., Cunha, A. R., Foster, B. A., Dahiya, R., et al. (1996a). Epithelial development in the rat ventral prostate, anterior prostate and seminal vesicle. Acta Anat (Basel), 155(2), 81-93.

Hayward, S. W., Baskin, L. S., Haughney, P. C., Foster, B. A., Cunha, A. R., Dahiya, R., et al. (1996b). Stromal development in the ventral prostate, anterior prostate and seminal vesicle of the rat. Acta Anat (Basel), 155(2), 94-103

Hendrickson, W. K., Flavin, R., Kasperzyk, J. L., Fiorentino, M., Fang, F., Lis, R., et al. (2011). Vitamin D receptor protein expression in tumor tissue and prostate cancer progression. J Clin Oncol, 29(17), 2378-2385.

Hoenderop, J. G., Nilius, B., & Bindels, R. J. (2005). Calcium absorption across epithelia. Physiol Rev, 85(1), 373-422.

Holick, M. F. (1989). Phylogenetic and evolutionary aspects of vitamin D from phytoplankton to humans. In: Pang, P. K. T., Schreibman, M. P., editors. Vertebrate endocrinology: fundamentals and biomedical implications, vol. 3. Orlando, FL: Academic Press, Inc (Harcourt Brace Jovanovich).

Holick, M. F. (2004). Vitamin D: importance in the prevention of cancers, type 1 diabetes, heart disease, and osteoporosis. Am J Clin Nutr, 79(3), 362-371.

Holick, M. F. (2006). Resurrection of vitamin D deficiency and rickets. J Clin Invest, 116(8), 2062-2072.

Holick, M. F. (2009). Vitamin D and health: evolution, biologic functions, and recommended dietary intakes for vitamin D. Clinic Rev Bone Miner Metab, 7, 2–19.

Holick, M. F. (2017). The vitamin D deficiency pandemic: approaches for diagnosis, treatment and prevention. Rev Endocr Metab Disord,18, 153–165.

Holick, M. F. (2018). Photobiology of Vitamin D. *in* Vitamin D (4th Edition), Academic Press, 45-55.

Holick, M. F., MacLaughlin, J. A., Clark, M. B., Holick, S. A., Potts, J. T., Jr., Anderson, R. R., et al. (1980). Photosynthesis of previtamin D3 in human skin and the physiologic consequences. Science, 210(4466), 203-205.

Holt, S.K., Kolb, S., Fu, R., et al. (2013). Circulating levels of 25-hydroxyvitamin D and prostate cancer prognosis. Cancer Epidemiol, 37, 666–670.

Hosseinpour, F., & Wikvall, K. (2000). Porcine microsomal vitamin D3 25-hydroxylase (CYP2D25): catalytic properties, tissue distribution, and comparison with human CYP2D6. J Biol Chem, 275(44), 34650-34655.

Housman, T. S., Feldman, S. R., Williford, P. M., Fleischer, A. B., Goldman, N. D., & Acostamadiedo, J. M. (2003). Skin cancer is among the most costly of all cancers to treat for the Medicare population. J Am Acad Dermatol,48,425–429.

Hsu, J. Y., Feldman, D., McNeal, J. E., & Peehl, D. M. (2001). Reduced 1alpha-hydroxylase activity in human prostate cancer cells correlates with decreased susceptibility to 25-hydroxyvitamin D3-induced growth inhibition. Cancer Res, 61(7), 2852-2856.

Hu, W. Y., et al. (2011). Estrogen-initiated transformation of prostate epithelium derived from normal human prostate stem-progenitor cells. Endocrinology 152(6), 2150-2163.

Hu, W. Y., et al. (2012). Actions of estrogens and endocrine disrupting chemicals on human prostate stem/progenitor cells and prostate cancer risk. Mol Cell Endocrinol 354(1-2), 63-73.

Huhtakangas, J. A., Olivera, C. J., Bishop, J. E., Zanello, L. P., & Norman, A. W. (2004). The vitamin D receptor is present in caveolae-enriched plasma membranes and binds 1 alpha,25(OH)2-vitamin D3 in vivo and in vitro. Mol Endocrinol, 18(11), 2660-2671.

Hypponen, E., Laara, E., Reunanen, A., Jarvelin, M., & Virtanen, S. M. (2001). Intake of vitamin D and risk of type 1 diabetes: a birth-cohort study. The Lancet, 358, 1500-1503.

INCA 2020. Incidência de Câncer no Brasil. *Instituto Nacional do Câncer – Ministério da Saúde:* http://www2.inca.gov.br.

Ittmann, M. (2018). Anatomy and histology of the human and murine prostate. Cold Spring Harb Perspect Med, 1;8(5).

John, E. M., Schwartz, G. G., Koo, J., Van Den Berg, D., & Ingles, S. A. (2005). Sun exposure, vitamin D receptor gene polymorphisms, and risk of advanced prostate cancer. Cancer Res, 65(12), 5470-5479.

Johnson, J. A., Grande, J. P., Roche, P. C., & Kumar, R. (1996). Immunohistochemical detection and distribution of the 1,25-dihydroxyvitamin D3 receptor in rat reproductive tissues. Histochem Cell Biol, 105(1), 7-15.

Jones, G., Ramshaw, H., Zhang, A., Cook, R., Byford, V., White, J., et al. (1999). Expression and activity of vitamin D-metabolizing cytochrome P450s (CYP1alpha and CYP24) in human nonsmall cell lung carcinomas. Endocrinology, 140(7), 3303-3310.

Kinuta, K., Tanaka, H., Moriwake, T., Aya, K., Kato, S., & Seino, Y. (2000). Vitamin D is an important factor in estrogen biosynthesis of both female and male gonads. Endocrinology, 141(4), 1317-1324.

Kivineva, M., Blauer, M., Syvala, H., Tammela, T., & Tuohimaa, P. (1998). Localization of 1,25-dihydroxyvitamin D3 receptor (VDR) expression in human prostate. J Steroid Biochem Mol Biol, 66(3), 121-127.

Krill, D., DeFlavia, P., Dhir, R., Luo, J., Becich, M. J., Lehman, E., et al. (2001). Expression patterns of vitamin D receptor in human prostate. J Cell Biochem, 82(4), 566-572.

Krishnan, A. V., & Feldman, D. (2011). Mechanisms of the anti-cancer and anti-inflammatory actions of vitamin D. Annu Rev Pharmacol Toxicol, 51, 311-336.

Kumar, V. L., & Majumder, P. K. (1995). Prostate gland: structure, functions and regulation. Int Urol Nephrol, 27(3), 231-243.

Kurita, T., Medina, R. T., Mills, A. A., & Cunha, G. R. (2004). Role of p63 and basal cells in the prostate. Development, 131(20), 4955-4964.

Kwiecinski, G. G., Petrie, G. I., & DeLuca, H. F. (1989). Vitamin D is necessary for reproductive functions of the male rat. J Nutr, 119(5), 741-744.

Laczko, I., Hudson, D. L., Freeman, A., Feneley, M. R., & Masters, J. R. (2005). Comparison of the zones of the human prostate with the seminal vesicle: morphology, immunohistochemistry, and cell kinetics. Prostate, 62(3), 260-266.

Lee, D. K., et al. (2014). The prostate basal cell (BC) heterogeneity and the p63-positive BC differentiation spectrum in mice. Int J Biol Sci 10(9), 1007-1017.

Leitzmann, M. F., & Rohrmann, S. (2012). Risk factors for the onset of prostatic cancer: age, location, and behavioral correlates. Clinic Epidemiol, 4, 1-11.

Li, Y. C., Kong, J., Wei, M., Chen, Z. F., Liu, S. Q., & Cao, L. P. (2002). 1,25-Dihydroxyvitamin D(3) is a negative endocrine regulator of the renin-angiotensin system. J Clin Invest, 110(2), 229-238.

Lilja, H., Ulmert, D., Vickers , A. J. (2008). Prostate-specific antigen and prostate cancer: prediction, detection and monitoring. Nat Rev Cancer, 8(4),268-278.

Lim, K. B. (2017). Epidemiology of clinical benign prostatic hyperplasia. Asian J Urol, 4, 148-151.

Liu, P. T., Stenger, S., Li, H., Wenzel, L., Tan, B. H., Krutzik, S. R., et al. (2006). Toll-like receptor triggering of a vitamin D-mediated human antimicrobial response. Science, 311(5768), 1770-1773.

MacLaughlin, J., & Holick, M. F. (1985). Aging decreases the capacity of human skin to produce vitamin D3. J Clin Invest, 76(4), 1536-1538.

Mangelsdorf, D. J., Thummel, C., Beato, M., Herrlich, P., Schutz, G., Umesono, K., et al. (1995). The nuclear receptor superfamily: the second decade. Cell, 83(6), 835-839.

Mao, G. E., Reuter, V. E., Cordon-Cardo, C., Dalbagni, G., Scher, H. I., DeKernion, J. B., et al. (2004). Decreased retinoid X receptor-alpha protein expression in basal cells occurs in the early stage of human prostate cancer development. Cancer Epidemiol Biomarkers Prev, 13(3), 383-390.

Marini, F., Bartoccini, E., Cascianelli, G., Voccoli, V., Baviglia, M. G., Magni, M. V., et al. (2010). Effect of 1alpha,25-dihydroxyvitamin D3 in embryonic hippocampal cells. Hippocampus, 20(6), 696-705.

Marshall, D. T., Savage, S. J., Garrett-Mayer, E., Keane, T. E., Hollis, B. W., Horst, R. et al. (2012). Vitamin D3 supplementation at 4000 international units per day for one year results in a decrease of positive cores at repeat biopsy in subjects with low-risk prostate cancer under active surveillance. J Clin Endocrinol Metab 97(7), 2315-2324.

McNeal, J. E. (1981). The zonal anatomy of the prostate. Prostate, 2(1), 35-49.

McNeal, J. E. (1988). Normal histology of the prostate. Am J Surg Pathol, 12(8), 619-633.

Mokry, L. E., Ross, S., Morris, J. A., Manousaki, D., Forgetta, V., & Richards, J. B. (2016). Genetically decreased vitamin D and risk of Alzheimer disease. Neurololy, 87, 1-8.

Morais-Santos, M., Nunes, A. E., Oliveira, A. G., Moura-Cordeiro, J. D., Mahecha, G. A., Avellar, M. C., et al. (2015). Changes in Estrogen Receptor ERbeta (ESR2) Expression without Changes in the Estradiol Levels in the Prostate of Aging Rats. PLoS One, 10(7), e0131901.

Morais-Santos, M., Werneck-Gomes, H., Campolina-Silva, G. H., Santos, L. C., Mahecha, G. A. B., Hess, R. A., & Oliveira, C. A. (2018). Basal Cells Show Increased Expression of Aromatase and Estrogen Receptor α in Prostate Epithelial Lesions of Male Aging Rats.

Endocrinology 159(2), 723-732.

Nemere, I., Farach-Carson, M. C., Rohe, B., Sterling, T. M., Norman, A. W., Boyan, B. D., et al. (2004). Ribozyme knockdown functionally links a 1,25(OH)2D3 membrane binding protein (1,25D3-MARRS) and phosphate uptake in intestinal cells. Proc Natl Acad Sci U S A, 101(19), 7392-7397.

Okano, T., Tsugawa, N., Morishita, A., & Kato, S. (2004). Regulation of gene expression of epithelial calcium channels in intestine and kidney of mice by 1alpha,25-dihydroxyvitamin D3. J Steroid Biochem Mol Biol, 89-90(1-5), 335-338.

Ozten, N., Vega, K., Liehr, J., Huang, X., Horton, L., Cavalieri, E. L., Rogan, E. G., & Bosland, M. C. (2019). Role of Estrogen in androgen-induced prostate carcinogenesis

Park, J. W., Lee, J. K., Phillips, J. W., Huang, P., Cheng, D., Huang, J., & Witte, O. N. (2016). Prostate epithelial cell of origin determines cancer differentiation state in an organoid transformation assay. Proc Natl Acad Sci USA 113(16): 4482-4487.

Park, S.Y., Cooney, R.V., Wilkens, L.R., et al. (2010). Plasma 25-hydroxyvitamin D and prostate cancer risk: the multiethnic cohort. Eur J Cancer, 46, 932–936.

Pike, J. W., Meyer, M. B., Benkusky, N. A., Lee, S. M., John, H. St., Carlson, A., et al. (2016). Genomic determinants of vitamin D-regulated gene expression. Vitamin Horm, 100, 21-44.

Pollock, P. A., Ludgate, A., & Wassersug, R. J. (2015). In 2124, half of all men

Prins, G. S., & Korach, K. S. (2008). The role of estrogens and estrogen receptors in normal prostate growth and disease. Steroids, 73(3), 233-244.

Rago, V., et al. (2016). Identification of the G protein-coupled estrogen receptor (GPER) in human prostate: expression site of the estrogen receptor in the benign and neoplastic gland. Andrology, 4(1), 121-127.

Raman, M., Milestone, A. N., Walters, J. R. F., Hart, A. L., & Ghosh, S. (2011). Vitamin D and gastrointestinal diseases: inflammatory bowel disease and colorectal cancer. Ther Adv Gastroenterol, 4(1), 49-62.

Rawla, P. (2019). Epidemiology of prostate cancer. World J Oncol, 10(2), 63-89.

Risbridger, G. P., Ellem, S. J., & McPherson, S. J. (2007). Estrogen action on the prostate gland: a critical mix of endocrine and paracrine signaling. J Mol Endocrinol, 39, 183-188.

Risbridger, G. P; Taylor, R.A. (2006). Physiology of the male accessory sex structures: the prostate gland, seminal vesicles, and bulborethral glands. In: D. N. Jimmy (Ed). Knobil and Neill=s Physiology of reproduction. Victoria: Elsevier. Physiology of the male accessory sex structures: the prostate gland, seminal vesicles, and bulborethral glands, p. 1149-1172.

Rodriguez, R., Pozuelo, J. M., Martin, R., Henriques-Gil, N., Haro, M., Arriazu, R., et al. (2003). Presence of neuroendocrine cells during postnatal development in rat prostate: Immunohistochemical, molecular, and quantitative study. Prostate, 57(2), 176-185.

Rondanelli, M., Miccono, A., Lamburghini, S., Avanzato, I., Riva, A., Allegrini, P., et al. (2018). Self-Care for Common Colds: the pivotal role of vitamin d, vitamin c, zinc, and echinacea in three main immune interactive clusters (physical barriers, innate and adaptive immunity) involved during an episode of common colds—practical advice on dosages and on the time to take these nutrients/botanicals in order to prevent or treat common colds. Evidence-Based Compl and Altern Med, 2018, 1-36.

Roy, J., Kim, B., Hill, E., Visconti, P., Krapf, D., Vinegoni, C., Weissleder, R., Brown, D., & Breton, S. 2016. Tyrosine kinase-mediated axial motility of basal cells revealed by intravital imaging. Nat Comm, 7: 10666.

Sawada, N., Sakaki, T., Ohta, M., & Inouye, K. (2000). Metabolism of vitamin D3 by human CYP27A1. Bioch and Biophys Res Comm, 273, 977-984.

Schiffer, L., Arlt, W., & Storbeck, K. (2018). Intracrine androgen biosynthesis, metabolism and action revised. Mol Cell Endo, 465, 4-26.

Segersten, U., Correa, P., Hewison, M., Hellman, P., Dralle, H., Carling, T., et al. (2002). 25-hydroxyvitamin D(3)-1alpha-hydroxylase expression in normal and pathological parathyroid glands. J Clin Endocrinol Metab, 87(6), 2967-2972.

Segersten, U., Holm, P. K., Bjorklund, P., Hessman, O., Nordgren, H., Binderup, L., et al. (2005). 25-Hydroxyvitamin D3 1alpha-hydroxylase expression in breast cancer and use of non-1alpha-hydroxylated vitamin D analogue. Breast Cancer Res, 7(6), R980-986.

Shappell, S. B., Thomas, G. V., Roberts, R. L., Herbert, R., Ittmann, M. M., Rubin, M. A., et al. (2004). Prostate pathology of genetically engineered mice: definitions and classification. The consensus report from the Bar Harbor meeting of the Mouse Models of Human Cancer Consortium Prostate Pathology Committee. Cancer Res, 64(6), 2270-2305.

Shinkyo, R., Sakaki, T., Kamakura, M., Ohta, M., & Inouye, K. (2004). Metabolism of vitamin D by human microsomal CYP2R1. Bioch and Biophys Res Comm, 324, 451-457.

Shum, W. W., Da Silva, N., McKee, M., Smith, P. J., Brown, D., & Breton, S. (2008). Transepithelial projections from basal cells are luminal sensors in pseudostratified epithelia. Cell, 135(6), 1108-1117.

Signoretti, S., Waltregny, D., Dilks, J., Isaac, B., Lin, D., Garraway, L., Yang, A., Montironi, R., McKeon, F., & Loda, M. (2000). p63 is a prostate basal cell marker and is required for prostate development. Am J Pathol 157(6), 1769-1775.

Skowronski, R. J., Peehl, D. M., & Feldman, D. (1993). Vitamin D and prostate cancer: 1,25 dihydroxyvitamin D3 receptors and actions in human prostate cancer cell lines. Endocrinology, 132(5), 1952-1960.

Stoyanova, T., Cooper, A. R., Drake, J. M., Liu, X., Armstrong, A. J., Pienta, K. J., Zhang, H., Kohn, D. B., Huang, J., Witte, O. N., & Goldstein, A. S. (2013). Prostate cancer

originating in basal cells progresses to adenocarcinoma propagated by luminal-like cells. Proc Natl Acad Sci USA 110(50): 20111-20116.

Sugimura, Y., Cunha, G. R., & Donjacour, A. A. (1986). Morphogenesis of ductal networks in the mouse prostate. Biol Reprod, 34(5), 961-971.

Swami, S., Krishnan, A. V., & Feldman, D. (2011). Vitamin D metabolism and action in the prostate: implications for health and disease. Mol Cell Endocrinol, 347(1-2), 61-69.

Tan, M. H., Li, J., Xu, H. E., Melcher, K., & Yong, E. L. (2015). Androgen receptor: structure, role in prostate cancer and drug discovery. Acta Pharmacol Sinica, 36(1), 3-23.

Tannour-Louet, M., Lewis, S. K., Louet, J. F., Stewart, J., Addai, J. B., Sahin, A., et al. (2014). Increased expression of CYP24A1 correlates with advanced stages of prostate cancer and can cause resistance to vitamin D3-based therapies. FASEB J 28(1), 364-372.

Taylor, R. A., Toivanen, R., Frydenberg, M., Pedersen, J., Harewood, L., Australian Prostate Cancer Bioresource, Collins, A. T., Maitland, N. J., & Risbridger, G. P. (2012). Human epithelial basal cells are cells of origin of prostate cancer, independent of CD133 *status*. Stem Cells 30(6), 1087-1096.

Trump, D. L., Deeb, K. K., & Johnson, C. S. (2010). Vitamin D: considerations in the continued development as an agent for cancer prevention and therapy. Cancer J, 16(1), 1-9.

van der Rhee, H., Coebergh, J. W., & de Vries, E. (2012). Is prevention of cancer by sun exposure more than just the effect of vitamin D? A systematic review of epidemiological studies. Eur J Cancer, 49(6), 1422-1436.

van Etten, E., & Mathieu, C. (2005). Immunoregulation by 1,25-dihydroxyvitamin D3: basic concepts. J Steroid Biochem Mol Biol, 97(1-2), 93-101.

Verze, P., Cai, T., Lorenzetti, S. (2016). The role of the prostate in male fertility, health and disease. Nature Rev Urol, 13(7), 379-386.

Wadhera, P. (2013). An introduction to acinar pressures in BPH and prostate cancer. Nat Rev Urol, 10(6), 358-366.

Wang, H., Chen, W., Li, D., Yin, X., Zhang, X., Olsen, N., &. Zheng, S. G. (2017). Vitamin D and Chronic Diseases. Aging Dis 8(3): 346-353.

Wang, Z. A., et al. (2013). Lineage analysis of basal epithelial cells reveals their unexpected plasticity and supports a cell-of-origin model for prostate cancer heterogeneity. Nat Cell Biol 15(3), 274-283.

Wang, Z. A., Toivanen, R., Bergren, S. K., Chambon, P., & Shen, M. M. (2014). Luminal cells are favored as the cell of origin for prostate cancer. Cell Rep 8(5): 1339-1346.

Webb, A. R., DeCosta, B. R., & Holick, M. F. (1989). Sunlight regulates the cutaneous production of vitamin D3 by causing its photodegradation. J Clin Endocrinol Metab, 68(5), 882-887.

Werneck-Gomes, H., Campolina-Silva, G. H., Maria, B. T., Barata, M. C., Mahecha, G. A. B., Hess, R. A., & Oliveira, C. A. (2020). Tumor-Associated Macrophages (TAM) are recruited to the aging prostate epithelial lesions and become intermingled with basal cells. Andrology, s/n, 1-12.

Woenckhaus, J., & Fenic, I. (2008). Proliferative inflammatory atrophy: a background lesion of prostate cancer? Andrologia, 40(2), 134-137.

Xie, D. D., Chen, Y. H., Xu, S., et al. (2017). Low vitamin D *status* is associated with inflammation in patients with prostate cancer. Oncotarget, 8, 22076–22085.

Yamasaki, T., Izumi, S., Ide, H., & Okyama, Y. (2004). Identification of a novel rat microsomal vitamin D3 25-Hydroxylase. J Biol Chem, 270(22), 22848-22856.

Zehnder, D., Bland, R., Williams, M. C., McNinch, R. W., Howie, A. J., Stewart, P. M., et al. (2001). Extrarenal expression of 25-hydroxyvitamin d(3)-1 alpha-hydroxylase. J Clin Endocrinol Metab, 86(2), 888-894.

Zhou, C. K., Check, D. P., Lortet-Tieulent, J., Laversanne, M., Jemal, A., Felay, J., Bray, F., et al. (2016). Prostate cancer incidence in 43 populations worldwide: An analysis of time trends overall and by age group. Int Journal of Cancer, 138, 1388-1400.

Zhu, J. G., Ochalek, J. T., Kaufmann, M., Jones, G., & Deluca, H. F. (2013). CYP2R1 is a major, but not exclusive, contributor to 25-hydroxyvitamin D production in vivo. Proc Natl Acad Sci U S A, 110(39), 15650-15655.

Zierold, C., Mings, J. A., & DeLuca, H. F. (2003). Regulation of 25-hydroxyvitamin D3-24-hydroxylase mRNA by 1,25-dihydroxyvitamin D3 and parathyroid hormone. J Cell Biochem, 88(2), 234-237.